



Caracterización funcional de la proteína scavenger AIM en la respuesta anti-infecciosa del macrófago

Lucía Sanjurjo Bouza

ADVERTIMENT. La consulta d'aquesta tesi queda condicionada a l'acceptació de les següents condicions d'ús: La difusió d'aquesta tesi per mitjà del servei TDX (www.tdx.cat) i a través del Dipòsit Digital de la UB (diposit.ub.edu) ha estat autoritzada pels titulars dels drets de propietat intel·lectual únicament per a usos privats emmarcats en activitats d'investigació i docència. No s'autoritza la seva reproducció amb finalitats de lucre ni la seva difusió i posada a disposició des d'un lloc aliè al servei TDX ni al Dipòsit Digital de la UB. No s'autoritza la presentació del seu contingut en una finestra o marc aliè a TDX o al Dipòsit Digital de la UB (framing). Aquesta reserva de drets afecta tant al resum de presentació de la tesi com als seus continguts. En la utilització o cita de parts de la tesi és obligat indicar el nom de la persona autora.

ADVERTENCIA. La consulta de esta tesis queda condicionada a la aceptación de las siguientes condiciones de uso: La difusión de esta tesis por medio del servicio TDR (www.tdx.cat) y a través del Repositorio Digital de la UB (diposit.ub.edu) ha sido autorizada por los titulares de los derechos de propiedad intelectual únicamente para usos privados enmarcados en actividades de investigación y docencia. No se autoriza su reproducción con finalidades de lucro ni su difusión y puesta a disposición desde un sitio ajeno al servicio TDR o al Repositorio Digital de la UB. No se autoriza la presentación de su contenido en una ventana o marco ajeno a TDR o al Repositorio Digital de la UB (framing). Esta reserva de derechos afecta tanto al resumen de presentación de la tesis como a sus contenidos. En la utilización o cita de partes de la tesis es obligado indicar el nombre de la persona autora.

WARNING. On having consulted this thesis you're accepting the following use conditions: Spreading this thesis by the TDX (www.tdx.cat) service and by the UB Digital Repository (diposit.ub.edu) has been authorized by the titular of the intellectual property rights only for private uses placed in investigation and teaching activities. Reproduction with lucrative aims is not authorized nor its spreading and availability from a site foreign to the TDX service or to the UB Digital Repository. Introducing its content in a window or frame foreign to the TDX service or to the UB Digital Repository is not authorized (framing). Those rights affect to the presentation summary of the thesis as well as to its contents. In the using or citation of parts of the thesis it's obliged to indicate the name of the author.

Cover art: Original digital illustration by Amagoia Agirre,
concept by Eneritz Agirre.



**Programa de Doctorado en Biomedicina
Universitat de Barcelona**

**Caracterización funcional de la
proteína scavenger AIM en la respuesta
anti-infecciosa del macrófago**

Tesis presentada por Lucía Sanjurjo Bouza
para obtener el título de Doctora en Biomedicina por
la Universidad de Barcelona

Directora:

Dra. Maria Rosa Sarrias Fornés

Institut d'Investigació en Ciències de la Salut Germans
Trias i Pujol

*O verdadeiro heroísmo consiste en trocar os
anceios en realidade, as ideas en feitos.*

A.D.R. Castelao en "Sempre en Galiza", 1928

A Mamá

INDEX

LIST OF ABBREVIATIONS	1
INTRODUCTION	5
1. General introduction. Innate immunity, macrophages and inflammation.....	5
2. Pattern Recognition Receptors (PRRs).....	9
2.1. Toll-Like Receptors (TLRs).....	10
2.2. NOD-Like Receptors (NLRs) and inflammasome	22
2.3. Scavenger Receptors (SRs).....	27
3. Apoptosis Inhibitor of Macrophages (AIM).....	35
3.1. Cloning of AIM	35
3.2. Regulation	37
3.3. Presence in serum.....	40
3.4. Role of AIM.....	42
4. Autophagy	54
4.1. Molecular signaling of autophagy.....	56
4.2. Autophagy in immunity	63
5. Tuberculosis	68
5.1. General introduction to tuberculosis.....	68
5.2. Macrophage mycobactericidal mechanisms.....	70
OBJECTIVES	79
MATERIAL & METHODS	81
1. Cells.....	81
1.1. Peripheral blood monocytes	81
1.2. Murine bone marrow-derived macrophages (BMDM)	82
1.3. Stably transfected THP1-vector and THP1-hAIM cell lines.....	83
2. Production of recombinant proteins	85
2.1. rhAIM.....	85
2.2. rmAIM	86
3. Quantitative Real Time PCR (qRT-PCR)	88

4.	Western blot analysis of cell lysates	90
5.	Measurement of cytokine and chemokine secretion.....	91
5.1.	Multi-Analyte Profiling (MAP) technology	91
5.2.	Enzyme-linked ImmunoSorbent Assay (ELISA).....	93
6.	Immunocytochemistry (ICC) and fluorescent microscopy	94
7.	Immunostaining for flow cytometry analysis.....	96
8.	Analysis of macrophage intracellular signalling	97
8.1.	MAPK and PI3K	97
8.2.	Autophagy pathway.....	100
9.	Silencing of ATG7 and CD36 expression.....	104
10.	Phagocytosis assays	105
11.	Measurement of <i>Escherichia coli</i> ingestion and killing by counting colony forming units (CFUs).....	107
12.	Study of the antimicrobial response against <i>Mycobacterium tuberculosis</i>	108
12.1.	Bacteria	108
12.2.	In <i>vitro</i> Mtb infection model	109
12.3.	Determination of hAIM in serum of Mtb infected mice.....	115
13.	Statistical analysis.....	119
	RESULTS & DISCUSSION	121
	WORK I: The hAIM-CD36 axis is a novel mechanism of autophagy induction in monocytes.....	123
	DISCUSSION I.....	144
	WORK II: Human AIM enhances macrophage intracellular killing of <i>Escherichia coli</i>	151
	DISCUSSION II.....	156
	WORK III: The scavenger protein AIM potentiates the antimicrobial response against <i>Mycobacterium tuberculosis</i> by enhancing autophagy	161
	DISCUSSION III	175
	GENERAL DISCUSSION	181
	CONCLUSIONS	191
	REFERENCES	195

LIST OF ABBREVIATIONS

3-MA: 3-methyladenine

AIM: apoptosis inhibitor of macrophage

AKT: protein kinase B

Alb: human albumin

Ab: antibody

BMDM: bone marrow-derived macrophages

CD: cluster of differentiation

cDNA: complementary DNA

cRNA: complementary RNA

Ct: control

DC: dendritic cell

DEFB4: Defensin B4

DNA: deoxyribonucleic acid

e.g.: from Latin, *exempli gratia*, which means “for example”

et al.: from Latin, *et alii*, which means “and others”

FCS: fetal calf serum

FITC: fluorescein isothiocyanate

G418: geneticin

h: hour

hAIM: human AIM

HEK: human embryonic kidney

HRP: horseradish peroxidase

ICC: immunocytochemistry

IFN: interferon

Ig: immunoglobulin

IL: interleukin

LC3: microtubule-associated protein 1A/1B-light chain 3

LL-37: cathelicidin peptide

LPS: Lipopolysaccharide

LS: laser scanning

MΦ: macrophage

mAIM: mouse AIM

ABBREVIATIONS

MAP: multi-analyte profiling

Min: minutes

Mo: monoclonal

MAPK: mitogen-activated protein kinase

MoAb: monoclonal antibody

Mtb: *Mycobacterium tuberculosis*

MW: molecular weight

NLR: NOD-like receptor

NO: nitric oxide

NR: non-reducing

ODN: oligodeoxynucleotide

OxLDL: oxidized low-density lipoprotein

PAMP: pathogen-associated molecular pattern

PBMC: peripheral blood mononuclear cell

PB Monocytes: peripheral blood monocytes

PBS: phosphate buffer saline

PCR: polymerase chain reaction

PE: phycoerythrin

PFA: paraformaldehyde

PI: phosphatidylinositol

PI3K: phosphatidylinositol 3 kinase

PMA: phorbol 12-myristate 13-acetate

poAb: polyclonal antibody

PRR: pattern recognition receptor

qRT-PCR: quantitative real-time PCR

R: reducing

rhAIM: recombinant human AIM

rmAIM: recombinant mouse AIM

RNA: ribonucleic acid

ROS: reactive oxygen species

s: seconds

SEM: standard error mean

SRCR: scavenger receptor cysteine rich

SRCR-SF: scavenger receptor cysteine rich superfamily

TB: tuberculosis

TBS: tris-buffered saline

TLR: toll-like receptor

TMB: tetramethylbenzidine

TNF: tumor necrosis factor

W: wortmannin

xg: multiples of standard acceleration due to gravity (g), centrifugal force



Most mentioned terms in this work. Word cloud from Jason Davis word cloud generator.

INTRODUCTION

1. General introduction. Innate immunity, macrophages and inflammation.

Infectious diseases are still a major cause of morbidity and mortality worldwide. The mammalian innate immune system is a remarkable complex of biochemical processes enabling efficient detection and prosecution of pathogens that threaten host viability.

The innate immune system is based on physical and chemical barriers to infection, as well as on different cell types recognizing invading pathogens and activating antimicrobial immune responses (Janeway and Medzhitov 2002). In the 20th century innate immunity was defined as “a primitive stopgap measure to hold the fort before the arrival of specific and more sophisticated adaptive immune responses”. This conception began to change in 1989 with a publication by Charles Janeway that outlined a new theory for immune system activation. Janeway suggested for the first time that recognition by the innate immune system is specific and that this specificity relies on a limited number of germ line-encoded receptors called pattern recognition receptors (PRR), which bind to molecular structures expressed by invading pathogens (pathogen associated molecular patterns, PAMPs) (Janeway 1989). PAMPs are characterized by being invariant among entire classes of pathogens, essential for the survival of the pathogen, and distinguishable from “self” (Janeway 1989). Later on, PRRs were shown to also recognize host factors as

“danger” signals, when they are present in aberrant locations or abnormal molecular complexes as a consequence of infection, inflammation, or other types of cellular stress (Matzinger 2002).

In the present work we focused on the innate immune response to pathogenic organisms.

The discovery of Toll-like receptors (TLRs) (Medzhitov, Preston-Hurlburt et al. 1997), a family of membrane bound PRR that signal in response to conserved microbial products, led to realize that the innate immune response not only provides a first line of defense but also is critical for prodding the adaptive immune response into action (Medzhitov, Preston-Hurlburt et al. 1997; Medzhitov, Preston-Hurlburt et al. 1998; Ravikumar, Sarkar et al. 2010; O'Neill, Golenbock et al. 2013; Parzych and Klionsky 2013). Moreover, these findings remarkably helped revitalize the study of innate immunology. PRRs trigger intracellular signaling cascades ultimately culminating in the expression of a variety of inflammatory molecules. Although the generation of a potent immune response is of crucial importance for the containment and eradication of microbial infection, excessive or inappropriate inflammation may be harmful to the host and result in immunopathology or autoimmunity (Kundu and Surh 2008; Mantovani, Allavena et al. 2008). The innate immune system therefore is able to control inflammatory signaling during infection and, not least, to downregulates the inflammatory response once the infection has been resolved (Barton 2008).

Among the cellular components of innate immunity, the monocyte/macrophage ($M\Phi$) is a key cell type. $M\Phi$ /monocytes,

together with other professional phagocytic cells including neutrophils and dendritic cells, play a crucial role in host-defense through recognition and elimination of invading pathogenic bacteria (Mosser and Edwards 2008). Since their initial description as professional phagocytes, we have learned a great deal about the distribution of M Φ throughout the body, their heterogeneous phenotype and their effector mechanisms in their encounter with pathogens. M Φ are strategically located throughout the body tissues, where they ingest and process foreign and host materials, pathogens, dead cells and debris. Interestingly, they are highly heterogeneous cells that can rapidly change their function in response to local microenvironmental signals.

With regard to their antimicrobial function, M Φ have the means to destroy pathogens directly or indirectly via innate and adaptive immune responses, respectively. The direct bactericidal features of these cells include the generation of reactive oxygen species (ROS), nitric oxide (NO) and phagocytosis, a process involving the engulfment of bacteria into phagosomes. The bacteria-containing phagosomes fuse with late endosomes or lysosomes in a process of “maturation” leading to the eventual degradation of the bacteria (Flannagan, Cosio et al. 2009). The indirect macrophage immune response involves T cell activation via antigen processing and presentation (Hume 2008) and induction of inflammation, a process characterized by the increased production of many inflammatory cytokines and chemokines, which together promote the recruitment of blood leukocytes to the site of infection and the activation of additional immune cells (Flannagan, Cosio et al. 2009). Moreover, recent studies suggest that autophagy, a conserved process involved in the turnover of

cellular material, plays an important role in the host immune response against invading bacteria. Autophagy is induced by various bacterial virulence factors. Once engaged, the autophagic machinery recognizes and targets bacteria in different ways. In addition to direct killing of bacteria in autophagosomes (xenophagy), autophagy also regulates many immune functions including the inflammatory process, phagocytosis (LAP, LC-3 associated phagocytosis), antigen presentation, and the release of bactericidal factors (ROS, NO) (Gong, Devenish et al. 2012).

As a front-line component of host defense, macrophages represent a useful model to study host-pathogen interactions. Moreover, understanding M Φ -pathogen interactions is crucial to understanding the pathogenesis of many infectious diseases. The balance between the macrophage's ability to recognize and correctly destroy bacterial pathogens and the pathogen's ability to modulate macrophage signaling often determines the outcome of an infection.

2. Pattern Recognition Receptors (PRRs)

The initial interaction of $M\Phi$ with a newly invaded pathogen is mediated by PRR, germ line-encoded receptors that can be expressed on the cell surface, in intracellular compartments, or secreted into the bloodstream and tissue fluids. PRRs recognize PAMPs, molecular structures that are broadly shared by pathogens. The best known examples of PAMPs include lipopolysaccharide (LPS) of gram-negative bacteria and peptidoglycan of gram-positive bacteria, among a long list of molecules (Janeway 1989). However, the concept of pattern recognition has to be broadened to include modified self-ligand (induced or altered self, e. g. externalized phosphatidylserine in apoptotic cells) and absence of self (missing self, e.g. cells that express few or no MHC class I protein on the cell surface) (Medzhitov and Janeway 2002).

Upon recognition, PRRs are able to mount a coordinated response to pathogen infection. Briefly, PRRs signaling results in induction of inflammation at the site of infection and recruitment of cells and mediators, which together orchestrate the early host response to infection and at the same time modulate of the second line of host defense called adaptive immunity. The principal functions of PRRs include opsonization, phagocytosis, activation of complement and coagulation cascades, activation of inflammatory signaling pathways and induction of apoptosis. Moreover, in order to avoid immunopathology, this system is tightly regulated by a number of endogenous molecules that limit the magnitude and duration of the inflammatory response (Medzhitov and Janeway 1997; Takeuchi and Akira 2010).

Several structurally and functionally distinct classes of PRR evolved to induce various host defense pathways. Accordingly, PRRs are classified into different families: toll-like receptors (TLRs); nucleotide binding leucine rich repeat (NLR) containing receptors, also known as NOD-like receptors; scavenger receptors (SRs); retinoic acid-inducible gene I (RIG-I)-like receptors; and the C-type lectin receptors are the main families of PRRs. This diversity allows the recognition of a wide repertoire of molecules found in either the extracellular space or an intracellular environment. By having multiple sites for detection of diverse targets, it is unlikely that any given pathogen will be able to evade all of the levels of detection.

Given their relevance in the present thesis, among the different families of PRR we want to highlight TLRs, NOD-like receptors and SRs, which will be introduced below.

2.1. Toll-Like Receptors (TLRs)

TLRs are among the most well-studied and well-characterized PRRs. Structurally, TLRs are type I transmembrane proteins consisting of an ectodomain comprised of leucine-rich repeats (LRRs) that mediate the recognition of PAMPs, a transmembrane domain, and a cytoplasmic domain containing a toll-interleukin 1 (IL-1) receptor (TIR) domain, which is required for downstream signal transduction (**Figure 1**).

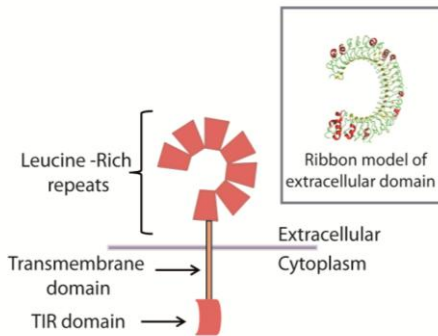


Figure 1. TLR structure. TLR structure scheme and Ribbon 3D protein structure diagram of TLR3 extracellular domain. Adapted from (Bell, Botos et al. 2006). TIR: Toll-interleukin 1 (IL-1) receptor.

To date, 10 and 13 functional TLRs have been identified in human and mice, respectively. Each TLR has a specific set of ligands that it can detect, these include distinct PAMPs derived from viruses, bacteria, fungi and parasites (Table 1) (Kawai and Akira 2007; Kumar, Kawai et al. 2009).

Receptor	Typical ligands
TLR2/TLR1	Triacyl lipopeptides
TLR2	Peptidoglycan, lipopeptide and lipoproteins
TLR3	Double-stranded RNA
TLR4	Lipopolysaccharide (LPS), viral envelope proteins
TLR5	Flagellin
TLR2/TLR6	Diacyl lipopeptides, zymosan
TLR7	ssRNA, imidazoquinolines
TLR8	ssRNA, imidazoquinolines
TLR9	Bacterial and viral deoxycytidylate-phosphate-deoxyguanylate (CpG) DNA motifs, malaria pigment hemozoin
TLR10	Undetermined. Participates in the innate immune response against influenza virus infection (Lee, Kok et al.)
TLR11/12 (mouse)	Protozoan profiling
TLR13 (mouse)	Bacterial 23S ribosomal RNA (bRNA)

Table 1. TLRs and selected ligands. Adapted from (Kawai and Akira 2007; Kumar, Kawai et al. 2009; Raetz, Kibardin et al.).

As mentioned, recognition of PAMPs by TLRs occurs in various cellular compartments, including the plasma membrane, endosomes, lysosomes and endolysosomes. The correct cellular localization of TLRs is thought to be important for ligand accessibility, maintenance of tolerance to self molecules and downstream signal transduction (**Figure 2**) (Akira, Uematsu et al. 2006). In this regard, upon ligand binding, extracellular TLRs signal intracellularly and then undergo internalization (Husebye, Halaas et al. 2006; Triantafilou, Gamper et al. 2006). This was initially thought to attenuate ligand-induced responses, but is now widely accepted that receptor internalization permits both the propagation of the signaling cascade from endosomal compartments and the generation of distinct signaling events (Barton and Kagan 2009). Moreover, it has been reported by different groups that blockade of TLR internalization results in a sustained anti-inflammatory response (Husebye, Halaas et al. 2006; Triantafilou, Gamper et al. 2006; Brandt, Fickentscher et al. 2013). Intracellular localization of nucleic acid-sensing may limit access to self nucleic acids and in this way establish the threshold for self and non-self discrimination by these receptors (Blasius and Beutler 2010).

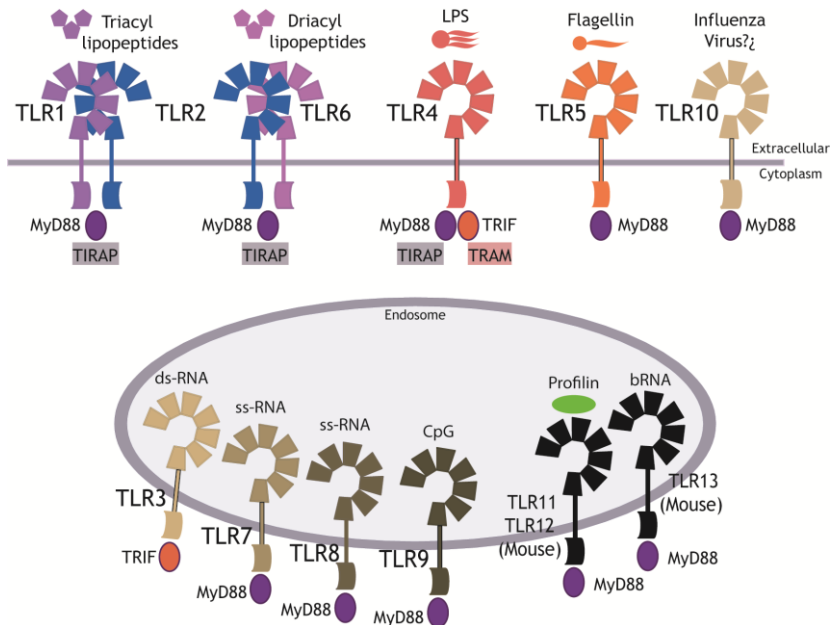


Figure 2. TLR location, ligands and adaptors. Human TLR1, TLR2, TLR4, TLR5, TLR6 and TLR10 are localized on the cell surface and largely recognize microbial membrane components. In contrast, human TLR3, TLR7, TLR8, TLR9 and mouse TLR11, TLR12 and TLR13 are expressed within intracellular vesicles and recognize nucleic acids and intracellular protozoan parasites. Figure also shows the typical ligand for each TLR and the specific adaptors, myeloid differentiation primary response gen 88 (MyD88) and/or TIR-domain containing adapter-inducing interferon- β (TRIF), used by each TLR. The activation of a MyD88-dependent pathway downstream of TLR2 and TLR4 is mediated by the adapter TIRAP (Toll-interleukin 1 receptor domain-containing adapter protein), the adapter TRAM (Toll-interleukin 1 receptor domain-containing adapter-inducing IFN- β -related adapter molecule) selectively participates in the activation of the TRIF-dependent pathway downstream of TLR4, but not TLR3.

2.1.1. Toll-like receptor signaling

Upon recognition of respective PAMPs, signaling is initiated by either receptor homodimerisation (e.g. TLR3) or heterodimerisation (e.g. TLR2 with TLR1 or TLR6). Moreover, it is known that TLRs 2, 3 and 4 form multicomplex structures with additional receptors and/or cofactors (e.g. CD14, CD36,

CD11b/CD18, Dectin-1, and MD2) for the recognition of some PAMPs. These co-receptors increase the efficiency and specificity of PAMP/TLR interactions (West, Koblansky et al. 2006; Jin and Lee 2008).

After PAMP recognition, a fundamental basis of TLR signaling is the recruitment and association of adaptor molecules that contain the structurally conserved TIR domain (**Figure 2**). Different adaptors engage different receptors, and the particular adaptor used determines which signaling pathway will be activated (Brown, Wang et al. 2010).

Myeloid differentiation primary response gene 88 (MyD88) is a universal adaptor shared by all TLRs (with the exception of TLR3) that activates inflammatory pathways. Recruitment of MyD88 leads to the activation of mitogen-activated protein kinases (MAPKs) pathways and the induction of nuclear transcription factor kappa-light-chain-enhancer of activated B cells (NF- κ B) to control the expression of cytokine and chemokine genes. A second, MyD88-independent pathway, operates in endosomal compartments, is initiated by the adaptor TRIF (TIR-domain containing adaptor-inducing interferon- β) recruited to endosomal TLR3 as well as to TLR4 upon its internalization (Kagan, Su et al. 2008). This pathway culminates in activation of the transcription factors NF- κ B and interferon regulatory factor 3 (IRF3) with the consequent induction of cytokines and type I interferon (INF) (Akira and Takeda 2004; Kawai and Akira).

In M Φ a generic model to explain TLR signaling is: receptors that induce an inflammatory response engage a MyD88-dependent

signaling pathway, whereas those that also induce a type I IFN response engage a TRIF-dependent signaling pathway. TLR4 is the only that uses four adaptors, it is thought that the MyD88 pathway is first activated in the plasma membrane and upon dynamin-dependent endocytosis it transits sequentially into TRIF signaling in endosomes. This leads to IRF3 activation as well as later-phase activation of NF- κ B (**Figure 3**) (Kagan, Su et al. 2008).

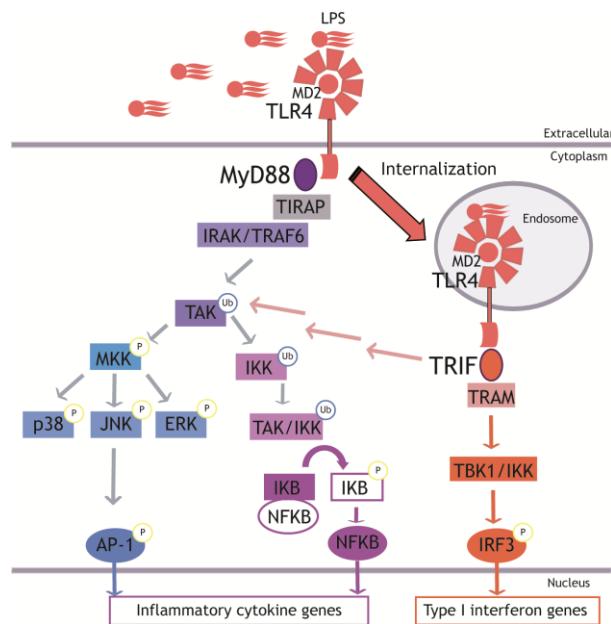


Figure 3. Oversimplified scheme for LPS signaling in M Φ . The figure shows MyD88 and TRIF-dependent pathways downstream TLR4. **MyD88 dependent pathway:** MyD88 recruits the IL-1 receptor associated kinases (IRAK) that are activated sequentially and this results in an interaction with IRAK6, an E3 ligase that catalyzes the synthesis of polyubiquitin linked to Lys63 (K63) on target proteins, namely TGF- β activated kinase (TAK) and I κ B kinase complex (IKK). Polyubiquitin chains (Ub) might be responsible for recruiting TAK1 to form a complex with IKK, thus allowing TAK1 to phosphorylate IKK, which leads to NF- κ B translocation to the nucleus via phosphorylation and subsequent degradation of I κ B proteins. The activated TAK1 complex simultaneously activates the MAPK pathway resulting in phosphorylation (P) and activation of various transcription factors, including AP-1. **MyD88 independent, TRIF-dependent pathway:** TRIF forms a multiprotein signaling complex for the activation of TAK1, with in later-phase activation of NF- κ B and MAPK pathways. TRIF also recruits a signaling complex involving the noncanonical IKKs and TANK-binding kinase 1 (TBK1), which catalyze the phosphorylation of IRF3 and induce its nuclear translocation (Laird, Rhee et al. 2009; Kawai and Akira). Figure adapted from (Guo and Friedman 2010).

pathogens, the inability to regulate the nature or duration of the host's inflammatory response can be detrimental as it occurs in chronic inflammatory, autoimmune or infectious diseases. TLR signaling is negatively controlled by accessory signaling pathways and multiple mechanisms such as dissociation of adaptor complexes, degradation of signal proteins, and transcriptional regulation (Kondo, Kawai et al. 2012). Endotoxin tolerance, defined as a reduced responsiveness to a lipopolysaccharide (LPS) challenge following a first encounter with endotoxin, is one example of utilization of multiple mechanisms to avoid sustained stimuli (Biswas and Lopez-Collazo 2009).

Phosphoinositide 3-kinases (PI3Ks) are also a possible safety system to control the magnitude of cellular responses to pathogens (Guha and Mackman 2002; Fukao and Koyasu 2003; Schabbauer, Tencati et al. 2004; Luyendyk, Schabbauer et al. 2008). TLR-signaling results in the activation of the PI3K pathway (Arbibe, Mira et al. 2000; Sarkar, Peters et al. 2004; Rhee, Kim et al. 2006; Santos-Sierra, Deshmukh et al. 2009), and whether PI3K plays a positive or negative role in TLR signaling was a controversy for many years. With the generation of PI3K KO mice the impact of the PI3K pathway on the host anti-inflammatory response was appreciated. PI3K (p85 α regulatory subunit of class IA PI3K) KO mice highlighted the anti-inflammatory role of PI3K through a negative feedback mechanism directed to IL-12 production (Fukao, Tanabe et al. 2002; Fukao, Yamada et al. 2002). PI3K negative TLR regulation differs from the tolerance systems, in that it acts at the first encounter to pathogens as an “early-phase safety system” (Biswas and Lopez-Collazo 2009) (**Figure 4**).

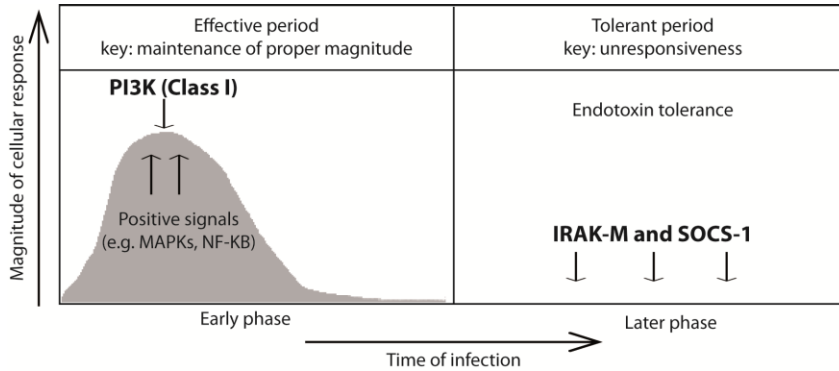


Figure 4. Dual-phase negative regulatory mechanism of innate immune response. In the first interaction between innate immune cells and pathogens, activation of class I Phosphoinositide 3-kinases (PI3K) negatively regulates TLR-mediated signaling. This ‘early-phase safety system’ controlled by PI3K confers a proper magnitude of cell activation rather than complete suppression of TLR-triggered signaling. Simultaneously, interleukin-1 receptor associated kinase-M (IRAK-M) and suppressor of cytokine signaling-1 (SOCS-1) are induced and have an essential role in a ‘late-phase safety system’ by inhibiting TLR signaling elicited by the second or continuous exposure of the cells to PAMPs-bearing pathogens. In this phase, IRAK-M and SOCS-1 stringently suppress TLR-mediated signaling, resulting in the unresponsiveness of innate immune cells (endotoxin tolerance). Figure adapted from (Fukao and Koyasu 2003).

2.1.2. Phosphoinositide 3-kinases (PI3Ks)

PI3Ks belong to an evolutionarily conserved family of proteins (enzymes) and their activation results in the phosphorylation of phosphoinositides on the 3 position of the inositol ring, leading to the transient accumulation of phospholipids in cell membranes. These lipid products serve as second messengers and/or signaling molecules to control many cellular events, including mitogenic responses, cell differentiation, survival, cytoskeletal organization, glucose homeostasis, vesicular trafficking, phagocytosis and autophagy (Vanhaesebroeck, Leever et al. 1997; Vanhaesebroeck, Guillermet-Guibert et al. 2010). The importance of these enzymes for the host is illustrated by the fact that deregulation of PI3K-dependent cellular pathways is

INTRODUCTION

associated with several diseases, including cancer and diabetes (Wong, Engelman et al. 2009; Foukas and Withers 2010).

PI3Ks are classified into three classes (I, II and III) on the basis of their structural characteristics and substrate specificities (Table 2).

	Catalytic subunits		Regulatory subunits		Main product	Activated by
	Gene	Protein	Gene	Protein		
Class IA	<i>PIK3CA</i>	p110 α	<i>PIK3R1</i>	p85 α , p55 α , p50 α	PI(3,4,5)P ₃	RTKs
	<i>PI3KCB</i>	p100B	<i>PIK3R2</i>	p85B		
	<i>PI3KCD</i>	p100 δ	<i>PIK3R3</i>	p85 γ		
Class IB	<i>PIK3CG</i>	p100 γ	<i>PIK3R5</i>	p101	PI(3,4,5)P ₃	GPCRs
			<i>PIK3R6</i>	p84		
Class II	<i>PIK3C2A</i>	C2 α			PI(3,4)P ₂ and PI3P	Insulin receptor, GPCRs, TNFr
	<i>PIK3C2B</i>	C2B				
	<i>PIK3C2C</i>	C2 γ				
Class III	<i>PIK3C3</i>	VPS34	<i>PIKCR4</i>	VPS15	PI3P	Glucose, aminoacids

Table 2. List of genes, proteins, products and activators of the mammalian PI3K family. Adapted from (Okkenhaug 2013).

All isoenzymes possess a catalytic subunit with the so-called 'PI3K core', consisting of a C2 domain, a helical domain and a catalytic domain. Class I PI3K catalytic subunits form part of a dimer with one regulatory subunit, and they are further divided

into two subclasses: IA and IB. Class IA comprises three distinct catalytic subunits (p110 α , p110 β and p110 δ) which bind the p85 type of regulatory subunit, whereas p110 γ is the only catalytic subunit within the class IB subfamily (Vanhaesebroeck, Guillermet-Guibert et al. 2010). Class IA PI3Ks are mainly activated by tyrosine kinase receptors (RTKs), whereas class IB PI3Ks are mainly activated by G protein-coupled receptor (GPCRs). Class II PI3K are monomers, they do not possess regulatory subunits. Mammals possess three class II isoforms: PI3K-C2 α , PI3K-C2 β and PI3K-C2 γ . Different receptors, such as insulin receptor, GPCRs, and tumor necrosis factor family receptors (TNFr), have been reported to activate class II PI3Ks (Yang and Klionsky 2009; Falasca and Maffucci 2012). The class III PI3K hVps (human vacuolar protein sorting) 34 is a monomer, structurally it comprises the protein kinase Vps15 which associates with Vps34 that has been described as a regulatory protein (Backer 2008; Okkenhaug 2013). Emerging evidence suggests that distinct PI3Ks activate different signaling pathways, indicating that their functional roles are probably not redundant (Okkenhaug 2013). The main functional characteristics of each class of PI3Ks will be discussed below.

- **Class I PI3K**

In mammals, class I PI3Ks are present in all cell types, with p110 δ and p110 γ highly enriched in leukocytes (Kok, Geering et al. 2009). All the class I PI3K have in common that their preferred substrate is phosphatidylinositol 4,5-bisphosphate, PI(4,5)P₂, which is converted to phosphatidylinositol 3,4,5-trisphosphate, PI(3,4,5)P₃. The latter is the most studied PI3K effector and a very well established second messenger involved in many cellular

functions. It acts as membrane tether for the recruitment of signaling molecules that possess a plekstrin homology domain, namely Ser/Thr and Tyr protein kinases such protein kinase B (AKT) and Bruton's tyrosine kinase (BTK), respectively; adaptor proteins such as Grb2-associated binder 2 (GAB2); and regulators of small GTPases. AKT plays a central role in multiple signaling pathways involved in cell survival, cell metabolism and proliferation. This is the reason why PI3K signaling studies have mainly focused on AKT and its downstream targets (Vanhaesebroeck, Guillermet-Guibert et al. 2010). In many cell types including MΦ and DCs the PI3K-AKT axis is activated downstream of TLRs (Koyasu 2003). Several targets of AKT, including mammalian target of rapamycin complex 1 (mTORC1), glycogen synthase kinase 3 (GSK3) and Forkhead box transcription factors (FOXO) have been identified to play pivotal roles in controlling the inflammatory response downstream of AKT (Ohtani, Nagai et al. 2008; Brown, Wang et al.). Recently, an additional mechanism of negative TLR regulation by PI3K was identified. The p100δ isoform contributes to negative regulation of TLR signaling by modulation of the “topology” and compartmentalization of TLR4 through depletion of local PI(4,5)P₂ (Aksoy, Taboubi et al. 2012).

- **Class II PI3K**

Class II PI3Ks are monomers of high molecular mass. They are the less studied and characterized PI3Ks. Although it is generally well accepted that class II PI3Ks do not catalyze the synthesis of PI(3,4,5)P₃, a general consensus of the specific lipid product(s) generated by these enzymes has not yet been reached. *In vitro*

studies showed that class II PI3Ks can generate both PI3P (phosphatidylinositol 3-phosphate) and PI(3,4)P₂, but some reports have simply assumed that the enzymes generate PI(3,4)P₂ without directly demonstrating it (Falasca and Maffucci 2012). Class II PI3Ks are involved in intracellular membrane trafficking, endocytosis, exocytosis (Falasca and Maffucci 2012) and autophagy (Devereaux, Dall'Armi et al. 2013). Loss of the *PiK3C2A* gene encoding C2 α catalytic subunit in the mouse has been reported to cause early embryonic lethality, initially ascribed to defective vasculogenesis (Yoshioka, Yoshida et al.), and more recently also to defects primary cilium organization (Franco, Gulluni et al. 2014).

- **Class III PI3K**

Class III PI3K Vps34 is the only PI3K that is evolutionarily conserved from yeast to mammals (Engelman, Luo et al. 2006). Vps34 phosphorylates phosphatidylinositol to generate PI3P, which is the most abundant of the phosphoinositides and which acts as a docking site for proteins that contain PX (for the Phox homology domain of the p47*phox* and p40*phox* subunits of the phagocyte NADPH oxidase) or FYVE (zinc-finger domains named for the first four proteins known to contain the domain: Fab1p, YOTB, Vac1p, EEA1) domains (Backer 2008). Vps34 was originally identified as a kinase required for protein sorting to the lysosome-like vacuole in yeast (Schu, Takegawa et al. 1993), and was subsequently shown to also control endocytosis, phagocytosis, and autophagy in various cell types (Simonsen, Wurmser et al. 2001). In this regard, it was demonstrated that Vps34 inhibitors impair autophagy and that the exogenous addition of PI3P increases the rate of autophagy in

mammalian cells, providing evidence for a role for PI3P in this process (Petiot, Ogier-Denis et al. 2000). Later studies showed that germ-line loss of Vps34 leads to embryonic lethality (Zhou, Takatoh et al. 2011), whereas a conditional loss-of function mouse model of Vps34 in mouse embryonic fibroblasts, liver and heart revealed its essential role in regulating autophagy, indispensable for heart and liver function (Jaber, Dou et al. 2012). The complexity of Vps34 biology could be due in part to its ability to associate with other proteins and form multiple complexes. In autophagy, Vps34 forms part of a key complex required for the initial steps of autophagosome formation (This information is extended in Introduction section 4.1.3 “PI3Ks and autophagy”).

2.2. NOD-Like Receptors (NLRs) and inflammasome

Although the key function of TLRs in innate immunity is evident and supported by a dense literature, certain observations had indicated the possibility that all features of the host response to pathogens could not be accounted for by TLRs alone. The initial evidence came with the observation that only an invasive form of the enteric bacterium *Shigella flexneri* triggers the activation of the transcription factor NF- κ B pathway in cultured epithelial cells (Philpott, Yamaoka et al. 2000). Subsequent studies demonstrated that the protein nucleotide-binding oligomerization domain 1 (NOD1) is responsible for the NF- κ B-dependent response of epithelial cells to *Shigella in vitro* (Girardin, Tournebize et al. 2001).

NOD1 is the founding member of the so-called NOD-like receptor (NLR) family. NLRs are PRRs that detect the presence of PAMPs and endogenous molecules in the cytosol. In their structure, all NLRs contain a central NACHT (named for its presence in NAIP, CIITA, HET-E and telomerase-associated protein) domain that facilitates oligomerization, and bear multiple LLRs on their C-terminal site for ligand sensing (Figure 5).

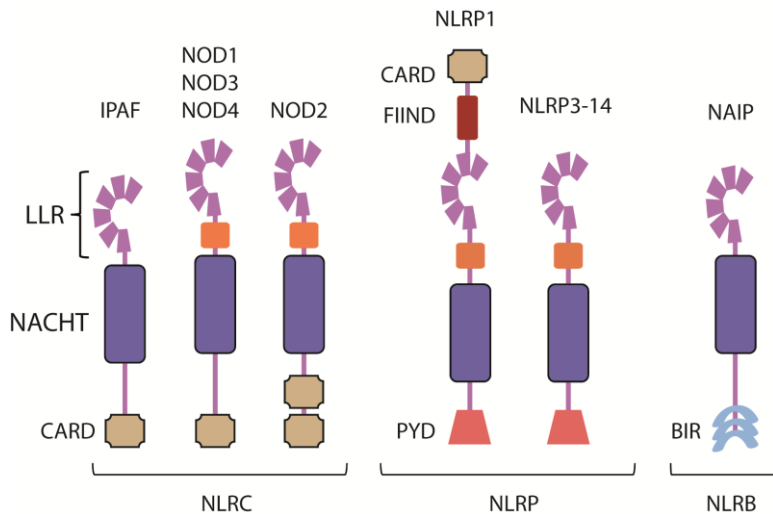


Figure 5. Domain structure of several NLRs. Abbreviations: BIR, baculoviral inhibitor of apoptosis repeat; CARD, caspase-recruitment domain; FIIND, domain with function to find; IPAF, interleukin 1 β -converting enzyme protease-activating factor; LLR, leucine rich repeat; NACHT (domain present in NAIP, CIITA, HET-E and telomerase-associated protein); NAIP, neuronal apoptosis inhibitor protein; PYD, pyrin domain. Adapted from (Martinon, Mayor et al. 2009).

The 23 human NLRs can be distinguished into different subfamilies by their N-terminal effector domains that bestow unique functional characteristics to each NLR (Werts, Girardin et al. 2006). N-terminal caspase activation and recruitment domain (CARD) distinguishes the NLRC (C for CARD, NLRC 1-5) subfamily and allows direct interaction between members of this family and other CARD carrying adaptor proteins. Among these, NOD1 and

NOD2, are key sensors of bacterial peptidoglycan and are crucial for tissue homeostasis and host defense against bacterial pathogens (Franchi, Warner et al. 2009). Once activated, NOD1 and NOD2 oligomerize and drive the activation of MAPKs and NF- κ B via interaction with serine-threonine kinase RICK (also called RIPK2, receptor-interacting serine-threonine kinase) and activation of TGF- β activated kinase (TAK1); as well as type I interferon responses (Philpott, Sorbara et al. 2013). Therefore, NOD1, NOD2, and TLR signaling converge to common pathways. A reasonable purpose for having multiple PRRs which induce overlapping signaling pathways is to increase the sensitivity for pathogen detection and to potentiate the cellular response. Consistently, there is extensive evidence that NOD1 and NOD2 agonists synergize with TLR ligands to produce proinflammatory cytokines and anti-microbial molecules (Franchi, Warner et al. 2009).

A second subclass, the members of the pyrin domain containing NLRP (P for pyrin) subfamily (NLRP 1-14), are best known for their role in inducing the formation of the inflammatory complex inflammasome. Inflammasome complex are assembled by self-oligomerizing scaffold proteins, NLR proteins that are capable of forming an inflammasome include: NLRP1, NLRP3, NLRP6, NLRP7, NLRP12, NLRC4 and NAIP (Barbe, Douglas et al.).

Inflammasomes are molecular platforms activated upon cellular infection or stress that in most cases can trigger activation of the enzyme caspase-1. One of the consequences of caspase-1 activation is the promotion of cleavage and secretion of IL-1 β and IL-18, potent pro-inflammatory cytokines (Martinon, Burns et al. 2002). IL-1 β and IL-18 are synthesized as a pro-forms and their

secretion requires two steps, induction and processing, which are independently regulated by separate classes of PRRs and intracellular pathways (**Figure 6**). Thus, the canonical model of inflammasome activation leading to IL-1 β and IL-18 production involves “signal 1” which is often induced by TLR stimulation and that induces transcriptional up-regulation of pro-IL-1 β and pro-IL-18. A second signal, “signal 2”, involves inflammasome mediated caspase cleavage of pro-IL-1 β and pro-IL-18 into their mature forms (Davis, Wen et al. 2011). Although “signal 2” has been described mainly mediated by caspase-1 cleavage, recently mouse caspase-11 (and homologous human caspase-4) an understudied pro-inflammatory caspase, has taken center stage in responses to Gram-negative bacteria. This has stemmed from the evidence that mice lacking caspase-11 fail to produce active caspase-1 and IL-1 β leading to an increased resistance to endotoxic shock induced by bacterial toxins (Kayagaki, Warming et al. 2011). Active caspase-11 co-operates with components of the NLRP3 inflammasome to induce caspase-1-dependent maturation of pro-IL-1 β and pro-IL-18. TLR4/TRIF-mediated type-I-IFN production is essential for caspase-11 activity (Broz and Monack 2013) (**Figure 6**).

In 2013, Hagar et al. and Kayagaki et al. modified the conception of this canonical inflammasome activation model by demonstrating that LPS from Gram-negative bacteria (a TLR4 ligand) could directly activate caspase-11 intracellularly without the need of TLR4 or other PRRs (**Figure 6**). These findings established a novel proinflammatory TLR4-MyD88-TRIF-independent response triggered by LPS (Kayagaki, Warming et al. 2011; Hagar, Powell et al. 2013). Thus reinforcing the emerging topic in antimicrobial defense that multiple sensors recognize the

same microbial product in a way that is specific to different cellular compartments.

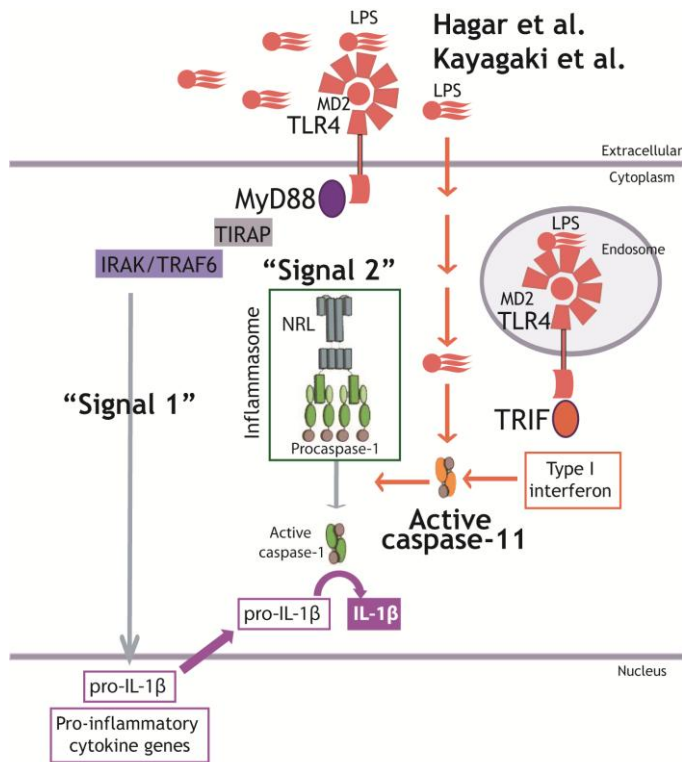


Figure 6. Inflammasome activation and IL-1 β processing. Schematic diagram of the canonical inflammasome activation (“Signal 1” and “Signal 2”), the involvement caspase-11 in inflammasome activation and the novel proinflammatory response TLR4-MyD88-TRIF-independent triggered by LPS (Hagar, Powell et al. 2013). Adapted from (Rathinam and Fitzgerald).

Under certain conditions, activation of inflammasomes and thus activation of inflammatory caspases leads to a particular type of programmed cell death termed pyroptosis. Pyroptosis (from the Greek “pyro”-fire and “ptosis”-fallin, death) is a highly inflammatory caspase 1-dependent cell death, in which inflammation is a key feature distinguishing it from silent apoptosis death. Pyroptosis frequently occurs upon infection with

intracellular pathogens. The mechanisms that direct caspase-1-mediated cell death versus cytokine maturation remain to be determined (Thornberry, Bull et al. 1992; Schroder and Tschopp 2010; Skeldon and Saleh 2011).

2.3. Scavenger Receptors (SRs)

SRs are a huge family of molecules firstly defined by their ability to recognize modified lipoproteins (Brown and Goldstein 1979). It is now appreciated that the range of ligands that they recognize is extremely diverse, including endogenous (e.g. collagen or thrombospondin), modified host-derived molecules (e.g. oxidized or acetylated LDL, apoptotic cells) as well as exogenous molecules (e.g. PAMPs: LPS, LTA) (Greaves and Gordon 2009). Based on their broad ligand-binding specificities and expression in M Φ , Dr. Krieger and colleagues proposed that SRs could serve as PRRs (Krieger 1997).

Since their initial discovery in 1979, a variety of proteins have been included in the SR family. At present, SRs are divided in ten classes (A-J) according to their structural features (**Figure 7**). Most SR are multidomained proteins, and in fact, no common domain has been identified that confers scavenger activity (Prabhudas, Bowdish et al. 2014). However, the receptor surfaces that are engaged in ligand binding share a high degree of similarity in terms of shape and charge distribution, displaying clusters of cationic residues that are in general centrally located linked by anionic patches. The electrostatic patch model helps to explain the

preference of SRs for polyanionic ligands; however, the precise structural determinants of the ligands themselves are less clear (Canton, Neculai et al. 2013).

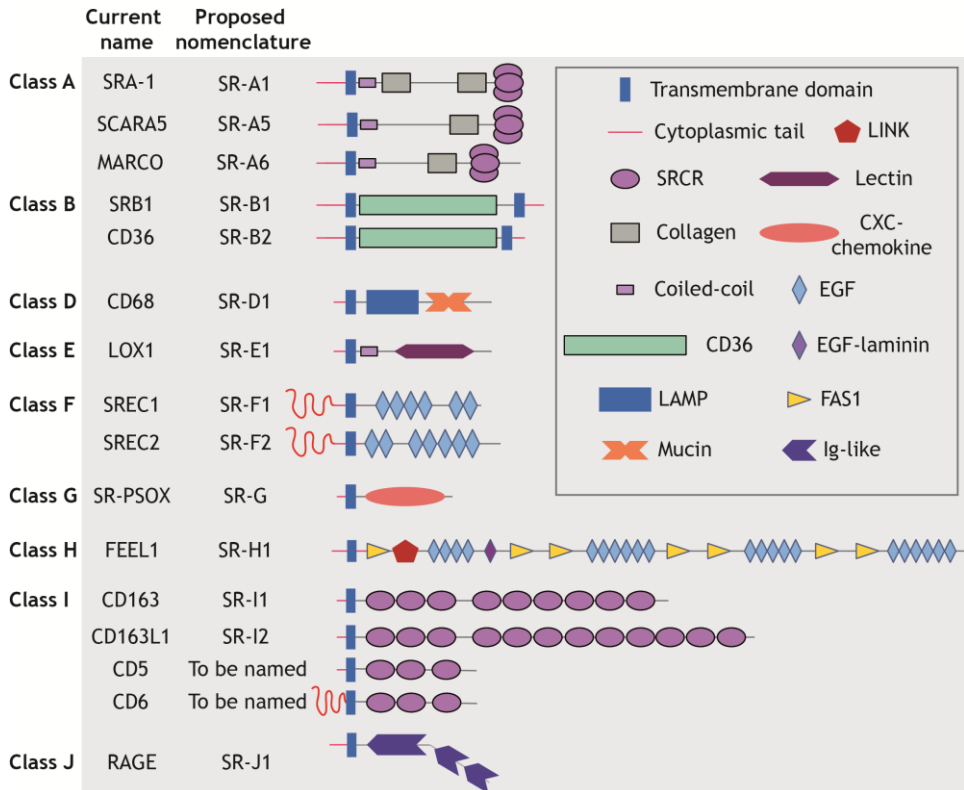


Figure 7. Domain architecture of SRs. Figure represents notorious members of the ten classes of SRs (the class C is not listed as it is only present in *Drosophila melanogaster*). Figure shows classical as well as recently proposed nomenclature and domain architecture of each receptor. Abbreviations: EGF, epidermal growth factor; EGF-laminin, laminin-type EGF-like; FAS1, fasciclin 1; FEEL1, fasciclin EGF-like laminin-type EGF-like and link domain-containing scavenger receptor 1 ; LAMP, lysosome-associated membrane glycoprotein; LINK, link domain-containing scavenger receptor 1; LOX1, lectin-like oxidized LDL receptor 1; MARCO, macrophage receptor with collagenous structure; RAGE, receptor for advanced glycation endproducts; SR-PSOX, scavenger receptor for phosphatidylserine and oxidized low-density lipoprotein; SCARA5, scavenger receptor class A member 5; SRCL, scavenger receptor with C-type lectin (also known as SCARA4 and CLP1); SREC, scavenger receptor expressed by endothelial cells; SRCR, scavenger receptor cysteine-rich domain. Figure adapted from (Canton, Neculai et al. 2013).

Among the different classes of SRs, the presence of the scavenger receptor cysteine-rich (SRCR) domain is the common

feature of a superfamily of proteins so-called SRCR superfamily (SRCR-SF), which is an ancient and highly conserved family of receptors. SRCR-SF members are closely related from the structural point of view. They are characterized by the presence a single SRCR domain, tandem SRCR domain repeats or SRCR domain as part of multidomain mosaic proteins (in combination with e.g. epidermal growth factor, serine protein, collagenous regions, or other domains) (**Figure 8**). The SRCR domain consists of 90 to 110 amino acid residues containing 6-8 cysteines with a well conserved disulfide bond pattern (Resnick, Pearson et al. 1994; Sarrias, Gronlund et al. 2004). Depending on the characteristics of their SRCR domains, two types of SRCR-SF members are reported: those with type A domains, which are encoded by at least two exons and contain six cysteine residues, and those with type B domains, encoded by a single exon and containing eight cysteine residues. There are, however, some exceptions: for instance SR-AIII that presents truncated SRCR domains containing four cysteines (Rohrer et al., 1990).

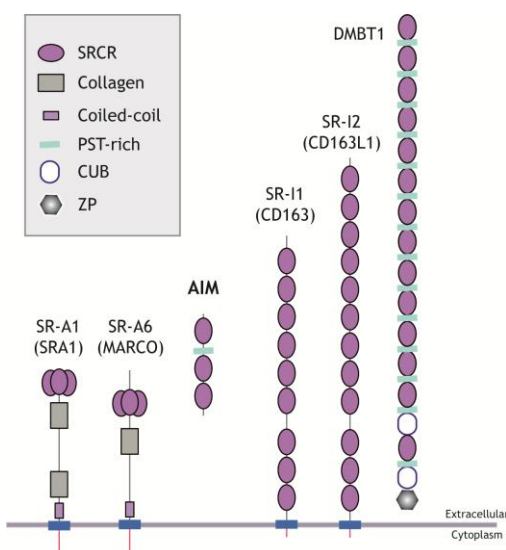


Figure 8. SRCR proteins expressed by MΦ. Abbreviations: AIM, apoptosis inhibitor of MΦ; CUB, complement C1r/C1s-Uegf-Bmp1; DMBT1, deleted in malignant brain tumors 1; MARCO, macrophage receptor with collagenous structure; PST-rich, proline-serine-theonine-rich; SR, scavenger receptor; SRCR, scavenger receptor cysteine rich; ZP, zona pellucida.

The overall function of SRs is to identify and remove unwanted entities, but now is accepted that SRs are involved as well in a broad range of complex functions such as antigen presentation, phagocytosis, lipid transport and the clearance of apoptotic cells (Canton, Neculai et al. 2013).

Accumulating evidences show that SRs participates in innate immunity to pathogens and macrophage regulation (Peiser and Gordon 2001). In addition to scavenging modified lipoproteins, many of the SRs have the ability to recognize conserved PAMPs on microbial surfaces and participate in the phagocytosis and clearance of various microbial species (Pluddemann, Mukhopadhyay et al. 2011). SRs have been shown to interact with and to influence signaling pathways by itself or through other PRRs. A typical case of SRs that have discernible signaling motifs is CD36 (one of the most extensively studied SRs), CD36 C-terminal intra-cytoplasmatic tail is thought to be the site of signal transduction, and indeed it associates with SRC family kinases (Huang, Bolen et al. 1991; Bull, Brickell et al. 1994; Rahaman, Lennon et al. 2006). SRs could also function as components of heteromultimeric signaling complexes, in which a particular receptor may form various types of complexes with different co-receptors, in different cell types but also in single cell type. Some examples of a synergistic relationship between SRs and other PRRs are SR-A1 interaction with TLR4 to promote *E. coli* phagocytosis (Amiel, Alonso et al. 2009) or cooperation between MARCO and TLR2 and CD14 for *M. tuberculosis* recognition (Bowdish, Sakamoto et al. 2009). It was recently highlighted that SRs also rely on the formation of multimolecular complexes to achieve their ligand-internalization function. Internalization of their ligands can alter

the mode of signaling or terminate it, and can also have metabolic functions (Heit, Kim et al. 2013). Regarding the participation of SRs in M Φ regulation, it is now extensively accepted that they also contribute to the functional phenotype of polarized M Φ . SRs are more prominently expressed by M2 M Φ which is congruent with the function of M2 cells in apoptotic cell clearance and in the suppression of inflammation, but they are not exclusive to this M Φ population and can contribute to pro-inflammatory macrophage responses in certain contexts or as a part of complex signaling platforms (Canton, Neculai et al. 2013). This is well illustrated by CD36: the net amount of this receptor increases in M2 M Φ , which suggests that it has an anti-inflammatory function; however, CD36 is also present in M1 cells in which it can interact with TLRs to produce pro-inflammatory cytokines in response to microbial ligands (Triantafilou, Gamper et al. 2006).

- **CD36**

CD36 is an 88-kDa transmembrane glycoprotein expressed in a wide variety of cell types, such as the microvascular endothelium; "professional" phagocytes including M Φ , dendritic cells, microglia; retinal pigment epithelium, erythroid precursors, hepatocytes, adipocytes, cardiac and skeletal myocytes, and specialized epithelia of the breast, kidney, and gut (Silverstein and Febbraio 2009).

CD36 is a cellular receptor for modified lipoproteins (e.g. oxidized low-density lipoprotein). The very first observations of the capacity of CD36 to bind and endocytose oxidized low-density lipoprotein (oxLDL) are linked to research by Endemann et al.

using a human epithelial kidney cell line (HEK293) transfected with CD36, they showed the capacity of the SR to bind specifically to oxLDL (Endemann, Stanton et al. 1993). At present, extensive evidence corroborates these findings. In fact, the capacity of CD36 to facilitate cholesterol accumulation in macrophages links this receptor to the initiation and perpetuation of atherosclerosis (Silverstein 2009; Silverstein, Li et al. 2010). Also, CD36 is intimately involved in the regulation of fatty acid uptake across the plasma membrane and the subsequent metabolism of this substrate (Coburn, Hajri et al. 2001; Ibrahimi and Abumrad 2002). Thus, it has been proposed that CD36 expression or function influences susceptibility to certain metabolic diseases, such as obesity, insulin resistance, and fatty liver disease (Coburn, Hajri et al. 2001; He, Lee et al. 2011; Kennedy and Kashyap 2011; Armengol, Bartoli et al. 2013).

In phagocytes, CD36 is also involved in phagocytosis and inflammation in response to pathogen aggression (Hoebe, Georgel et al. 2005; Stuart, Deng et al. 2005; Means, Mylonakis et al. 2009). For example, CD36-deficient mice are more susceptible to infection with *S. aureus* compared with WT mice, thereby demonstrating that CD36 is required for the defense against this bacterial pathogen (Hoebe, Georgel et al. 2005; Stuart, Deng et al. 2005). By analogy with membrane protein CD14, it has been suggested that CD36 functions as an accessory protein to present bacterial as well as modified host proteins to some TLRs. This notion is based on the findings that, depending on the ligand, TLR2 and TLR4 require CD36 as co-receptor (Abe, Shimamura et al. 2010; Hoebe, Georgel et al. 2005; Triantafilou, Gamper et al.

2006; Jimenez-Dalmaroni, Xiao et al. 2009; Seimon, Nadolski et al. 2010).

Accumulating evidence shows that CD36 recognizes many types of ligands including thrombospondin (Asch, Barnwell et al. 1987), *Plasmodium falciparum* (Barnwell, Asch et al. 1989; Ockenhouse, Tandon et al. 1989), bacterial cell wall components (Hoebe, Georgel et al. 2005), phosphatidyl serine and oxidized phosphatidylserine that are expressed on the surface of apoptotic cells (Mikolajczyk, Skrzeczynska-Moncznik et al. 2009), among others. The multivariate ligand recognition of CD36 allows it to exert several functions, depending on the cell type. Recently, mouse protein Apoptosis Inhibitor of M Φ (mAIM) has been identified as a novel CD36 ligand. Both *in vitro* and *in vivo* evidences support the finding that mAIM is incorporated into adipocytes through CD36-mediated endocytosis (Kurokawa, Arai et al. 2010; Iwamura, Mori et al. 2012). Incorporation of mAIM to adipocytes is drastically decreased in the presence of CD36-neutralizing antibody. Indeed, *in vivo* AIM incorporation is markedly less in CD36 $-/-$ mice compared with wild-type mice upon intravenously mAIM injection (Kurokawa, Arai et al. 2010). In fact, mAIM also gets internalized into M Φ through CD36, suggesting this may serve as its cellular receptor for endocytosis (Kurokawa, Arai et al. 2010; Miyazaki, Kurokawa et al. 2011). In line with these findings, our group demonstrated that in M Φ AIM increases CD36-mediated oxLDL uptake, suggesting that AIM may serve as a soluble protein that transfers oxLDL to CD36 (Amezaga, Sanjurjo et al. 2013). These results suggested that CD36 may function as a cellular receptor for AIM.

3. Apoptosis Inhibitor of Macrophages (AIM)

Among the SRs, the central protein studied in the present work is the scavenger protein AIM, also called soluble protein alpha (Sp α), CD5-like (CD5L) protein and apoptosis inhibitor-6 (Api-6). In this work we will distinguish the data reported for to human (hAIM) to that for mouse (mAIM) and when we refer globally to both of them we will do it as AIM. AIM comprises three SRCR domains and belongs to the group B of SRCR-SF. Is a ~37-kDa glycoprotein secreted by tissue M Φ under inflammatory conditions (Gebe, Kiener et al. 1997; Gebe, Llewellyn et al. 2000).

3.1. Cloning of AIM

In 1997 Gebe et. al. reported the cloning of a cDNA encoding human AIM (formerly called Sp α). They identified RNA transcripts encoding hAIM in bone marrow, spleen, lymph node, thymus, and fetal liver but not in non-lymphoid tissues. In cell binding studies using a hAIM-immunoglobulin (hAIM-mIg) fusion protein they showed that it is capable of binding to peripheral blood monocytes but not to T or B cells. So they presented hAIM as a novel secreted protein produced in lymphoid tissues that may regulate monocyte activation, function, and/or survival (Gebe, Kiener et al. 1997). Two years later Toru Miyazaki group reported the cloning of a novel murine macrophage secreted protein which inhibits apoptosis, and they termed it AIM (mAIM), for Apoptosis Inhibitor expressed by M Φ (Miyazaki, Hirokami et al. 1999). Characterization of both proteins revealed that AIM protein

sequence consists of a N-terminal secretory signal followed by three C-terminal SRCR domains; it closely resembles that of extracellular region of the lymphocyte receptors CD5 and CD6 (48.3/23.1% and 52.1/27.3% similarity/identity, respectively). However, AIM displays higher sequence homology with fellow group B members T19/WC1 and SRI1/CD163 (Gebe, Llewellyn et al. 2000) (64/39.3% and 60.9/37.2% similarity/identity, respectively). Although human and mouse AIM homologues share a high level of sequence homology (70%) and their predicted sizes from amino acid sequences are similar (37 kDa), both were detected in serum at different molecular weights that are attributable to different post-transductional modifications. In this regard, two forms of the human protein were defined at 38 and 40 kDa resulting for different sialic acid content (**Figure 9**). Accordingly, the primary sequence of hAIM contains a potential region of O-linked glycosylation in a Pro-Ser-Thr-rich polypeptide (PST) separating SRCR domains 1 and 2 (Sarrias, Padilla et al. 2004). Whereas hAIM contains no N-linked glycans, mAIM sequence presents four putative N-glycosylation sites and two of them were verified to bind N-glycans. Therefore, those post traductional modifications can explain the observed larger molecular weight (55kDa) than predicted from its aminoacid sequence (37 kDa) (Gebe, Llewellyn et al. 2000; Mori, Kimura et al. 2012).

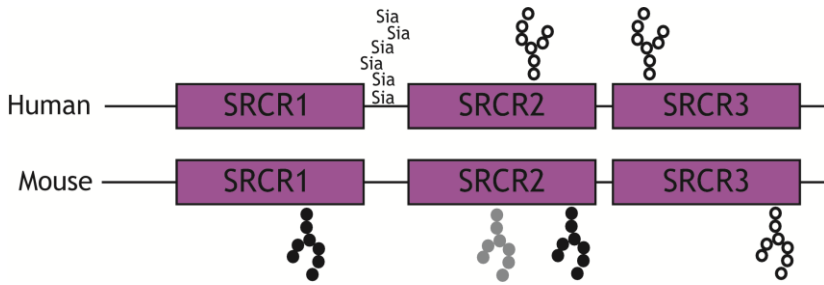


Figure 9. AIM glycosylation sites. Potential N-glycosylation sites (asparagine-X-serine/threonine, NXS/T) (branches) and O-glycosylation sites (Sia, Sialic acid) along the human and murine AIM aminoacid sequences. Filled branch: N-glycan detected by PNGase treatment. Gray branch: N-glycan detected depending of the mice strain (only in FVB/N and BALB/c). Open branch: potential N-glycosylation but not N-glycan detected by PNGase treatment. Figure adapted from (Mori, Kimura et al. 2012).

It has been recurrently hypothesized that differences in glycosylation patterns between human and mice proteins may result in distinct activities. In this regard, a recent publication confirmed the relevance of glycosylation in mAIM function, by reporting that mutation of two N-glycosylation sites in mAIM protein affects its secretion and enhances its lipolytic activity in adipocytes (Mori, Kimura et al. 2012).

3.2. Regulation

Mouse experimental models revealed that mAIM is synthesized in tissue M Φ and upregulated under inflammatory conditions such as fulminant hepatitis (Haruta, Kato et al. 2001), *Cryptosporidium parvum* injection (Kuwata, Watanabe et al. 2003), atherosclerotic lesions (Arai, Shelton et al. 2005), *Listeria monocytogenes* infection (Joseph, Bradley et al. 2004), obese conditions (Kurokawa, Arai et al. 2010) and exposure to conserved

microbial cell wall components (Martinez, Escoda-Ferran et al. 2014). In contrast to tissue M Φ , *in vitro* cultured M Φ do not express AIM. mAIM expression disappears completely from freshly isolated thioglycollate-activated peritoneal M Φ after 16 hours of culture in plastic dishes, and its expression could not be re-induced by PMA, LPS, INF or interleukins (Miyazaki, Hirokami et al. 1999; Joseph, Bradley et al. 2004). These data suggested that cell interactions in tissue might be necessary for mAIM gene expression. Our results indicated that in cultured human monocyte-derived macrophages (HMDM) hAIM mRNA and protein expression can be induced by maturation with macrophage colony-stimulating factor (M-CSF) or with granulocyte macrophage colony-stimulating factor (GM-CSF). These data reinforced the notion that AIM expression is tightly regulated (Amezaga 2013; Amezaga, Sanjurjo et al. 2013).

Regulation of AIM expression is controlled by the transcription factors of the nuclear receptor family liver X receptor/ retinoid X receptor (LXR/RXR) heterodimers (Joseph, Bradley et al. 2004). LXR/RXR receptors are cholesterol-sensing receptors that have emerged as key regulators of lipidic metabolism and transport. LXR/RXR also regulates inflammatory responses, providing a link between metabolism and inflammation in M Φ . They were identified as potential targets for the treatment of Alzheimer disease, rheumatoid arthritis or asthma (Kiss, Czimmerer et al. 2013).

AIM expression is induced through LXR/RXR activation by its natural ligands, either exogenous (oxLDL) or endogenous (25-hydroxycholesterol, produced by cholesterol-25-hydroxylase

enzyme) or by the synthetic LXR/RXR ligands (T1317, 9cRA, GW3965) (Figure 10) (Joseph, Bradley et al. 2004; Valledor, Hsu et al. 2004; Zou, Garifulin et al. 2011; Amezaga, Sanjurjo et al. 2013). Two different transcription factors expressed in a high level in MΦ and upregulated by LXR/RXR activation also participates in AIM regulation. Sterol regulatory element binding protein (SREBP-1), that connects lipidic metabolism with diverse physiologic responses (Repa, Liang et al. 2000; Im and Osborne 2012) and MafB, that induces myelomonocytic differentiation and has recently been associated with atherogenesis (Hamada, Nakamura et al. 2014).

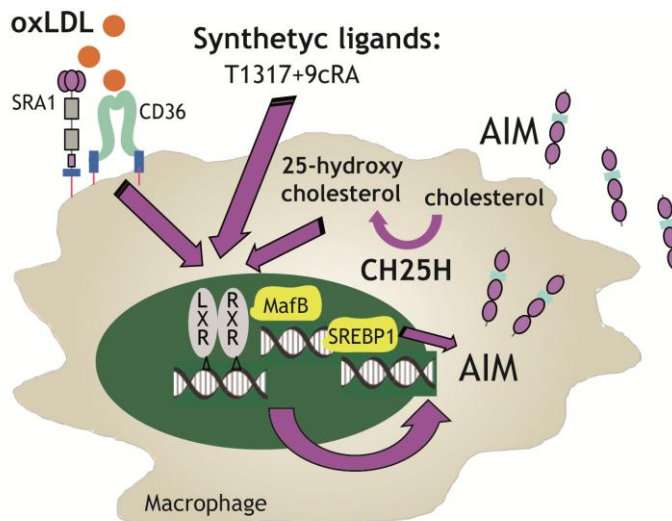


Figure 10. Regulation of AIM expression by LXR/RXR ligands and transcription factors involved. Abbreviations: CH25H, cholesterol-25-hydroxylase; MafB, LXR/RXR, liver X receptor/ retinoid X receptor ;OxLDL, oxidized low-density lipoprotein; SREBP-1, sterol regulatory element binding protein.

3.3. Presence in serum

AIM is detected in serum in relatively high amounts ($\mu\text{g}/\text{mL}$ range) where it circulates associated to IgM (Tissot, Sanchez et al. 2002; Sarrias, Padilla et al. 2004). This interaction allows mAIM to modulated IgM homeostasis by contributing to autoantibody production under obese conditions (Arai, Maehara et al. 2013). It is well known that obesity in humans often increases the serum levels of multiple autoantibodies causing autoimmune diseases. Among them, pathogenic immunoglobulin (Ig) G antibodies, including a unique profile of autoantibodies, have been found in obese humans and mice (Winer, Winer et al. 2011). In these settings AIM-IgM association inhibits IgM binding and internalization by follicular dendritic cells, preventing an IgM-dependent auto-antigen presentation to B cells, that would stimulate IgG autoantibody production (Arai, Maehara et al. 2013). Therefore, the AIM-IgM interaction may play an important role in obesity-associated autoimmune processes. It has been recently found that in turn, the AIM-IgM interaction protects AIM from renal excretion and thus maintains relatively high circulating concentrations ($\sim 2.5\text{--}10 \mu\text{g}/\text{mL}$) (Kai, Yamazaki et al. 2014).

Different plasma/serum proteomic studies (**Table 3**) have founded hAIM protein differentially expressed in several conditions that arise in an inflammatory background, highlighting its potential as a plasmatic biomarker.

Disease	Origin of samples	Discovery	Comparison	AIM	Validation	AIM presumed function	References
Atshma	BALF	SDS-PAGE and MS	Asthmatic (n: 4) Vs healthy (n: 3). 24h after segmental allergen challenge	↑	X	X	(Wu, Kobayashi et al. 2005)
Liver cirrhosis in HCV infection	Serum	2D-PAGE and MS	Cirrhorrhic (n:6) Vs mild fibrosis (n:3) patients	↑	X	Immune response to HCV infection	(Gangadharan, Antrobus et al. 2007)
Liver cirrhosis and HCC in fatty liver disease	Serum	2D-PAGE and MS	Cirrhotic (n:5) and HCC (n:5) Vs pre-cirrhotic (n:5)	↑	Serum ELISA Steatohepatitis patients With and without cirrhosis (n: 113). AIM mRNA expression in liver tissues NAFLD (n:21) Vs normal liver (n:13)	Anti-apoptotic role, supporting hepatocyte regeneration	(Gray, Chattopadhyay et al. 2009)
HCC in HCV infection	Serum	2D-PAGE and MS	HCV-HCC (n:5) Vs HCV-cirrhotic (n:7)	↑	X	Immune response to HCV infection	(Sarvari, Mojtahedi et al. 2013)
Chronic liver disease due to HCV infection	Serum	ELISA	Advanced hepatic fibrosis among different stages of liver damage (n:77)	↑	X	X	(Mera, Uto et al. 2014)
Atopic dermatitis	Plasma	2D-PAGE and MS	Children with AD (n:8) Vs healthy children (n:8)	↑	WB of plasma AD (n:6) and healthy (n:6)	Antiapoptotic role. Promoting eosinophilia	(Kim, Hwang et al. 2008)
Kawasaki disease	Serum	2D-PAGE and MS	KD patients (n:10) Vs febrile controls (n:10)	↑	X	Antiapoptotic role. Dysregulation of apoptosis in coronary artery lesions	(Yu, Kuo et al. 2009)
Turner syndrome	Plasma	2D-PAGE and MS	Pregnant women: TS (n:10) Vs healthy (n:10) fetuses	↑	X	X	(Koliateli, Anagnostopoulos et al. 2010)
CLI in diabetic patients	Plasma	2D-DIGE and MS	Diabetic patients with hemodialysis CLI (n:10) Vs non CLI (n:10)	↑	X	X	(Hung, Chen et al. 2011)
Pulmonary TB	Serum	iTRAQ-2DLC-MS	TB (n:10) Vs healthy (n:10)	↑	WB and ELISA (n:132) of serum samples	Macrophage recognition of Mtb	(Xu, Deng et al. 2013)
Osteoarthritis	Synovial fluid of affected knees	iTRAQ-2DLC-MS	Osteoarthritic (n:10) Vs rheumatoid arthritic (n:10)	↑	X	X	(Balakrishnan, Bhattacharjee et al. 2014)
Extreme physical stress	Plasma	2DE and MS	8 healthy men who completed the "spartatlon" in less than 36h. Prior the race start (Phase I), after the end (Phase II), recovery period (Phase III). II Vs I and III Vs I.	↓	X	Antiapoptotic role. Preventing stress-induced apoptosis.	(Balfoussi, Skenderi et al. 2013)

Table 3. Please see table legend on next page

Table 3: Role of hAIM as a biomarker. List of proteomic studies where hAIM was found differentially expressed. Abbreviations: 2DE, two-dimensional electrophoresis; 2D-DIGE, two-dimensional difference gel electrophoresis; 2DLC, two-dimensional liquid chromatography; 2D-PAGE, two-dimensional polyacrylamide gel electrophoresis; AD, atopic dermatitis; BALF, bronchoalveolar lavage fluid; CLI, critical limb ischemia; ELISA, enzyme-Linked ImmunoSorbent assay; HCC, hepatocarcinoma; HCV, hepatitis C virus; iTRAC, isobaric tag for relative and absolute quantization; KD, Kawasaki disease; MS, mass spectrometry; Mtb, *Mycobacterium tuberculosis*; SDS-PAGE, sodium dodecyl sulfate polyacrylamide gel electrophoresis; TB, tuberculosis; TS, Turner syndrome; WB, western blot.

3.4. Role of AIM

AIM has been implicated in a wide spectrum of biological functions by modulating the activity of M Φ and other cell types, thereby participating in the pathogenesis of several infectious and inflammatory processes. The discovery of most of its important functions and characteristics has been achieved using mouse models.

3.4.1. Antiapoptotic Role

Apoptosis is a programmed form of cell death generally characterized by distinct morphological characteristics and energy-dependent biochemical mechanisms. It is considered a vital component of various processes, and inappropriate apoptosis is a factor in many human conditions including neurodegenerative diseases, ischemic damage, autoimmune disorders and many types of cancer (Elmore 2007).

In 1999, AIM's "parents" chose its name including the antiapoptotic concept on it based on *in vivo* and *in vitro* evidences: in AIM-deficient mice before thymic selection CD4/CD8

double-positive (DP) thymocytes were more susceptible to apoptosis induced by both dexamethasone and irradiation. *In vitro*, recombinant mAIM (rmAIM) protein significantly inhibited cell death of DP thymocytes as well as reduced CD95/Fas-crosslinking-mediated apoptosis of the monocyte-derived cell line J774A.1 (Miyazaki, Hirokami et al. 1999). Shortly afterwards, using also rmAIM they showed an AIM-dependent inhibition of proliferation induced by LPS in combination with TGF- β in B lymphocytes (Yusa, Ohnishi et al. 1999). The authors suggested for the first time, that AIM may exhibit different functions depending on the target cell types and/or on the combination with other cytokines.

Later, the antiapoptotic function of mAIM was corroborated in the AIM-/- KO model, when challenged with heat-killed *Corynebacterium parvum* also showed a reduction of T and NKT cells within liver granulomas compared with WT mice (Kuwata, Watanabe et al. 2003), suggesting that these cell types were rescued from apoptosis by mAIM. These results were confirmed demonstrating that rmAIM addition significantly inhibited apoptosis of NKT and T cells obtained from *C. parvum* stimulated livers *in vitro* (Kuwata, Watanabe et al. 2003).

In line with the previous findings, mouse AIM also contributes to protect M Φ against apoptosis mediated by different pathogens, namely, *Bacillus anthracis*, *Escherichia coli*, *Salmonella typhimurium* and *Listeria monocytogenes* (Joseph, Bradley et al. 2004; Valledor, Hsu et al. 2004; Zou, Garifulin et al. 2011). Moreover, both in human and mice M Φ AIM was identified as a factor that protects from the apoptotic effects of diverse

agents such as anisomycin (Valledor, Hsu et al. 2004), cycloheximide (Amezaga, Sanjurjo et al. 2013), and oxidized lipids (Arai, Shelton et al. 2005; Amezaga, Sanjurjo et al. 2013), the latter facilitating the progression of atherosclerotic disease (see below).

Under different experimental settings, in a mice model overexpressing AIM (Haruta, Kato et al. 2001), the authors linked its antiapoptotic role with increased numbers of liver infiltrating M Φ in response to fulminant hepatitis. In this work the authors also showed that mAIM promotes M Φ phagocytosis, and thus hypothesized that AIM-dependent support of survival and phagocytic activity of M Φ may result in an efficient clearance of dead cells and infectious or toxic reagents in hepatitis. However, overexpression of AIM can also be damaging. In two mice models of specific AIM overexpression in myeloid cells (Qu, Du et al. 2009) or in lung in alveolar type II (AT II) epithelial cells (Li, Qu et al. 2011), mAIM overexpression promoted inhibition of apoptosis and activation of oncogenic signaling pathways, resulting in increased incidence of lung adenocarcinoma.

Taking into account all these data, AIM could be defined as an apoptosis inhibitor that supports the survival of M Φ and other cell types against various apoptosis-inducing stimuli of infectious origin and chemical compounds, both in mouse and human cell types.

3.4.2. Role in atherosclerosis

Atherosclerosis is an inflammatory pathology characterized by an accumulation of fatty deposits and cellular debris within the arterial wall. Two major factors contributing to the pathophysiology of atherosclerosis are hyperlipidemia and inflammation. Low-density lipoprotein (LDL) is a major extracellular carrier of cholesterol and, as such, it plays important physiologic roles distributing cholesterol through the circulatory system to peripheral tissues. However, under conditions of hyperlipidemia specific components of LDL become oxidized (oxLDL) or otherwise modified and these modifications substantially alter its function. Modified LDL are chemotactic for monocytes, induce migration, initiate inflammatory responses, alter the endothelium, induce differentiation of monocytes into macrophages and are avidly taken up by macrophages via SRs generating lipid-rich foam cells. Accumulation of foam cells is the hallmark of the disease. This pathologic deposition and the attendant proinflammatory reactions in the artery wall lead to the development of atherosclerotic lesions, which may obstruct the arterial lumen and/or eventually rupture and thrombose, causing myocardial infarction or stroke (Ross 1999; Libby 2002).

Both in human and mice, AIM is highly expressed in lipid-laden M Φ at atherosclerotic lesions. In this regard, its induction is associated with atherogenesis by supporting M Φ survival within atherosclerotic plaques (**Figure 11A**). Indeed, atherosclerotic plaques were markedly reduced in size in a mice model of atherosclerosis double deficient for AIM and LDL receptor (AIM^{-/-}, LDL^{-/-}) undergoing high-cholesterol diet compared with WT mice

(Arai, Shelton et al. 2005). Accordingly, a recent report shows that MafB, a transcription factor activated by LXR/RXR in macrophages that directly regulates AIM expression, also participates in the acceleration of atherogenesis by inhibiting foam-cell apoptosis (Hamada, Nakamura et al. 2014).

Besides its antiapoptotic effects, AIM participates in other key aspects of atherosclerosis-related mechanisms. Recently, our group demonstrated that hAIM increases M Φ foam cell formation. Together with the finding that rhAIM binds to oxLDL, we hypothesized that it may serve as a soluble protein that transfers oxLDL to CD36 and showed that, indeed hAIM promotes CD36-mediated oxLDL uptake (Amezaga, Sanjurjo et al. 2013). Furthermore, hAIM may contribute to macrophage cell adhesion to endothelial intercellular adhesion molecule 1 (ICAM-1) by enhancing expression of the integrins lymphocyte function-associated antigen (LFA-1) and macrophage 1 antigen (Mac-1) (**Figure 11B**) (Amezaga, Sanjurjo et al. 2013).

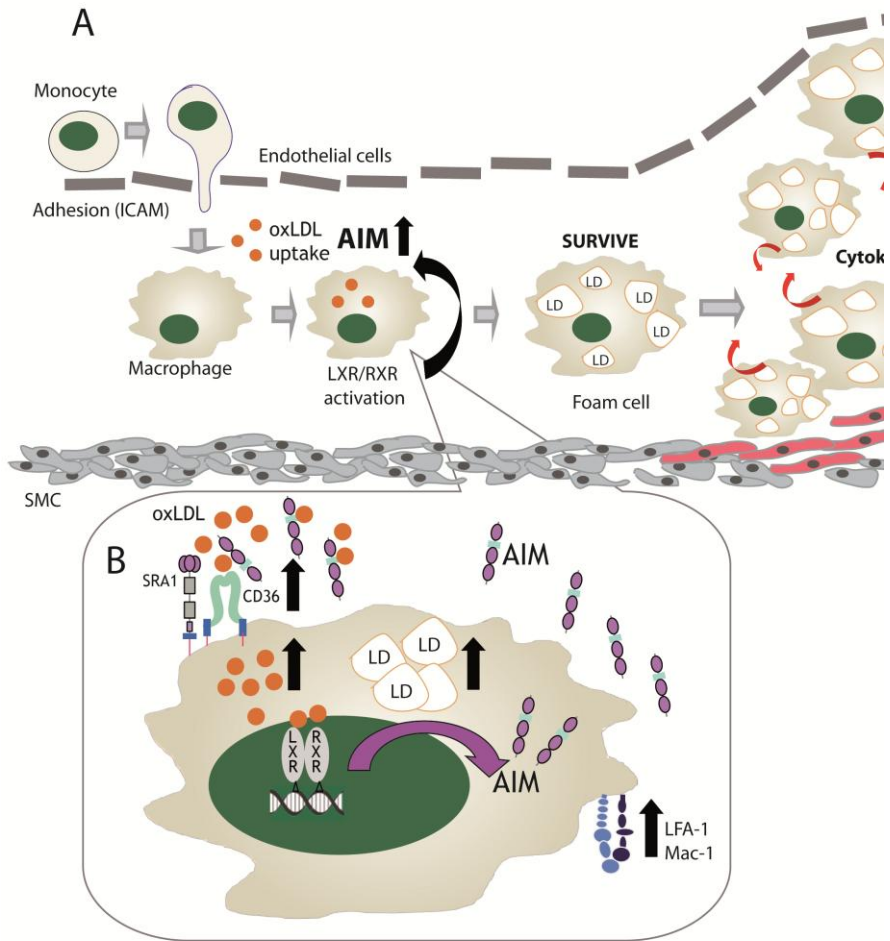


Figure 11. Role of AIM in atherosclerosis. (A) Model for the putative role of AIM in atherosclerosis development. Incorporation of oxLDL by macrophages in subendothelial space induces AIM production in migrating macrophages via LXR/RXR. This supports the survival of mature foam macrophages, which harbor a large amount of lipid droplets. This response results in accumulation of foam cells within intima, leading to expansion of the lesions (Arai, Shelton et al. 2005). **(B) Participation of hAIM in the atherosclerosis-related mechanism in the macrophage.** hAIM enhances macrophage oxLDL uptake, binds to oxLDL, increase cell surface CD36 expression and facilitates CD36-mediated oxLDL endocytosis. Consequently hAIM increases macrophage lipid accumulation. Moreover hAIM increases LFA-1 and Mac-1 expression conferring macrophages a enhanced adhesion capacity to VCAM-1 (Amezaga, Sanjurjo et al. 2013). Abbreviations: ICAM-1, intercellular adhesion molecule 1; LD, lipid droplets; LFA-1, lymphocyte function-associated antigen; LXR/RXR, liver X receptor/retinoid X receptor; Mac-1, macrophage 1 antigen; oxLDL, oxidized low-density lipoprotein; SMC, smooth muscle cell; SRA1, scavenger receptor A1.

Obesity is closely associated with insulin resistance, which triggers and/or accelerates multiple metabolic disorders including type 2 diabetes, cardiovascular diseases, and fatty liver dysfunction. It is known that insulin resistance is caused, in part, by chronic, low-grade inflammation in obese adipose tissue (Shoelson, Lee et al. 2006). This subclinical state of inflammation is dependent mainly on the innate immune system. Activation of TLRs expressed on adipocytes by fatty acids leads to the production of inflammatory adipokines and the recruitment of classically activated inflammatory macrophages (M1 macrophages) into the obese adipose tissue enhancing chronic subacute inflammatory stage (Weisberg, McCann et al. 2003; Xu, Barnes et al. 2003).

In this regard, mAIM was shown to induce obesity-associated lipolysis in adipose tissue. As mentioned above, mAIM is incorporated into adipocytes through CD36. Once in the cytosol mAIM associates with fatty acid synthase (FASN). FASN is a metabolic enzyme that is highly expressed in adipose tissue and that catalyzes the synthesis of saturated fatty acids such as palmitate, from acetyl-CoA and malonyl-CoA precursors. mAIM binding remarkably reduced the enzymatic activity of FASN, thereby reducing the amount of saturated fatty acids in adipocytes (Kurokawa, Arai et al. 2010). This response ablated transcriptional activity of peroxisome proliferator-activated receptor (PPAR γ), a master transcription factor for the differentiation of adipocytes, leading to diminished gene expression of lipid-droplet coating proteins including fat-specific protein 27 (FSP27) and Perilipin, which are indispensable for triacylglycerol (TG) storage in adipocytes. This resulted in decreased lipid droplet size, lower

numbers of mature adipocytes and decreased weight and fat mass induced by high-fat diet in mice, which is physiological relevant to the prevention of obesity (**Figure 12**) (Kurokawa, Arai et al. 2010; Iwamura, Mori et al. 2012). However, AIM-dependent lipolytic response also induced an efflux of free fatty acids (FA) from adipose cells. This response stimulated chemokine production in surrounding adipocytes through TLR4 activation concomitant with an infiltration of inflammatory M Φ (**Figure 12**). Supporting this fact, the progression of obesity-associated inflammation was prevented both locally and systemically in obese AIM $-/-$ mice due to the abolished infiltration of inflammatory macrophages. Similarly, whole-body glucose intolerance and insulin resistance were ameliorated in obese AIM $-/-$ mice. Thus, the absence of mAIM apparently prevents insulin resistance under obese conditions in mice (Kurokawa, Nagano et al. 2011). Regulation of hAIM could therefore be therapeutically applicable to obesity-associated inflammation diseases such as metabolic syndrome (Miyazaki, Kurokawa et al. 2011).

Interestingly, serum mAIM levels increase with the progression of obesity in mice fed with a high fat diet (Kurokawa, Nagano et al. 2011). Thus, the authors of all these discoveries concluded that the combined application of AIM agonists (to prevent obesity progression) and AIM antagonists (to prevent obesity-associated diseases) could have the potential to serve as a next-generation therapy for preventing harmful obesity-associated inflammatory diseases brought about by modern lifestyles (Miyazaki, Kurokawa et al. 2011; Arai and Miyazaki 2014). In this regard, they developed a novel strategy based on a synthetic Fc portion of IgM heavy chain to safely control AIM blood levels. That

could be applied in obese patients to promote lypolysis, and at the same time avoiding inflammation (Kai, Yamazaki et al. 2014).

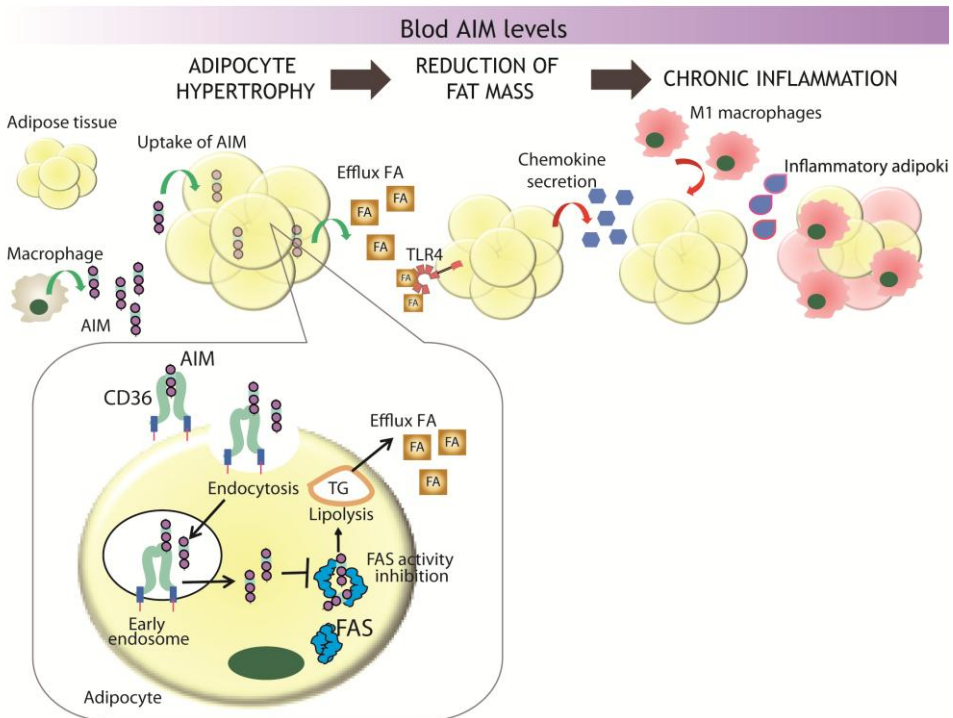


Figure 12. A scheme for the putative role of AIM in the establishment of adipose tissue inflammation and insulin resistance. Abbreviations: FA, free fatty acids; FAS, fatty acid synthase; TG, triacylglycerol; TLR4, toll-like receptor 4. Figure adapted from (Arai and Miyazaki 2014).

3.4.4. Role in pathogen aggression and inflammation

Like other members of the SRCR-SF such SRA-I/II (Dunne, Resnick et al. 1994), MARCO (Brannstrom, Sankala et al. 2002), DMBT1/SAG/gp340 (Bikker, Ligtenberg et al. 2004), CD6 (Sarrias, Farnos et al. 2007), CD163 (Fabriek, van Bruggen et al. 2009), gp340, (Loimaranta, Hytonen et al. 2009), CD5 (Vera, Fenutria et al. 2009) or S5D-SRCRB (Miro-Julia, Rosello et al. 2011), AIM is able to bind bacteria. Both human and mouse AIM proteins binds and aggregates Gram-negative and Gram-positive bacteria as well as saprophytic or pathogenic fungi (Sarrias, Rosello et al. 2005; Martinez, Escoda-Ferran et al. 2014). Moreover, hAIM has been found to act as a PRR for LPS and LTA, and competition-binding studies revealed that the binding to LPS and LTA is mediated by two independent sites (Sarrias, Rosello et al. 2005). Further roles for AIM regarding host-pathogen interactions involve its antiinflammatory function, whereby AIM influences the monocyte inflammatory response to LPS and LTA by inhibiting monocyte TNF- α secretion (Sarrias, Rosello et al. 2005; Martinez, Escoda-Ferran et al. 2014).

Additionally to its pathogen-binding properties, AIM may have antimicrobial functions. Initial evidence showed that mAIM increases M Φ phagocytosis of latex beads (Haruta, Kato et al. 2001). Moreover, in a study on mice lacking LXR (LXR $^{-/-}$) (Joseph, Bradley et al. 2004) these mice became highly susceptible to infection with the intracellular bacteria *L. monocytogenes*. This was mainly because of altered M Φ function: accelerated apoptosis and defective bacterial clearance. Most interestingly for our studies, the LXR $^{-/-}$ mice showed a loss of AIM expression, which

led to enhanced M Φ apoptosis. Moreover, the authors of this study suggested that, independent of its ability to inhibit apoptosis, mAIM could also have antimicrobial functions.

In another experimental model of *L. monocytogenes* infection (Zou, Garifulin et al. 2011), transient overexpression of cholesterol-25-hydroxylase (Ch25h, the enzyme that synthesizes 25-hydroxycholesterol, a natural endogenous ligand of LXR), promotes survival of *L. monocytogenes*-infected cells through mAIM induction. In this scenario, infected mice showed higher bacterial loads in liver and spleens, which correlated with higher bacterial loads in M Φ infected *in vitro*. Therefore, in terms of antimicrobial activity, these data are apparently contradictory with those of LXR $-/-$ mice. The authors suggested that this may reflect the different effects of constitutive vs. transient changes in M Φ apoptosis. This was supported by the notion that increased survival of *L. monocytogenes* infected M Φ by transient Ch25h overexpression at the time of infection could intensify the disease.

Interestingly, in this work the authors also showed that mAIM inhibited *L. monocytogenes*-induced M Φ death in part by inhibiting caspase-1 cleavage. The authors proposed that these events could be part of a strategy evolved by the pathogen to maintain a protected cellular environment for its replication and to prevent immune activation by pyroptotic death of M Φ .

Overall, these two studies revealed new points of intersection of metabolic and inflammatory pathways and also highlighted the delicate balance of cell survival that has to be maintained by the host to resist infection.

Even though the existence of all these studies, no direct evidences of AIM putative antimicrobial properties neither mechanism involved in its anti-inflammatory function had been described before the beginning of the present work.

4. Autophagy

Autophagy is a highly conserved cellular degradative process, used to recycle obsolete, damaged or superfluous cell components into basic biomolecules, which are then recycled back into cytosol. In this regard, autophagy drives a flow of biomolecules in a continuous degradation-regeneration cycle (Feng, He et al. 2013).

In mammalian cells, there are three primary types of autophagy: microautophagy, chaperone-mediated autophagy and macroautophagy (Parzych and Klionsky 2013). While each is morphologically distinct, all three culminate in the delivery of cargo to the lysosome. During microautophagy, invaginations of the lysosomal membrane are used to capture cargo that can include intact organelles (Mijaljica, Prescott et al. 2011). Chaperone-mediated autophagy differs in that it does not use membranous structures to sequester cargo, but instead uses chaperones to identify cargo proteins that contain a particular peptide motif; these substrates are then unfolded and translocated individually directly across the lysosomal membrane (Massey, Kiffin et al. 2004). In contrast, in macroautophagy *de novo* synthesis of double-membrane vesicles, called autophagosomes, is used to sequester cargo and subsequently transport it to the lysosome (Yorimitsu and Klionsky 2005). Because mouse models only exist for macroautophagy, so far, extensive research has been dedicated to the understanding of this type. In this work, we focus on macroautophagy, and for the sake of simplicity, it will be referred as autophagy.

Autophagy occurs at a low level constitutively, and plays an important role in cellular homeostasis maintaining quality control of essential cellular components. It also participates in general processes such as development, differentiation, ageing and cell death (Wirawan, Vanden Berghe et al. 2011). On the other hand, when cells encounter environmental stresses, autophagy can be further induced to degrade cytoplasmic material into metabolites that can be used in biosynthetic processes or energy production, allowing cell survival (Ravikumar, Sarkar et al. 2010).

Autophagy has long been thought to be a non-selective bulk degradation mechanism. However, recent accumulating evidence highlighted the selective elimination of unwanted components by autophagy. Some examples are protein aggregates (aggrephagy), lipid droplets (lipophagy), dysfunctional organelles (mitophagy, perophagy, ribophagy, ERphagy) or pathogens (xenophagy). The molecular mechanisms underlying cargo selection are still largely unknown. In general these pathways appear to rely on the same molecular core machinery as non-selective (starvation-induced) autophagy that might also interact with specific adaptors which function as scaffolding proteins to allow the specific sequestration of the substrate (Fimia, Kroemer et al. 2012; Reggiori, Komatsu et al. 2012).

During the last decade autophagic dysfunction has been associated with a variety of human pathologies, including neuronal disorders, liver and heart diseases, infectious diseases, cancer, type II diabetes, cystic fibrosis and many more (Levine and Kroemer 2008). Therefore, the interest in autophagy has experienced an exponential growth. Yet many questions

concerning its specific role in these diverse cellular and patho/physiological processes remain unanswered, and the knowledge about its molecular signaling is far from complete.

4.1. Molecular signaling of autophagy

The precise molecular events in autophagy are complex and the core autophagic machinery described to date consists of nearly thirty proteins. Apart from these factors that execute the process of autophagy, several signaling pathways are involved in converting internal and external stimuli into an autophagic response.

4.1.1. Autophagy “effectors”

The hallmark of autophagy is the formation of double membrane vesicles called autophagosomes. Two characteristics make autophagosomes a unique type of transport carrier. First, the cargo is surrounded by two lipid layers and second, its big size (700 nm approximately) which can further expand to accommodate large structures such as organelles or bacteria. The autophagic process is divided into mechanistically distinct steps: initiation, elongation of autophagosomes, closure, and fusion with lysosomes (**Figure 13**) (Xie and Klionsky 2007; Yoshimori and Noda 2008).

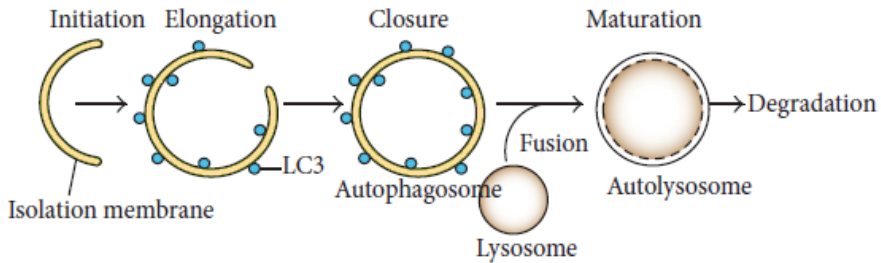


Figure 13. General scheme of autophagic process. The autophagic process starts with the formation of isolation membrane that originates from various intracellular membrane sources. Initiation of the isolation membrane is followed by elongation and closure leading to a complete autophagosome that surrounds the cargo. The fusion of lysosomes with autophagosomes causes the formation of autolysosomes, where autophagic substrates are exposed to hydrolytic interior of lysosome resulting in their degradation. Adapted from (Vural and Kehrl 2014).

The initial event upon autophagy induction is the formation of a membranous cistern called isolation membrane (or phagophore). The identity of the sources of autophagosome membrane is one of the key questions in the field that still lacks a clear answer. The plasma membrane, the endoplasmic reticulum, the mitochondria and the Golgi have been proposed to contribute to phagophore biogenesis (Mari, Tooze et al. 2011).

A large group of proteins assist in autophagosomal biogenesis. These proteins were initially characterized in yeast and designated autophagy related genes (ATGs) (Takeshige, Baba et al. 1992). Among these ATG proteins, one subset is essential for autophagosome formation, and is referred to as the ‘core’ molecular machinery that can be divided in different subgroups or complexes: the ATG1/ULK complex, the PI3K complex, ATG9 and its cyclin system, and two ubiquitin-like conjugation systems. See **Figure 14** for a brief outline of the different stages in autophagosome formation

INTRODUCTION

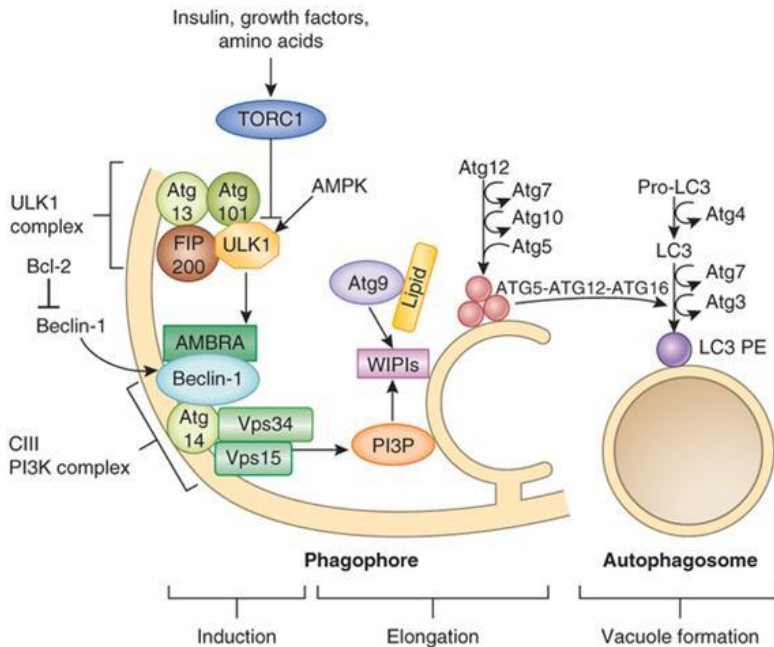


Figure 14. Mammal autophagosome biogenesis. The process can be divided into three steps: **Initiation:** Autophagosome formation is initiated by phosphorylation of Unc-51-like kinase (ULK1), which activates it and catalyzes the phosphorylation of other components of the Atg1-ULK complex (ULK1, ULK2, Atg13, FIP200 and Atg101). The phosphorylation of ULK1 triggers translocation of an ATG14-containing class III PI3K multiprotein complex (Vps34, Vps15, ATG14 and Beclin-1) from the cytoskeleton. This complex generates PI3P, which is required for autophagy both in yeast and mammals and is involved in the nucleation of the phagophore. **Elongation:** PI3P effectors WD repeat domain phosphoinositide-interacting 1 (WIPI1) and WIPI2 and catalyzes the first of two types of ubiquitination-like reactions that regulate isolation membrane elongation. Then two conjugation systems involving ubiquitin-like (UBL) proteins contribute to the expansion of the phagophore. The first system involves formation of the ATG5-ATG12-ATG16 complex that is irreversibly conjugated to each other in the presence of ATG7 and ATG10. ATG16L1 dimerizes and allows association with the phagophore, promoting membrane expansion. **Closure:** Attachment of the fully formed complex on the isolation membrane induces the second complex to covalently conjugate phosphatidylethanolamine to microtubule-associated protein 1 light chain 3 (LC3), which facilitates closure of the isolation membrane. LC3 is processed by ATG4 to reveal a C-terminal glycine (LC3-I). Then ATG7 activates LC3-I and transfers it to the E2-like enzyme ATG3. The ATG12-ATG5-ATG16L1 complex participates in the conjugation of PE to LC3-I to create LC3-II, which can associate with the phagophore. (Laird, Rhee et al. 2009; Guo and Friedman; Nixon 2013). Figure adapted from (Guo and Friedman; Nixon 2013).

Among all the autophagy-related proteins one of the best-defined autophagic markers is the microtubule-associated protein 1 (MAP1) light chain 3 (LC3). LC3 undergoes several modifications, among them C-terminal proteolysis of an 18 kDa fragment, to form LC3-I, which is then modified into the phosphatidylethanolamine-conjugated form, LC3-II (16 kDa), which is incorporated into autophagosomal membranes (Reggiori and Klionsky 2002; Ravikumar, Sarkar et al. 2010; Kang, Zeh et al. 2011). Accumulation of autophagosomes measured by accumulation of LC3-II or by electron microscopy (EM) image analysis could reflect either increased autophagosome formation due to increases in autophagic activity, or to reduced turnover of autophagosomes. The latter can occur by defects in fusion with lysosomes, or following inefficient degradation of the cargo. Therefore, the use of autophagy markers such as LC3 needs to be complemented by knowledge of the overall autophagic flux to permit a correct interpretation of the results. Autophagic flux refers to the complete process of autophagy including the delivery of cargo to lysosomes and its subsequent breakdown and recycling (Klionsky, Abdalla et al. 2012). Autophagosome-lysosome colocalization assays, turn-over of LC3-II or autophagic protein degradation assays are some examples of flux measurements of autophagy.

4.1.2. Cellular signaling pathways regulating autophagy

Autophagy helps cells to respond to a wide range of extra and intracellular stresses including nutrient starvation, the presence/absence of insulin and other growth factors, hypoxia and ER stress or pathogen invasion (Yang and Klionsky 2009). Multiple signaling pathways translate these inputs to a cellular response.

INTRODUCTION

Three of the major kinases that regulate autophagy are mammalian target of rapamycin (mTOR), protein kinase A (PKA) and adenosine monophosphate-activated protein kinase (AMPK). There is thought to be crosstalk between these kinases that allows them to operate in an interconnected way (Figure 15).

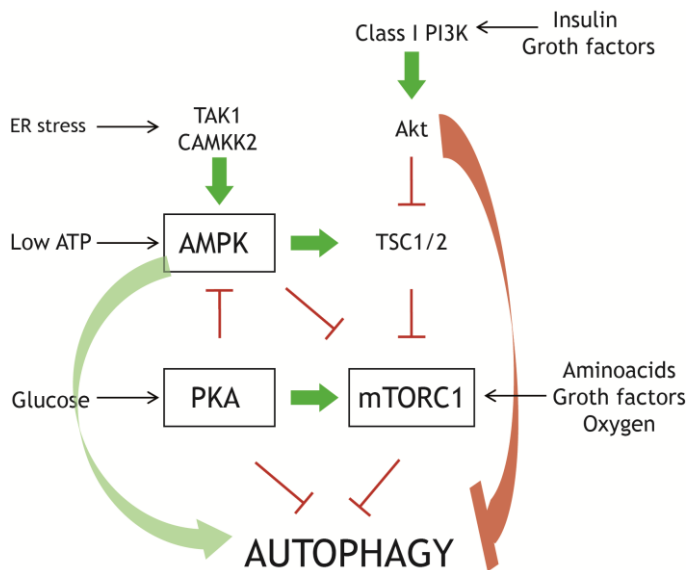


Figure 15. Main kinases regulating autophagy and their functional relationships. Green lines means activation, red lines means inhibition. Abbreviations: AMPK, adenosine monophosphate-activated protein kinase; ATP, adenosine triphosphate; CAMKK2, calcium/calmodulin dependent protein kinase; ER, endoplasmic reticulum; mTORC1, mammalian target of rapamycin complex 1; PI3K, phosphatidylinositol 3-kinase; PKA, protein kinase A; TAK1, TGF β -activated kinase 1; TSC ½ tuberous sclerosis complex ½. Adapted from (Nagelkerke, Bussink et al. 2014).

mTORC1 and PKA acts as nutrient-sensors, they sense primarily carbon and nitrogen, respectively. Both kinases negatively regulate autophagy; mTORC1 suppresses autophagy through direct interaction with the autophagy initiation complex ULK (Jung, Ro et al. 2010) and PKA through the phosphorylation of LC3 (Cherra, Kulich et al. 2010). The PI3K/Akt/mTOR pathway is

the most studied pathway regulating mammalian autophagy. Diverse signals such as growth factors, aminoacids, glucose or energy status activate the class I PI3K/AKT/mTOR pathway and consequently inhibit autophagy under nutrient-rich conditions (Jung, Ro et al. 2010). In contrast AMPK acts an autophagy inducer, is the major energy-sensing kinase in the cell and responds to intracellular AMP/ATP levels to regulate a variety of cellular processes, including autophagy (Akers, Loffler et al. 2011). It promotes autophagy via different pathways: by directly activating ULK1 complex through phosphorylation of Ser 317 and Ser 777, by directly inhibition of mTORC1 or by activating TSC1/2-complex which represses mTOR1 (Gwinn, Shackelford et al. 2008).

mTOR independent pathways of autophagy control were also reported, and examples are the MAPK pathway and PKCs, but their role in autophagy may depend on the cellular context and inducers used (Sridharan, Jain et al.).

4.1.3. PI3K and autophagy

Among the key pharmacological targets in regulation of autophagy are the PI3Ks. It is known that their catalytic products PI(3,4,5)P₃ and PI3P have opposing roles in autophagy. PI(3,4,5)P₃, the product of class I PI3K triggers mTOR pathway which inhibits autophagy. Numerous receptor types and hence a broad range of extracellular signals activate PI3K-I to generate a pool of inner plasma membrane PI(3,4,5)P₃. As previous commented, PI(3,4,5)P₃ acts as a ligand for a subset of Pleckstrin homology (PH) domain proteins. Phosphoinositide dependent kinase 1 (PDK1) and AKT1 are two key PI(3,4,5)P₃ effectors crucial for autophagy

suppression; among their diverse range of ligands several substrates directly impact on autophagy. The best studied mechanism of PDK1-AKT-dependent autophagy inhibition is through phosphorylation of tuberous sclerosis complex proteins 1 and 2 (TSC1/2) that possess GTPase activating protein required for activation of TOR in the context of TOR complex 1 (TORC1) (O'Farrell, Rusten et al. 2013). By contrast, PI3P, the product of class II and III PI3K, mediates recruitment of specific autophagy effectors to the sites of autophagy membranes and thereby plays a critical role in the initial steps of autophagosome biogenesis (**Figure 16**) (Devereaux, Dall'Armi et al. 2013).

PI3K class III, Vps34, is part of core autophagy machinery. Genetic and biochemical studies of autophagy in yeast and humans have led to identification of different Vps34 complexes (Kihara, Noda et al. 2001; Obara, Sekito et al. 2006; Backer 2008). Core components of the Vps34 complexes include Vps34 and p150 (Vps15). Beclin1, a mammalian homolog of Atg6, participates in Vps34 complex formation and recruits additional proteins, among them, ATG14L and ultra violet radiation resistance-associated gene protein (UVRAG) that devote the Vps34 complex to autophagy (Kim, Kim et al. 2013).

It was recently shown that AMPK plays a key role in regulating different Vps34 complexes. AMPK inhibits the non-autophagy Vps34 complex by phosphorylation of T163/S165 in Vps34 and therefore suppresses overall PI3P production (Kim, Kim et al. 2013). In parallel, AMPK activates the proautophagy Vps34-Atg14L complex by phosphorylating S91/S94 in Beclin1 to induce autophagy (Kim, Kim et al. 2013).

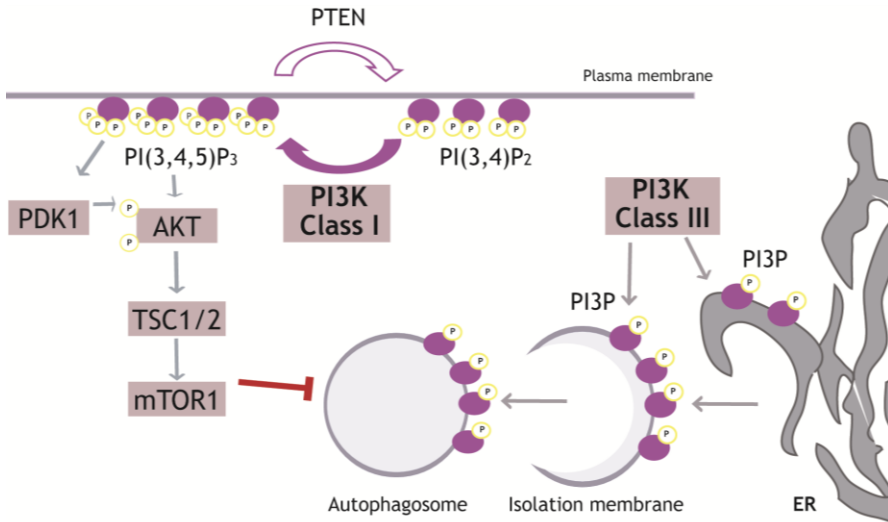


Figure 16. Oversimplified scheme of PI3K involvement in autophagy. Opposite functions of PI3K class I and III in autophagy are represented. Abbreviations: ER, endoplasmic reticulum; mTOR, mammalian target of rapamycin 1; PI3K, phosphoinositide 3-kinase; PTEN, phosphatase and tensin homolog; TSC1/2, tuberous sclerosis complex proteins 1 and 2 . Figure adapted from (Dall'Armi, Devereaux et al. 2013).

4.2. Autophagy in immunity

Four main roles of autophagy in immunity have been described: the direct elimination of microorganisms, the control of inflammation, the control of adaptive immunity through the regulation of antigen presentation and lymphocyte homeostasis and the secretion of immune mediators (such as immunoglobulin, preventing excessive antibody production) (Deretic, Saitoh et al. 2013). In the present work we were interested on the first two roles, namely microorganism elimination and control of inflammation.

4.2.1. Autophagy in the direct elimination of microorganisms

A decade ago it was demonstrated that the induction of autophagy following infection with Group A *Streptococcus* (GAS) acted as a defense mechanism (Nakagawa, Amano et al. 2004). The bacteria were found to colocalize with LC3 and lysosomal-associated membrane protein 1 (LAMP-1) positive vesicles and markers of autophagosomes and lysosomes, respectively (Nakagawa, Amano et al. 2004). A similar phenomenon was observed in *Mycobacterium tuberculosis* infected MΦ (Gutierrez, Master et al. 2004). Since then, a wealth of information has highlighted the relevance of autophagy in the control of intracellular infection by bacteria, mycobacteria and virus, reviewed in (Jo, Yuk et al. 2013). The importance of autophagy in protecting cells from microbial invasion is highlighted by the microbial adaptations that have evolved to evade autophagy (Ogawa, Mimuro et al. 2011).

Different antimicrobial functions targeting bacteria to the lysosome by components of autophagy machinery have been described, the main two are LC3-associated phagocytosis (LAP) and xenophagy (Cemma and Brumell 2012). LAP, involves the engagement of the autophagy machinery to enhance the maturation of the conventional single-membrane phagosomes through the same maturation pathway that is used in internally formed autophagosomes (Deretic, Saitoh et al. 2013). Similarly to conventional autophagy, LAP uses Class III PI3K complex and LC3 conjugation system, and involves ATG5 and ATG7 (Sanjuan, Dillon et al. 2007). However, it proceeds in the absence of ULK1

(Martinez, Almendinger et al. 2011) and FIP200 (Florey, Kim et al. 2011), two components of the autophagy initiation complex. In contrast, xenophagy, which is the uptake of intracellular pathogens into double-membrane autophagosomes and requires the participation of the full autophagy machinery, leads to engulfment of the microbe into double-membrane vesicles and ultimately, their delivery into lysosomes. The latter constitutes a defense mechanism of *MΦ* against *M.tuberculosis* infection, which will be extended in section 5.1.4. To initiate xenophagy (hereinafter referred as autophagy), mammalian cells detect the presence of cytoplasmic invasion of microbes by PRRs. Subsequently, autophagy is induced by different families of receptors that recognize PAMPS (such as TLRs, NOD-like receptors and the double-stranded RNA-binding protein PKR), by DAMPs (such as ATP, ROS) or by pathogen receptors (such as CD46) (Levine, Mizushima et al. 2011). This fact supports the idea that the participation in host defense by autophagy has been well integrated with other immune sensing systems, promoting a model in which immune and nutritional inputs converge in common signaling pathways to activate autophagy.

4.2.2. Autophagy in the control of inflammation

The role of autophagy in inflammatory diseases was initially described through genome-wide association studies in which polymorphisms in ATG genes were linked with Crohns disease (Kumar, Nath et al. 2010). A prominent example is autophagy suppression of inflammasome activation. Based on the association between Crohn's disease and ATG16L1 polymorphisms, Saitoh et al. generated an ATG16L1-deficient mouse strain that presented

total absence of autophagosomes and a significant reduction in autophagy-dependent degradation (Saitoh, Fujita et al. 2008). To assess the consequences of defective autophagy, M Φ from wild type and ATG16L1-deficient mice were treated with LPS for 24 hours. Although TNF- α , IL-6 and IFN- β production were unchanged, the level of IL-1 β was markedly elevated. Besides IL-1 β , elevations in IL-18 and active caspase-1 levels were observed in the ATG16L1 deficient M Φ . Similar results were found with ATG7-deficient M Φ . Further studies focused on how autophagy regulates IL-1 β secretion founded that pro-IL-1 β is targeted by autophagosomes and degraded following exposure of M Φ to various TLR agonists (Harris, Hartman et al. 2011). Inflammasome proteins AIM2 (absent in melanoma 2 protein) and NLRP3 also exhibited partial colocalization with autophagosomes and autophagolysosomes, suggesting that the autophagic pathway acted to limit inflammasome activity by engulfing and degrading them (Shi, Shenderov et al. 2012). At present, several studies indicate that autophagy is an anti-inflammatory mechanism that affects numerous pathways. Autophagy dependent degradation of proinflammatory factors also has been documented in effector T cells, where autophagy targets BCL-10-containing complexes, to reduce NF- κ B activation and modulate T-cell receptor (TCR) (Paul, Kashyap et al. 2012). Moreover, autophagy can affect PRR-mediated INF signaling, by bringing physically together cytosolic PAMPs to their cognate endosomal TLRs. This was best documented in the case of plasmacytoid dendritic cells in which autophagy was found needed to recognition of vesicular virus by TLR7 and subsequent INF- α production (Lee, Lund et al. 2007).

Interestingly, recent reports indicate that autophagy might play a role in manipulating tumor-associated immune responses by modulating TLR2 signaling in the macrophage. It has been shown that hepatoma cells can produce TLR2-related ligands that may modulate tumor associated macrophage (TAM) functions towards an M2 differentiation (Kim, Takahashi et al. 2009). Recently, it was shown that hepatoma-cell derived CM stimulates TLR2 signaling to induce NF- κ B cytosolic ubiquitination. This leads to its degradation by SQSTM1/p62-mediated autophagy, thus contributing to promote immunosupresion in the tumor microenviroment (Chang, Su et al. 2012; Chang, Su et al. 2013).

5. Tuberculosis

5.1. General introduction to tuberculosis

The causal agent of tuberculosis (TB), *Mycobacterium tuberculosis* (Mtb) is a human pathogen infecting over a billion people worldwide. The relevance of this disease for human health is reflected by the following figures. In 2011 alone, 8.7 million people fell ill with TB and 1.4 million died from the disease (Global tuberculosis report, 2012, World Health Organization, WHO). Infection with this pathogen is via the inhalation of aerosols containing a small number of bacilli (Kaufmann 2001). Once in the lung, bacilli can be phagocytized by alveolar M Φ (M Φ), in which they may survive intracellularly (Hart and Armstrong 1974; Armstrong and Hart 1975; Kaufmann 2001; Russell 2001) until the destruction of M Φ , which then allows the bacilli to infect new M Φ and thus to perpetuate the infection (**Figure 17**). However, host immunity is sufficient to control Mtb in 90% of infected people thanks to a combination of early innate and subsequent adaptive responses, as indicated by the fact that only 10% of those infected develop active TB (Global tuberculosis report, 2012, World Health Organization, WHO) (Pieters 2008).

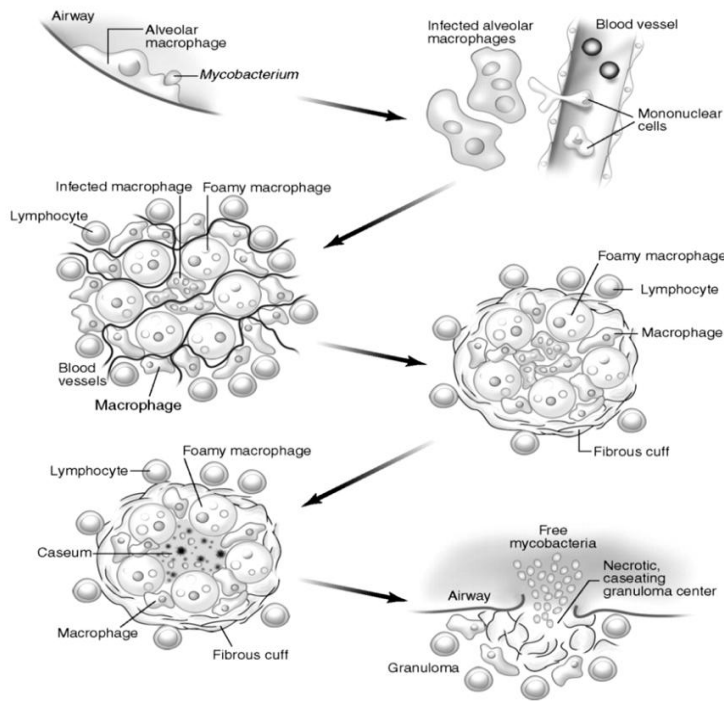


Figure 17 Progression of the human tuberculosis granuloma. Infection is initiated after inhalation of viable bacilli present in atmosphere. Once in the lung, the bacilli are phagocytized by alveolar M Φ , triggering a proinflammatory response that induces the macrophage to invade the subtending epithelium and the recruitment of mononuclear cells. In its early stage, the granuloma has a core of infected M Φ enclosed by foamy M Φ and surrounded by lymphocytes. This tissue response contains the infection and spells the end of the period of rapid replication of Mtb. As the granuloma matures, it develops an extensive fibrous capsule. At this stage there is a noticeable increase in the number of foamy M Φ in the fibrous capsule. In a progressive infection, the caseous, necrotic center of the granuloma liquefies and cavitates, spilling thousands of infectious Mtb into the airways completing bacterium's life cycle. Figure from (Russell, Cardona et al. 2009).

Traditionally, protective immunity to TB was ascribed to T-cell-mediated immunity, with CD4⁺ T cells playing a crucial role. More recently, immunological and genetic studies support the long-standing notion that innate immunity is also relevant in the fight against TB infection. In this regard M Φ , the primary target of

Mtb infection, responds to Mtb through multiple interconnected mechanisms. They produce reactive oxygen and nitrogen intermediates (Chan, Chan et al. 2001; Yang, Yuk et al. 2009; Miller, Velmurugan et al. 2010) and a wide spectrum of inflammatory mediators. Moreover, they activate intracellular autophagy mechanisms enhancing interaction between mycobacterial containing phagosomes and lysosomes (Gutierrez, Master et al. 2004). On the other hand, Mtb has evolved with powerful evasion strategies to protect itself and to achieve long-term persistence in human organs including preventing the recognition of infected MΦ by T cells, or evading macrophage mycobactericidal mechanisms (Flynn and Chan 2003). Mtb can protect itself against reactive oxygen and nitrogen intermediates (Zahrt and Deretic 2002) and arrest mycobacterial containing phagosome maturation and phagolysosomal fusion (Armstrong and Hart 1975; Deretic 2008).

5.2. Macrophage mycobactericidal mechanisms

5.2.1. Immune recognition and phagocytosis

Phagocytosis of Mtb by alveolar MΦ is the first event in the host-pathogen relationship that decides the outcome of infection. Phagocytosis of Mtb involves different receptors such complement receptors (CRs), mannose receptor (MR) and scavenger receptors (SRs). CRs are primarily responsible for the uptake of opsonized Mtb; the best-characterized receptor for non-opsonin-mediated phagocytosis is MR, important in environments low in opsonins,

such as the lung. When uptake by CRs and MR is blocked, M Φ may also internalize Mtb through the type A SR (van Crevel, Ottenhoff et al. 2003).

After mycobacterial infection innate immune responses are initiated through the recognition of mycobacterial components by intracellular and extracellular PRRs such as TLRs, NOD-like receptors or SRs. Then, intracellular signaling cascades are activated which will eventually lead to the activation of NF- κ B transcription and the production of pro- and anti-inflammatory cytokines and chemokines (Kleinnijenhuis, Oosting et al. 2011).

TLRs play a central role in immune recognition of Mtb. The TLRs known to be involved in recognition of Mtb are TLR2, TLR4, TLR9, and possibly TLR8 (Kleinnijenhuis, Oosting et al. 2011). The *in vivo* importance of the TLR-mediated signal in host defense to Mtb was highlighted in studies using mice lacking MyD88. MyD88-deficient mice are highly susceptible to airborne infection with Mtb (Fremond, Yeremeev et al. 2004). However, several findings have indicated that PRRs other than TLRs evoke innate immune responses. These include RIG-I-like receptors, NOD-like receptors (NLRs), C-type lectin receptors and SRs (Kleinnijenhuis, Oosting et al. 2011) (Figure 18). In this regard, recently, a functional redundancy in the PRRs in a long-term control of Mtb infection was reported. In this work the authors hypothesized that PRR might cooperate in a coordinated response to sustain the full immune control of Mtb infection (Court, Vasseur et al. 2010).

INTRODUCTION

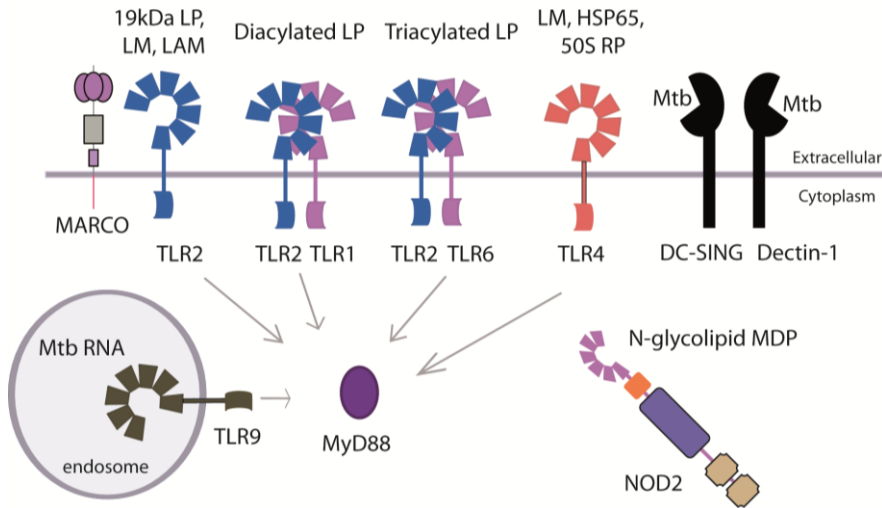


Figure 18: Immune recognition of Mtb. Several PRRs on phagocytic cells have been identified for the recognition mycobacterial PAMPs. TLR2 recognizes the 19 kDa lipoprotein (LP), lipomannan (LM), and lipoarabinomannan (LAM). TLR1-TLR2 and TLR6-TLR2 heterodimers bind diacylated and triacylated LP, respectively. TLR4 binds tri- and tetra-acylated LM, heat shock protein 65 (HSP65), and 50S ribosomal protein (50S RP), whereas mycobacterial DNA is recognized by phagosomal TLR9. Scavenger macrophage receptor with collagenous structure (MARCO) is a component required for TLR2 signalling pathway. C-type lectin receptors (DC-Sign and Dectin-1) have also been implicated in the innate recognition of Mtb. Cytosolic receptor NOD2 interacts with Mtb derived peptidoglycan component muramyl dipeptide (MDP). Adapted from (Hossain and Norazmi 2013).

Although the impact of SRs for recognition of Mtb has not been extensively studied, there are reports that show that SRCR-SF proteins contribute to the immune defense against Mtb infection. Some examples are macrophage SR-AI that modulates granuloma formation (Sever-Chroneos, Tvinnereim et al. 2011) and Macrophage Receptor with Collagenous Structure (MARCO), described as a novel component required for Mtb-TLR2 signaling (Bowdish, Sakamoto et al. 2009). Moreover, genetic variations of

MARCO have been associated with susceptibility to pulmonary tuberculosis in a Gambian population (Bowdish, Sakamoto et al. 2009). Interestingly, hAIM protein and the ectodomain of CD163 (sCD163), have been found to be elevated in the serum of TB patients (Knudsen, Gustafson et al. 2005; Xu, Deng et al. 2013). These observations open up the possibility that SRCR proteins may be predictors of TB disease in humans.

5.2.2. Generation of Reactive Nitrogen Species (RNS)

During infection, interferon- γ (IFN- γ) produced by newly recruited lymphocytes acts on the parasitized M Φ to trigger the expression of antimicrobial effectors, including the inducible isoform of nitric oxide synthase (iNOS) (MacMicking, North et al. 1997). iNOS oxidizes L-arginine to produce nitric oxide (NO) and citrulline. Then, NO rapidly reacts with molecular oxygen and water to eventually generate reactive nitrogen species (RNS) (Nathan and Shiloh 2000). NO itself is a very potent antimycobacterial agent that kills 99% of cultured Mtb at low concentrations (<100 parts per million) (Long, Light et al. 1999). Recently, besides its antimicrobial activity, an immunoregulatory function was described demonstrating that NO is also necessary to suppress the continual production of IL-1 β by the NLRP3 inflammasome, to inhibit persistent neutrophil recruitment and to prevent progressive tissue damage (Mishra, Rathinam et al.). However, the role of RNS in human tuberculosis is controversial. In fact, it is well known that NO production by human M Φ is not as high as that of murine M Φ (Weinberg, Misukonis et al. 1995). Moreover, in early human TB studies, RNS were difficult to detect

leading most researchers to discount their importance in disease control in humans (Yang, Yuk et al. 2009).

5.2.3. Generation of Reactive Oxygen Species (ROS)

A powerful M Φ defense mechanism to combat bacterial infections is to induce a process called “oxidative burst” or “respiratory burst” (Spooner and Yilmaz 2011). This process produces large quantities of reactive oxygen species (ROS) by activating phagocyte oxidase (phox), also known as nicotinamide adenine dinucleotide phosphate-oxidase (NADPH-oxidase), which reacts with molecular oxygen to form superoxide (O_2^-). O_2^- then can be converted to the toxic H_2O_2 and the hydroxyl radical. Free oxygen radicals are highly toxic to pathogens and are utilized as a tool to prevent colonization of tissues by microorganisms. The importance of ROS in controlling bacterial infections is illustrated in patients with chronic granulomatous disease (CGD), a congenital disorder where a mutation occurs in any of the four phox subunit proteins, resulting in a failure to produce a correct ROS response. These CGD patients show a high susceptibility to pyogenic infections (Segal, Leto et al. 2000) and also to Mtb infection in areas of endemic TB (Lau, Chan et al. 1998). However, there are no strong *in vitro* data implicating ROS produced by M Φ in the killing of Mtb. Note that besides a direct role of ROS in pathogen killing, these molecules are also a key part of the intracellular redox profile influencing a wide variety of signaling networks (Circu and Aw 2010). Thus, rather than acting as bactericidal effector, ROS might be important as signaling molecules coordinating the antimycobacterial host defense. In fact, moderate levels of ROS can serve as a signal in various signaling

pathways including autophagy (Gibson 2013; Deffert, Cachat et al. 2014).

5.2.4. Autophagy

Autophagy is emerging as a key antimicrobial strategy in antimycobacterial resistance, given that numerous studies have shown a crucial role for autophagy in the defense against mycobacterial infection in human cells (Deretic and Levine 2009). Physiological or pharmacological induction of autophagy results in increased Mtb-phagosome colocalization with the LC3 autophagosomes, which leads to the delivery of mycobacteria to lysosomes and results in bactericidal activity in M Φ (Gutierrez, Master et al. 2004). More recently, the crucial role of autophagy genes in restricting intracellular growth of Mtb was confirmed by genome-wide siRNA screenings (Kumar, Nath et al. 2010). Finally, the analysis of Mtb infection in autophagy-deficient mice validated the relevance of data obtained in *in vitro* systems and provided *in vivo* evidence that autophagy protects against active tuberculosis by suppressing bacterial burden and inflammation (Castillo, Dekonenko et al. 2012).

5.2.5. Vitamin D and Antimicrobial peptides

Recent findings have determined that autophagy is also the end result of the anti-mycobacterial activity of vitamin D, more specifically its active form 1,25-dihydroxyvitamin D₃ (1,25D₃) (Campbell and Spector 2012), which has long been known to activate a direct antimicrobial pathway in human M Φ (Martineau 2011). The 1,25D₃-induced autophagic antimicrobial pathway involves the generation of the peptides cathelicidin (hCAP-18/LL-

37) and defensin β 4 (DEFB4), which exert direct antimicrobial activity against Mtb (Liu, Stenger et al. 2007; Sonawane, Santos et al. 2011). However, LL-37 also induces autophagy through up-regulating expression of beclin-1 (BECN1) and autophagy protein 5 (ATG5) (Figure 19) (Yuk, Shin et al. 2009). This pathway also synergizes with other cellular responses, such as TLR activation. Indeed, TLR2/1 activation by mycobacterial components can also trigger the vitamin D-dependent induction of cathelicidin through the generation of IL-15 (Kruzick, Hewison et al. 2008), and in synergy with the IL-1 β pathway, the induction of DEFB4 (Liu, Schenk et al. 2009) (Figure 19). Moreover, the vitamin D pathway is also induced by two T-cell-mediated mechanisms, IFN- γ (Fabri, Stenger et al. 2012) and CD40 ligand (Klug-Micu, Stenger et al. 2013), both part of the host adaptive immune response.

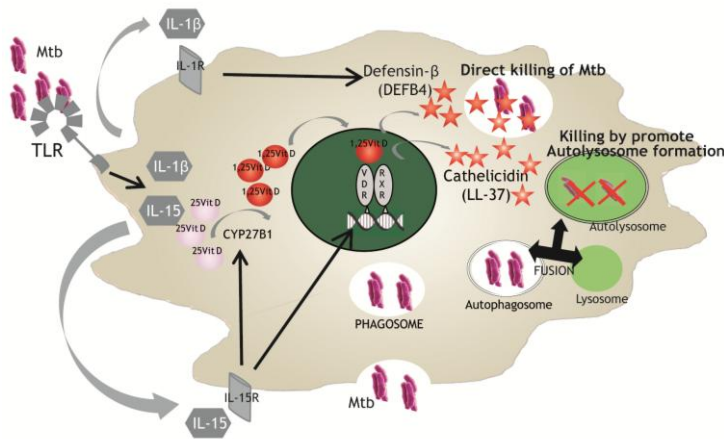


Figure 19. Model for the role of autophagy in the vitamin D-dependent induction of antimicrobial responses in humans. The active form of vitamin D (1,25VitD), by interaction with vitamin D nuclear receptor (VDR) promotes antimicrobial peptides cathelicidin (LL-37) and β -defensin 4 (DEFB4) expression, leading to a direct killing of Mtb. LL-37 also promotes macrophage autophagy to kill the bacterium. TLR activation by Mtb potentiates those responses by interleukin 15 (IL-15) and interleukin-1 β (IL-1 β) production. IL-15 up-regulates vitamin D-activating enzyme 1 α -hydroxylase (CYP27B1) and vitamin D receptor (VDR) expression, and IL-1 β promotes Mtb killing by human β -defensin 4 (DEFB4) induction.

5.2.6. Nuclear receptors in the control of *M. tuberculosis* infection

In $M\Phi$, other mechanisms, such as activation of nuclear liver X receptors (LXRs), contribute to the control of *Mtb* infection (Korf, Vander Beken et al. 2009). Their participation in mycobactericidal responses was demonstrated in a study showing that mice deficient in both LXR isoforms, LXR α and LXR β , were more susceptible to infection, developing higher bacterial burdens as well as increased size and number of granulomatous lesions (Korf, Vander Beken et al. 2009). As mentioned before, nuclear receptors control the expression of AIM (section 3.2 introduction), although the direct involvement of AIM in mycobactericidal response was unknown at the beginning of this thesis. For this reason, the study of the putative role of AIM in macrophage mycobactericidal mechanisms was one of the objectives of the present work.

OBJECTIVES

OBJECTIVES

The main objective of the present work was to analyze the immunomodulatory role of human AIM protein (hAIM) in macrophage response to bacterial aggression. More specifically, our objectives were:

1. To analyze the role of hAIM in the inflammatory response of macrophages to PAMPs and the subsequent intracellular signaling events.
2. To explore the effect of hAIM in macrophage phagocytosis.
3. To decipher the putative involvement of hAIM in *Mycobacterium tuberculosis* infection by:
 - Exploring AIM role in macrophage response against *Mycobacterium tuberculosis* in an *in vitro* infection model.
 - Analyzing AIM serum levels in a murine model of *M. tuberculosis* infection.

MATERIAL & METHODS

1. Cells

1.1. Peripheral blood monocytes

Buffy coats, provided by the Blood and Tissue Bank (BST, Barcelona, Spain) were obtained from healthy blood donors following the institutional standard operating procedures for blood donation and processing, all protocols were approved by the institutional Ethics Committee. Peripheral blood mononuclear cells (PBMCs) were isolated by Ficoll-Paque (GE Healthcare, Piscataway, NJ, USA) density gradient centrifugation at 400 xg for 25 min and CD3⁺ cells were depleted by RosetteSep human CD3 depletion cocktail (StemCell Technologies, Vancouver, BC, Canada). Recovered cells were washed twice in PBS and counted by flow cytometry using Perfect-Count microspheres (Cytognos, Salamanca, Spain) following the manufacturer's instructions. Peripheral blood monocytes (PB monocytes) were obtained by positive selection using human CD14 MicroBeads and autoMACS columns (Miltenyi Biotec, Auburn, CA, USA) (Naranjo-Gomez, Fernandez et al. 2005). To assess the effect of hAIM on PB monocytes, these were incubated for 24 h in RPMI 1640 2 mM glutamine (RPMI) containing 10% heat-inactivated fetal calf serum (FCS; Lonza, Basel, Switzerland), 100 U/mL penicillin and 100 µg/mL streptomycin (Sigma-Aldrich, St Louis, MO, USA) with 1 µg/mL albumin purified from human plasma (Alb), used as a control protein (Grifols, Barcelona, Spain), or 1 µg/mL endotoxin-free recombinant human AIM (rhAIM) (<1.0 EU per 1

µg of the protein by the LAL method). In these experiments, rhAIM was from two different sources; an affinity purified His-tagged rhAIM produced in the mouse myeloma cell line NS0 (R&D systems, Minneapolis, MN, USA), and an in-house produced rhAIM expressed in Chinese Hamster Ovary cells (section 2.1, material and methods).

1.2. Murine bone marrow-derived macrophages (BMDM)

BMDM were kindly provided by Dr. Annabel Fernández and Jonathan Matalonga (Nuclear Receptor Group, Department of Physiology and Immunology, University of Barcelona). BMDM were isolated as described (Celada, Gray et al. 1984). Briefly, Six-week-old BALB/C mice (Charles River Laboratories, Wilmington, MA) were killed by cervical dislocation, and both femurs were dissected free of adherent tissue. The ends of the bones were cut off and the marrow tissue was flushed by irrigation with media. The marrow plugs were dispersed by passing through a 25-gauge needle, and the cells were suspended by vigorous pipetting and washed by centrifugation. The cells were cultured in plastic tissue-culture dishes (150 mm) in 40 mL DMEM containing 20% FBS and 30% L-cell conditioned media as a source of macrophage colony-stimulating factor (M-CSF). Macrophages were obtained as a homogeneous population of adherent cells after 7 days of culture. The cells were incubated at 37°C in a humidified 5% CO₂ atmosphere.

1.3. Stably transfected THP1-vector and THP1-hAIM cell lines

To ease our functional studies and given that hAIM expression disappears in cultured cells (Miyazaki, Hirokami et al. 1999; Joseph, Bradley et al. 2004), the human acute monocytic leukemia cell line THP1 was transfected with the cDNA encoding full length hAIM. The generation of THP1-hAIM and THP1-Vector cells was described before (Amezaga 2013), but it is summarized below.

The cDNA-encoding hAIM was obtained by reverse transcription (Omniscript® Reverse Transcription kit; QIAGEN, Hilden, Germany) of human spleen mRNA (Clontech, Mountain View, CA, USA), where high expression of hAIM was detected by tissue northern blot (Gebe, Kiener et al. 1997), and subsequent PCR amplification (Expand High Fidelity PCR System; Roche, Mannheim, Germany). hAIM cDNA was introduced by NheI/NotI restriction in an appropriated digested mammalian expression pCI-neo vector (Promega), a kind gift of Dr. Maragarita Martín (University of Barcelona).

Subsequently, the human acute monocytic leukemia cell line THP1 (a kind gift of Dr. Alfonso del Rio, Fundació IGTP, Badalona) was transfected as described (Amezaga, Sanjurjo et al. 2013). Stably transfected cells were then maintained in RPMI supplemented with 10% FCS (Lonza), 250 µg/mL G418 (Invitrogen), 100 U/mL penicillin and 100 µg/mL streptomycin (Sigma-Aldrich) at a density of 10^5 to $5 \cdot 10^5$ cells/mL. Prior to the experiments, cells were differentiated to macrophages (MΦ) by incubation with 10 ng/mL of phorbol-12-myristate-13-acetate (PMA, Sigma-Aldrich) in culture medium for 48 h. They were then washed with PBS and grown in culture medium for 24 h

before experiments were performed. These cells are referred to as THP1 MΦ.

To validate hAIM expression, production and secretion in stably transfectant cell lines. hAIM mRNA expression was determined by quantitative Real Time PCR (qRT-PCR, as described in “section 3, material and methods”). Analysis of hAIM protein expression and secretion was performed by SDS-PAGE and western blotting of cell lysates as well as cell supernatants. Cell lysates were immunoprecipitated with a specific antibody and protein G-sepharose beads and protein content in cell supernatants by trichloroacetic acid/acetone protein precipitation, as described (Amezaga, Sanjurjo et al. 2013). As shown in **Figure 1A**, hAIM mRNA values in control cells were under the limit of detection of RT-qPCR whereas higher amounts were detected in hAIM expressing cells. Accordingly, in western blot analysis of cell lysates (**Figure 1B**) as well as culture supernatants (**Figure 1C**) a specific 37-40 kDa band was observed in hAIM-expressing cells.

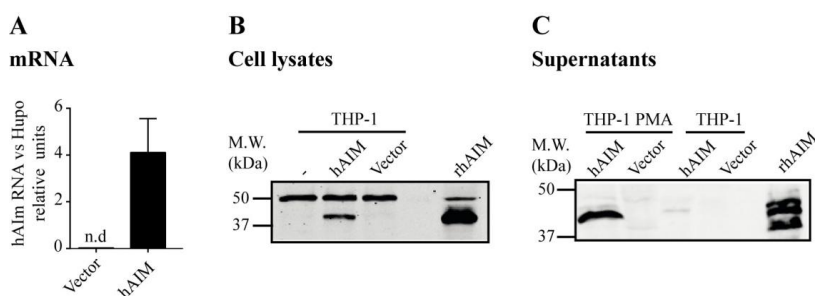


Figure 1. Validation of hAIM expression in stable transfectant THP1-hAIM cell line. (A) mRNA levels of hAIM were determined by RT-qPCR; gene expression values were normalized to the expression levels of human acidic ribosomal protein (HuPo). Graph showing mean \pm SEM of three independent experiments. (B-C) Representative images of hAIM protein detection analyzed by western blot with an specific antibody in cell lysates (B) and culture supernatants (C) showing a specific band at 37 KDa in hAIM expressing cells. rhAIM was used as positive control.

2. Production of recombinant proteins

A recombinant form of human (rhAIM) and mouse (rmAIM) AIM were produced in the laboratory as detailed below:

2.1. rhAIM

The cDNA of human AIM was obtained by gene synthesis (GenScript) following NCBI reference sequence NP_005885.1, with a modification in which the Immunoglobulin g chain signal peptide replaced that of hAIM. The cDNA was cloned into the p.evi vector and transiently transfected into CHO K1 cells using the eviFect system (Eviatria AG). Cells were grown in eviMake, a chemically defined, serum-free, animal component-free medium. The cell culture supernatant was harvested at day 8 after transfection, dialyzed to 20 mM Na₂HPO₄, pH 7.4 and subjected to MonoQ chromatography. Recombinant hAIM was eluted in a sodium chloride gradient, and purification was monitored by SDS-PAGE (Figure 2A). Purified protein

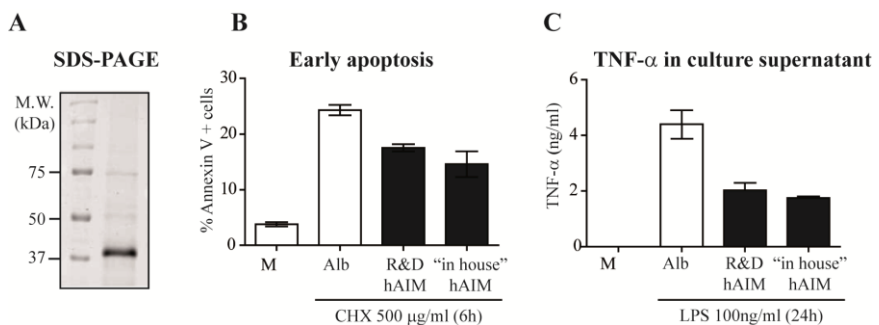


Figure 2. Validation of rhAIM purification and activity. (A) Representative image of 1 µg of purified rhAIM resolved by SDS-PAGE, showing a predominant band at 37-40 kDa. (B-C) PMA differentiated THP1 cells were incubated during 24h with 1 µg/ml of control protein human albumin (Alb), commercial rhAIM (R&D Systems) or “in-house” produced rhAIM. (B) Apoptosis was induced by 24 incubation with 500 µg/mL cycloheximide (CHX, Sigma-Aldrich), then cells were stained with 2.5 µL of Phycoerythrin (PE) conjugated Annexin V (BD biosciences), % of early apoptotic cell was determined by flow cytometry. (C) Cells were stimulated with LPS for 24h and culture supernatants were analyzed for TNF-α production by ELISA. The figure shows that rhAIM from both sources reduces percentage of annexin positive cells as well as MΦ TNF-α secretion to a similar extent.

was dialyzed to PBS, concentrated by centrifugation on Amicon ultra (Millipore), and possible endotoxin contamination was removed by Endotrap columns (Hyglos GmbH), following the manufacturer's protocol and as performed (Sarrias, Rosello et al. 2005). The purified rhAIM was tested in preliminary experiments, where its activity in terms of inhibition of M Φ apoptosis (**Figure 2B**) and TNF- α secretion (**Figure 2C**) were comparable to that of commercially available rhAIM (R&D Systems).

2.2. rmAIM

To obtain mAIM for its use as a positive control in phagocytosis experiments and for assisting in western blot determination of mAIM in mouse serum samples, a recombinant form of the protein was expressed in the laboratory as follows. mAIM cDNA was obtained by reverse transcription of C57BL/6 mouse spleen mRNA (Clontech) where high expression of mAIM was previously detected (Miyazaki, Hirokami et al. 1999) and subsequent PCR amplification with the following primers was performed. Forward primer incorporated the NheI restriction site (*GCTAGC*), while reverse primer incorporated stop codon followed by the BamHI restriction site (*GGATCC*):

Fw: 5'- GCCCGGCTAGCGGAGTCTCCAACCAAAGTG -3'

Rv: 5'- CGCGCGGATCCTCACACATCAAAGTCTG -3'

Mouse AIM cDNA was cloned into the *in* pGEM[®]-T vector (Promega); cDNA was further NheI/BamHI-restricted and cloned into appropriately digested pCEP-4 vector (Invitrogen). Subsequently, human embryonic kidney (HEK) 293 cells were transiently transfected with 4 μ g pCEP-4 vector or pCEP-4/mAIM

construct using transfectin lipid reagent (Bio-Rad Laboratories). Intracellular expression of mAIM in transfected cell lysates was assessed by western blot. Immunodetection was performed with anti-mouse AIM biotinylated poAb (0.1 µg/mL, R&D Systems). Given that AIM circulates in serum in relative high amounts (Tissot, Sanchez et al. 2002; Sarrias, Padilla et al. 2004; Arai, Maehara et al. 2013) 1µL of mouse C57Bl/6 serum was used as a positive control in western blot. As shown in **Figure 3**, a specific 50 KDa band was detected in mouse serum as well as in cell lysates of mAIM-expressing HEK cells.

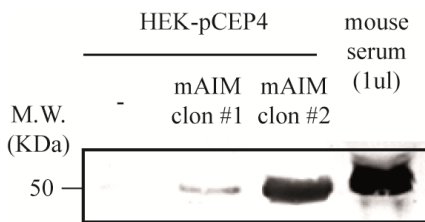


Figure 3. Validation of mAIM expression in HEK transiently transfectant cell lines. Representative image of mAIM detection analyzed by western blot of cell lysates with a specific antibody. 1µL of C57BL/6 mouse serum was used as positive control. A specific 50 kDa band was detected in cell lysates as well as in mouse serum sample.

3. Quantitative Real Time PCR (qRT-PCR)

RNA from 10^6 THP1 M Φ or PB monocytes was isolated using the QIAzol reagent and purified with an RNeasy mini kit (QIAGEN), following the manufacturer's instructions. Total RNA (1 μ g) was reverse-transcribed using the Transcriptor First Strand cDNA Synthesis Kit (Roche). Then, 2 μ l of each RT reaction was amplified in a LightCycler® 480 PCR system (Roche), using the KAPA SYBR Fast Master Mix (KAPA Biosystems, Woburn, MA, USA). Samples were incubated for an initial denaturation at 95°C for 5 min, followed by 40 PCR cycles under the following conditions: 95°C for 10 s, 60°C for 20 s and 72°C for 10 s. All the primer pairs used in this study are listed in Table 1.

Gene	Forward primer (5'-3')	Reverse primer (5'-3')
hAIM	GACGAGAAGCAACCCTTCAG	CCCAGAGCAGAGGTTGTCTC
TNF- α	GAGGAGGCGCTCCCCAAGAAG	GTGAGGAGCACATGGGTGGAG
IL-1 β	ACGCTCCGGGACTCACAGCA	TGAGGCCCAAGGCCACAGGT
IL-6	TCGAGCCCACCGGAACGAA	GCAGGGAAGGCAGCAGGCAA
IL-10	CGTGGAGCAGGTGAAGAATG	AGAGCCCCAGATCCGATTTT
GAPDH	TCTTCTTTTGCCTCGCCAG	AGCCCCAGCCTTCTCCA
DEFB4	GGTGTTTTTGGTGGTATAGGCG	AGGGCAAAAAGACTGGATGACA
LL-37	TGCCCAGGTCCTCAGCTAC	GTGACTGCTGTGTCGTCCT
HuPo	GAGAACTGTTATGGGGCTAT	TTCAACTGGAGAGGCCAAAGG

Table 1. List of primers used in this study

Gene expression values were normalized to the expression levels of glyceraldehyde 3-phosphate dehydrogenase (GAPDH). Based on a comparative study that described human acidic ribosomal protein (HuPo) as the most suitable housekeeping gene for normalizing mRNA

levels in human pulmonary tuberculosis (Dheda, Huggett et al. 2004), in *Mycobacterium tuberculosis* infected samples HuPo gene was used to normalize gene expression values. Fold induction was calculated using the levels of expression of each gene in unstimulated conditions in the control cell line as a reference.

4. Western blot analysis of cell lysates

Cells were washed in cold TBS and lysed in TBS lysis buffer [20 mM Tris (pH 7.5) containing 150mM NaCl, 1 mM EDTA, 1 mM EGTA, 1% Triton-X100, 1 mM Na₃VO₄, 1 mM PMSF (all from Sigma-Aldrich) and complete protease inhibitor mixture tablets (Roche)] for 30 min at 4°C. Nuclei and cell debris were removed by centrifugation at 8000 xg for 15 min, and protein concentration was measured with the BCA protein assay reagent kit (Thermo Fisher Scientific), following the manufacturer's instructions. 40-50 µg of cell lysates were resolved in 10% SDS-polyacrylamide gels (12% for LC3 analysis) under reducing conditions and electrophoretically transferred to nitrocellulose membranes (Bio-Rad Laboratories). These were then blocked with Starting Block TBS buffer (Thermo Fisher Scientific) for 1 h at RT and incubated overnight at 4°C with the indicated primary antibodies diluted in blocking buffer. The membranes were subsequently incubated with the appropriate fluorescently coupled secondary antibodies IRDye 680Cw conjugated goat anti rabbit IgG (0.05 µg/mL; Thermo Fisher Scientific) and IRDye 800Cw conjugated goat anti-mouse IgG (0.05 µg/mL; LI-COR Biosciences) or with IRDye 680Cw-conjugated streptavidin (0.05 µg/mL; LI-COR Biosciences) diluted in blocking buffer for 60 min at RT. Three 15-min washes between steps were performed with TBS-0.01% Tween 20. Bound antibody was detected with an Odyssey Infrared Imager (LI-COR Biosciences) and densitometric analysis was performed by using the Odyssey V.3 software (LI-COR Biosciences). Blots were also probed against β-tubulin or β-actin with specific mAbs (Sigma-Aldrich) to determine equal loading.

5. Measurement of cytokine and chemokine secretion

5.1. Multi-Analyte Profiling (MAP) technology

TNF- α , IL-6, IL-1 β and IL-10 amounts were determined on culture supernatants using a Procarta Human Cytokine Profiling kit (Affymetrix Inc., Santa Clara, CA, USA). The xMAP technology uses a 96-well plate format and polystyrene microspheres which are internally dyed with red and infrared fluorophores. The use of different intensities of each dye allows distinguishing one bead from another by its red/infrared mixture. Capture antibodies for a specific cytokine were coated on the microsphere surface. Then, different microspheres for the detection of different proteins were combined within the same assay in a single reaction volume (50 μ L). After an overnight incubation, a biotinylated detection antibody which binds to the proteins-bead complex was added. The sample was then incubated with the reporter molecule streptavidin-phycoerythrin, to complete the reaction on the surface of each microsphere. Detection of the multiplexed results was performed using the Luminex system (Luminex 100 analyzer, Luminex Corp., Austin, TX, USA). Based on the principle of flow cytometry, the microspheres were allowed to pass individually through a detection chamber. A first laser excites both the internal red and infrared dyes, distinguishing the microsphere. A second laser excites phycoerythrin, the fluorescent dye on the reporter molecule allowing the quantification of the cytokines/chemokines bound to the beads (**Figure 4**). These experiments were performed in BST facilities thanks to the assistance of Dr. Carina Cardalda.

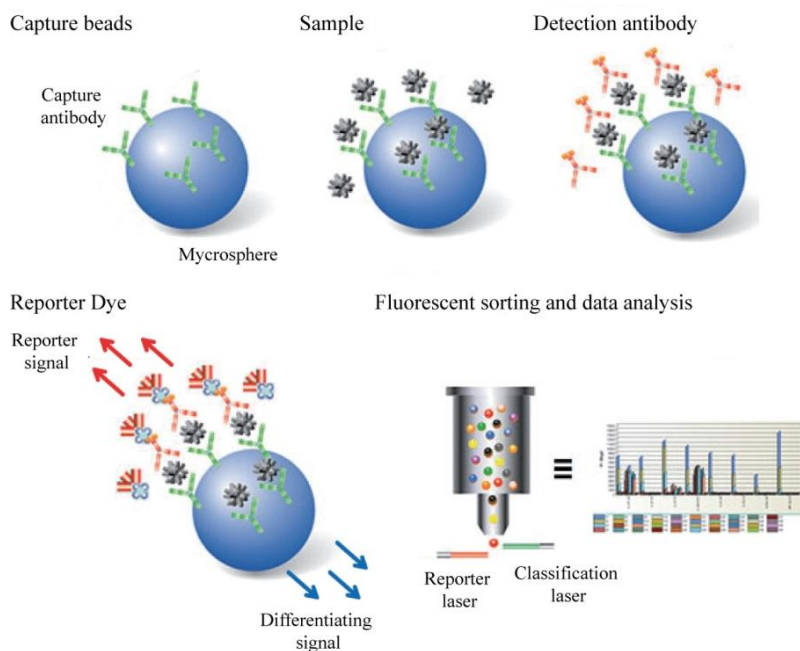


Figure 4. Principle of the xMAP technology. Distinctly colored bead sets are coated with specific capture antibodies. After an analyte from a sample is captured by the bead, a biotinylated detection antibody is introduced. The reaction mixture is then incubated with Streptavidin-PE, the reporter molecule, to complete the reaction on the surface of each microsphere. Fluorescent sorting allows distinguish each class of beads and quantify reporter signal intensity in each bead. Figure adapted from Bio-Rad Applications & Technologies (Bio-Rad).

The minimum detectable concentration (pg/mL) of each protein was 0.1 for TNF- α , 0.4 for IL-1 β , 0.3 for IL-6 and 0.3 for IL-10. All the cytokines measured were over the detection limit, and inside the detection range of their respective standard curves.

5.2. Enzyme-linked ImmunoSorbent Assay (ELISA)

Culture supernatants were assayed for the presence of TNF- α , IL-1 β , IL-8 and IL-10 with sandwich ELISA kits (OptEIA ELISA set, BD Biosciences, Franklin Lakes, NJ, USA). For each cytokine, capture Ab was previously coated overnight at 4°C on a Maxisorp® flat-bottom 96 well plate (NUNC, Thermo Fisher Scientific). Next, wells were blocked at room temperature for 1 h using PBS 20% FCS. The procedure continued with 2 h incubation with the appropriately diluted culture supernatants, followed by 1 h incubation with the biotin labeled detection Ab and the streptavidin-horseradish peroxidase (HRP). Three washes with PBS-0,1% Tween 20 (sigma-Aldrich) were performed between steps. Color was developed by adding 3,3',5,5'-tetramethylbenzidine liquid substrate (TMB) and the enzymatic reaction was stopped using 1M H₃PO₄ Stop solution. The optical density was read at 450 nm using a Varioskan Flash microplate reader (Thermo Fisher Scientific). The minimum detectable concentration (pg/mL) was 2.0 for TNF- α , 0.3 for IL-1 β , 0.8 for IL-8 and 0.2 for IL-10. All the cytokines measured were over the detection limit mentioned before and inside the detection range of their respective standard curves.

6. Immunocytochemistry (ICC) and fluorescent microscopy

THP1 cells (5×10^4 cells/well) or PB monocytes (10^5 cells/well) were plated in Millicell EZ slides (Merck Millipore, Darmstadt, Germany). Cells were washed once with PBS and fixed with PBS containing 5% paraformaldehyde (PFA; Panreac, Castellar del Vallès, Catalonia, Spain) for 30 min. They were then incubated with specific primary antibodies in PBS containing 0.3% Triton X-100 and 10% Human AB serum (Sigma-Aldrich) for 24 h at 4°C. Then cells were subsequently incubated with the appropriate FITC or Alexa Fluor® 647-conjugated antibodies for 1 h at RT in PBS containing 0.3% Triton X-100. Between steps, unbound antibodies were removed with three washes with PBS. Finally, nuclei were stained with PBS containing 800 nM Hoechst solution (Invitrogen) for 10 min at RT. Cells were washed three times with PBS, and coverslips were mounted in Fluoromount™ mounting medium (Sigma-Aldrich) and left at 4°C overnight. The slides were examined using the following three different types of microscopes as indicated: fluorescence inverted microscope, laser scanning (LS) microscope or confocal microscope. Inverted and LS microscopy analysis were conducted in IGTP Microscopy Unit (Badalona), thanks to the assistance of Gerard Requena, using Zeiss Axio Observer Z1 Inverted Microscope and AxioVision 4.8 software for inverted microscopy, and Laser scanning Axio Observer Z1 DUO LSM 710 confocal system and ZEN Black software for LS microscopy (Carl Zeiss, MicroImagin, Jena, Germany). Confocal studies were performed at the Microscopy Platform of Vall d'Hebron Research Institute (VHIR, Barcelona), thanks to the collaboration with Marta Valeri, and using

FluoView™ FV1000 Spectral Confocal microscope and FluoView™ FV10-ASW 3.1 software (Olympus, Shinjuku, Tokyo, Japan).

7. Immunostaining for flow cytometry analysis

2×10^5 THP1 M Φ or PB monocytes in culture medium or incubated with 1 $\mu\text{g}/\text{mL}$ of LPS or Pam3CSK4 for 2 h were detached from 24-well culture plates with accutase (PAA Laboratories, UK), washed twice in ice-cold PBS and incubated with 100 μl of PBS containing 10% human AB serum (Sigma-Aldrich), 2% FCS (Lonza) and 0.02% NaN₃ (blocking buffer) for 30 min on ice, cells were then incubated with 10 $\mu\text{g}/\text{mL}$ mouse moAb anti-TLR2 (clone 383936, R&D Systems), mouse moAb anti-TLR4 (clone HTA125, Affymetrix), or mouse FITC conjugated moAb anti-CD36 (ImmunoTools, Friesoythe, Germany), for 90 min at 4°C in blocking buffer. Cells were washed once with 3 mL PBS containing 2% FCS and 0.02% NaN₃ (washing buffer) and incubated, when needed, with FITC conjugated anti-mouse IgG/IgM antibody (BD Biosciences) in blocking buffer for 45 min at 4°C. After washing with 3 mL of washing buffer, acquisition was performed in a FacsCanto II flow cytometer using the standard FacsDiva software (BD Biosciences; Flow Cytometry Unit, IGTP, Badalona). Samples were gated using forward (FSC) and side (SSC) scatter to exclude dead cell and debris.

8. Analysis of macrophage intracellular signalling

To assay the effects of hAIM in macrophage intracellular signalling in response to inflammatory stimuli, two signalling pathways were assayed: the mitogen-activated protein kinases (MAPKs) and phosphatidyl inositol 3 kinase (PI3K) pathways by their relevance in TLR signalling (Brown, Wang et al. 2010), as well as the effect in nuclear factor kappa B (NF- κ B) activation. Then, based on the results obtained and in recent developments that reveal a crucial role for the autophagy pathway and proteins in immunity and inflammation (Deretic, Saitoh et al. 2013), hAIM involvement in the modulation of macrophage autophagy was also analyzed.

8.1. MAPK and PI3K

To address the intracellular signalling events modulated by hAIM in the settings of inflammation, two different experimental approaches were performed in TLR stimulated cells. First, cytokine production was analyzed in the presence of specific signalling inhibitors of kinases involved in macrophage TLR response. To corroborate the results obtained, MAPK activity was determined by time-course phosphorylation analysis, and PI3K activity was measured by quantification of its products of activation (phosphatidilinositols, PIs) by fluorescent microscopy.

8.1.1. Cell stimulation with TLR ligands and selective kinase inhibition

THP1 MΦ (5×10^4 cells/well) or PB monocytes (10^5 cells/well) were plated in 96-well plates and stimulated at 37°C with TLR agonists, including Pam3CSK4 (TLR2/1 agonist), FSL1 (TLR2/6 agonist) and LPS (TLR4 agonist) all from InvivoGen (San Diego, CA, USA) in culture medium containing 4% FCS, at indicated concentrations. Four h later, culture supernatants were collected and assayed for TNF- α production. Supernatants from Pam3CSK4 or LPS-stimulated cells were also collected at 24 h and analyzed for IL-6, IL-1 β and IL-10 production. For determine cytokine amounts in culture supernatants MAP or ELISA techniques were used when indicate. In the experiments performed in the presence of signalling inhibitors, listed in Table 2, these were added 45 min previous to TLR stimulation. DMSO used to dilute the inhibitors was added in control wells.

Pathway	Kinase	Subunit	Name	Working concentration	Supplier
MAPK	p38		SB203580	20 μ M	Invivogen
	JNK		SP600125	50 μ M	Invivogen
	MEK		PD98059	100 μ M	Invivogen
PI3K	PI3K	Pan- PI3K	LY294002	200 μ M	Invivogen
	PI3K	Pan- PI3K	Wortmannin	10 μ M	Invivogen
	Class I PI3K	Pan- Class I PI3K (P110 α , β , δ , γ)	Pi-103	1 μ M, 0.1 μ M, 0.01 μ M	Echelon Biosciences
	Class IA PI3K	P110 δ	IC87114	10 μ M, 1 μ M, 0.1 μ M	Echelon Biosciences
	Class IB PI3K	P110 γ	AS605240	10 μ M, 1 μ M, 0.1 μ M	Echelon Biosciences
	Class III PI3K	Vps34	3-Methyladenine	1mM, 0.1mM, 0.01mM	Sigma-Aldrich

Table 2. Signaling inhibitors used in this study.

8.1.2. MAPKs phosphorylation analysis

THP1 M Φ (1.5×10^6 cells/well) or PB monocytes (2×10^6 cells/well) were plated in 6-well plates and incubated at 37°C with 0.5 $\mu\text{g}/\text{mL}$ of Pam3CSK4 or LPS for the indicated periods of time. Time-course determination of MAPKs phosphorylation in total lysates was determined by SDS-PAGE and western blot as previously described. The following primary antibodies were used: rabbit moAb phosphorylation site-specific antibodies anti p38, ERK1/2, JNK1/2 (1/1000; Cell Signalling Technology, Boston, MA, USA). Equal loading in western blots was determined by probing against β -tubulin and fold induction was calculated using the levels of band intensity of each protein in unstimulated conditions in control cell line as a reference.

8.1.3. Quantification of PI3P

The cellular levels of the PI3K metabolite PI3P were measured as an indicator of class III PI3K activity. THP1 and PB monocyte PI3P cellular content was measured by ICC using a specific anti-PI3P MoAb (5 $\mu\text{g}/\text{mL}$, Echelon Bioscience Inc) and subsequently a secondary FITC-conjugated anti-mouse IgG/IgM antibody (BD Biosciences). Cells were pre-treated for 45 min with 0.1 mM 3-methyladenine (3-MA, -Vps34) and then incubated with 1 $\mu\text{g}/\text{mL}$ Pam3CSK4 for 30 min before cell fixation when indicated. The slides were examined using LS microscopy (Microscopy Unit, IGTP, Badalona) and fluorescence intensity quantification was performed using the “measure tool” of ImageJ software (National Institutes of Health, NIH, Maryland, US).

8.1.4. NF- κ B translocation assay

The inactive p50/p65 NF- κ B heterodimer is located in the cytoplasm, complexed to its I κ B inhibitory unit. Stimulation of M Φ by various reagents such as bacterial LPS leads to a dissociation of NF- κ B from I κ B and a rapid translocation of free NF- κ B to the nucleus. In this work, as indicator of NF- κ B activation, NF- κ B p65 translocation to the nucleus was measured by ICC and LS microscopy as follows. ICC slides were stained ON with poAb anti-NF- κ B p65 (Cell Signaling Technology) and subsequently with Alexa Fluor® 647 labeled F(ab')₂ Fragment of Goat Anti-Rabbit IgG (H+L) secondary antibody (Invitrogen). NF- κ B (p65) nuclear: cytoplasm ratio was quantified using ImageJ software (National Institutes of Health) in 250 cells of three independent experiments as described (Noursadeghi, Tsang et al. 2008).

8.2. Autophagy pathway

Autophagy is a dynamic, multi-step process that can be modulated at several points, both positively and negatively. Klionsky et al. in *Guidelines for the use and interpretation of assays for monitoring autophagy* (Klionsky, Abdalla et al. 2012) recommend the use of multiple assays to verify an autophagic response. In the present work we combined the measurement of autophagy induction analyzing both positive (LC-3) and negative (AKT phosphorylation) autophagy-related markers together with monitorization of double-membrane autophagosome formation by electron microscopy and determination of autophagic flux.

8.2.1. Monitoring of autophagy-related proteins

- **LC3 conversion**

THP1 cells (1.5×10^6 cells/well) or PB monocytes (2×10^6 cells/well) were plated in 6-well plates and incubated at 37°C with 0.5 µg/mL of Pam3CSK4 or LPS for the indicated periods. Microtubule-associated protein 1A/1B-light chain 3 (LC3) cytosolic form (LC3-I) and phosphatidylethanolamine conjugate (LC3-II), which is generated and recruited to autophagosomal membranes during autophagy, were detected by western blot with rabbit anti-LC3 poAb (5 µg/mL, Novus Biologicals, Littleton, CO, USA) in total cell lysates resolved in 12% SDS-polyacrylamide gels. LC3 protein signal intensities were plotted as LC3-II/LC3-I ratio.

- **LC3 puncta formation**

LC3 accumulation in autophagosomes was detected by ICC and LS microscopy (Microscopy Unit, IGTP, Badalona) as previously detailed. Cell preparations were stained ON with rabbit poAb anti-LC3 (5 µg/mL, Novus Biologicals) and subsequently with Alexa Fluor® 647 labeled F(ab')₂ Fragment of Goat Anti-Rabbit IgG (H+L) secondary antibody (2 µg/mL, Invitrogen). LC3 puncta per cell were determined using the ImageJ software and puncta analyzer plug-in (NIH), in thresholded images with size from 3 to 30 pixel² and puncta circularity 0.8-1 as described previously (Cannizzo, Clement et al. 2012). When indicated, cells were pre-incubated with the autophagy inhibitor 3-methyladenine (1mM, 3-MA) (Sigma-Aldrich) 45 min before cell fixation.

- **AKT phosphorylation**

THP1 cells (1.5×10^6 cells/well) or PB monocytes (2×10^6 cells/well) were plated in 6-well plates and incubated at 37°C with 0.5 µg/mL of Pam3CSK4 or LPS for the indicated periods of time. Time course-phosphorylation of AKT was determined by western blot as previously described. For immunodetection anti phospho-specific anti-AKT (Ser 473) and anti pan AKT antibodies (1/1000; Cell Signalling) were used. Equal loading in western blots was determined by probing against β -tubulin. Fold induction was calculated using the levels of band intensity of each protein in unstimulated conditions in the control cell line as a reference.

8.2.2. Ultrastructural analysis by electron microscopy

The hallmark of autophagy process is formation of double-membrane autophagosomes, given to autophagy and LC3-mediated phagocytosis (LAP) shares many components of the same cellular machinery. One way to differentiate these processes is to confirm by electron microscopy the presence of double membrane vesicles. THP1 M Φ (10^7) were fixed with 2.5% glutaraldehyde in phosphate buffer. They kept in the fixative during 2 h at 4°C. Then, they were washed with the same buffer and postfixed with 1% osmium tetroxide in the same buffer containing 0.8% potassium ferricyanide at 4°C. Then the samples were dehydrated in acetone, infiltrated with Epon resin during 2 days, embedded in the same resin and polymerised at 60°C during 48 h. Ultrathin sections were obtained using a Leica Ultracut UC6 ultramicrotome (Leica Microsystems, Vienna) and mounting on Formvar-coated copper grids. They were stained with 2% uranyl acetate in water and lead citrate. Then, 25 sections/cell line were

observed in a JEM-1010 electron microscope (Jeol, Japan). These assays were performed by the electron microscopy facility at Parc Científic de Barcelona, University of Barcelona, thanks to the kind assistance of Dr. Carmen Lopez-Iglesias.

8.2.3. Measurement of autophagic flux

The term “autophagic flux” is used to denote the dynamic process of autophagosome synthesis, delivery of autophagic substrates to the lysosome, and degradation of autophagic substrates inside the lysosome. To measure autophagy flux, colocalization of LC-3 puncta with acidic organelles was determined by LS microscopy (Microscopy Unit, IGTP, Badalona). Cells cultured in Millicell EZ slides were incubated with 100 nM of the *acidotropic* probe for labeling and tracking acidic organelles LysoTracker Red (Molecular Probes, Life Technologies, NY, USA) diluted in pre-warmed RPMI medium, then cells were fixed with PFA and LC3 was stained as previously indicated. LC3-LysoTracker double positive puncta per cell were determined using green and red puncta colocalization macro (Pampliega, Orhon et al. 2013) and ImageJ software (NIH) in thresholded images with size from 3 to 30 pixel² and puncta circularity 0.8-1.

9. Silencing of ATG7 and CD36 expression

To silence ATG7 and CD36 cell expression, undifferentiated THP1 MΦ were transfected with 10 nM of a set of 4 small-interfering RNAs (siRNAs) targeting either ATG7, CD36, or an equal concentration of a non-targeting negative control pool (ON-TARGET plus siRNA, Dharmacon; Thermo Fisher Scientific), by using INTERFERin® (Polyplus, France) following the manufacturer's instructions. After 24 h, the medium was replaced, and cells were differentiated for 24 h in culture medium supplemented with 50 ng/mL PMA, then PMA-containing medium was replaced by culture medium, and cells were incubated for further 24 h before being tested for ATG7 or CD36 expression by western blot and flow cytometry analysis, respectively (Figure 5).

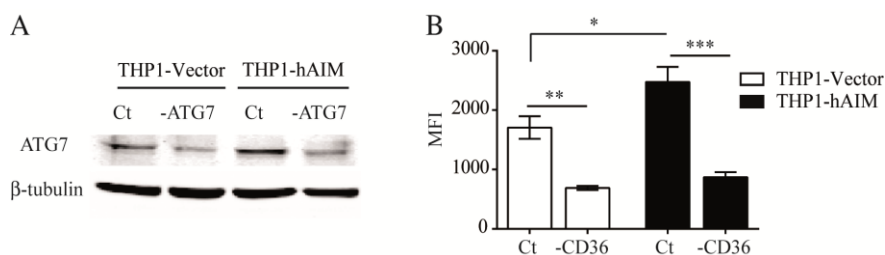


Figure 5. Validation of ATG7 and CD36 silencing in THP1 cells. THP1 MΦ were transfected with non-targeting negative control (Ct) or with siRNA targeting ATG7 (-ATG7) or CD36 (-CD36). (A) Western blot analysis of ATG7 protein silencing in THP1 MΦ. Detection of β -tubulin was used as a measure of equal loading. (B) CD36 surface expression was analyzed by flow cytometry with a specific antibody. The graph shows mean fluorescence intensity (MFI) values of four independent experiments performed in duplicate. Western blot shows a visible reduction of ATG7 intracellular protein content and data of flow cytometry shows that CD36 siRNA lowered surface expression over 60 % in both cell types.

10. Phagocytosis assays

2.5*10⁵ cells were plated in 24-well plates and incubated with 3 μM YG Fluoresbright™ microspheres (Polysciences, Warrington, PA, USA), fluorescent bioparticles *Escherichia coli* K-12 and *Staphylococcus aureus* (wood strain, without protein A) (Molecular Probes) or *Mycobacterium tuberculosis* H37Rv stained with FITC (see section 9.1 Math and Mets) at the indicated doses, lengths of time and at 37°C or 4°C. Incubation at 4°C was performed to measure extracellular attachment rather than internalization, since no uptake occurs at this temperature. Then cells were harvested by scrapping, extensively washed with cold PBS and fixed with PBS containing 5% PFA (Panreac) for 30 min. Phagocytosis was quantified by flow cytometry as follows: after incubation the percentage of FITC-positive cells were determined on a FACScalibur instrument using the CellQuest software (BD Biosciences). Samples were gated using forward (FSC) and side (SSC) scatter to exclude dead cell and debris. In experiments with Fluoresbright™ microspheres it was possible to differentiate cells that phagocytized 1, 2 or 3 or more microspheres (**Figure 6**) thanks to the assistance of Marco Fernandez (Cytometry unit IGTP, Badalona).

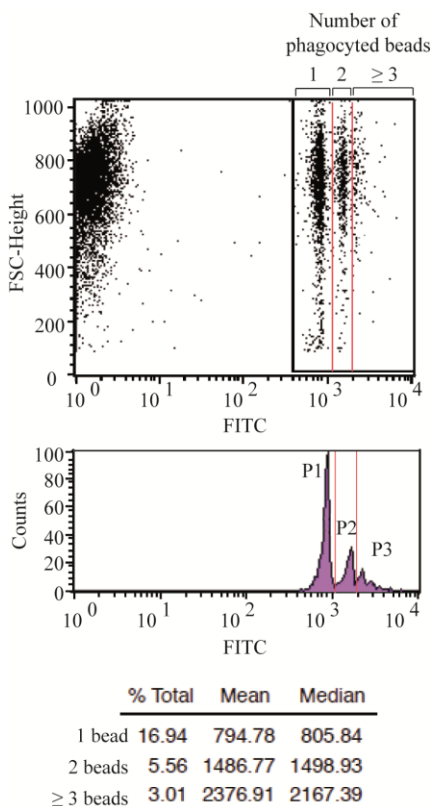


Figure 6. Optimization of Fluoresbriht™ microspheres phagocytosis experiments. THP1-Vector cells were incubated with 3 μ M YG Fluoresbriht™ microspheres at 10: 1 (beads: cells) ratio for 1 h at 37 °C, then phagocytosis was analyzed by flow cytometry. The figure shows a representative experiment. Upper panel: FITC dot plot. Lower panel: histogram of FITC positive populations, first peak (P1) correspond to the macrophages that had phagocytized a single bead, second peak (P2) correspond to macrophages that had phagocytized 2 beads and third peak (P3) to cells that had phagocytized 3 or more beads, showing that these 3 populations can be gated and analyzed separately.

11. Measurement of *Escherichia coli* ingestion and killing by counting colony forming units (CFUs)

10^5 THP1 M Φ were plated in 24-well plates and incubated at 37°C with *E coli* strain JM109 (Promega) at ratio of 10 bacteria: 1 cell. 30 and 90 min later cells were thoroughly washed with sterile PBS and then lysed with PBS 0.9% Triton X-100 (Sigma-Aldrich). Serial 10-fold dilutions of cell lysates were plated in LB-Agar plates. 24-48 h later, intracellular CFUs numbers were determined by colony counting setting the countable range as 10 to 200 visible colonies per plate.

12. Study of the antimicrobial response against *Mycobacterium tuberculosis*.

Thanks to the collaboration with the Experimental Tuberculosis Unit (UTE, IGTP, Badalona) a set of *in vitro* experiments were performed to assay the participation of hAIM in the macrophage response to *M. tuberculosis*. Moreover, mAIM serum levels were analyzed in an experimental murine model of tuberculosis infection. Material and methods of the *in vitro* *M. tuberculosis* infection model and animal experiment performed are detailed below.

12.1. Bacteria

M. tuberculosis H37Rv Pasteur strain (Mtb) was grown in 250-mL PYREX bottles in a shaking incubator at 37°C and at 120 rpm in Middlebrook 7H9 broth (BD Biosciences) supplemented with 0.2% glycerol, 0.5% albumin-dextrose catalase (BD Biosciences) and 0.05% Tween 80. Bottle caps were left half open to allow unlimited O₂ availability. Bacteria were grown to mid-log phase and stored at -70°C in 3 mL aliquots. For phagocytosis and autophagy experiments, bacteria were labeled with FITC (Mtb-FITC) (Sigma-Aldrich) as follows: 4*10⁷ bacteria were incubated for 1 h at RT in 0.2M Na₂CO₃-NaHCO₃ buffer (pH 9.5) (Merck Millipore) containing 0.01% (w/v) FITC. They were then washed three times with PBS and resuspended in medium RPMI supplemented with 10% FCS. The Mtb-FITC were prepared in large volumes, aliquoted, frozen, and stored at -80°C for later use. After each Mtb-FITC stock preparation number and viability of bacteria was assayed by plating serial dilutions of Mtb-FITC on Middlebrook 7H11

agar plates (BD Biosciences) and counting CFUs 21 days after 37°C incubation.

12.2. In vitro *M. tuberculosis* infection model

12.2.1. Infection solution preparation and experimental design

The infection solution was prepared by diluting the frozen aliquoted Mtb with RPMI medium supplemented with 10 % FCS to obtain a final concentration of 2×10^6 Colony Forming Units (CFU)/mL following centrifugation at 2000 xg for 20 min to remove the 7H9 Middlebrook medium. Pelleted bacilli were resuspended with culture medium keeping the 2×10^6 CFU/mL concentration, then serial dilutions were performed vortexing 1 min between steps. THP1-Vector and THP1-hAIM cells were PMA differentiated (10 ng/mL) during 48 h (THP1 MΦ) followed by one day of resting in RPMI 10% FCS without Abs. Monolayers were infected with infection solution at the indicated multiplicities of infection (MOIs). After 4 h non-ingested bacilli were removed by washing three times with PBS and RPMI 10% FCS medium was subsequently replenished. At the indicated time points, as summarized in **Figure 7**, different functional analysis were performed: macrophage and bacterial viability, foam cell formation, cytokine secretion and analysis of the following macrophage mycobactericidal mechanisms: nitric oxide (NO) and reactive oxygen species (ROS) production, expression of antimicrobial peptides and macrophage autophagy. Also hAIM mRNA and protein expression in response to Mtb infection were analyzed.

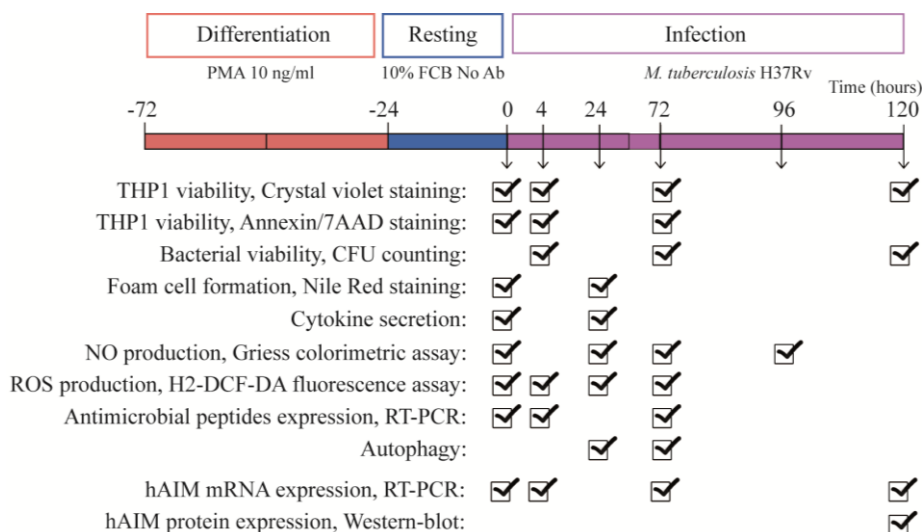


Figure 7. Experimental design of THP1 Mtb infection and subsequent functional analysis

12.2.2. Measurements of THP1 viability

- **Crystal violet staining**

THP1 MΦ (10^5 cells/well) were infected at MOI: 0.1, 1 or 10 in 24-well plates as described above. Cells were washed with PBS at the indicated time points, fixed by incubation with 10% formamide (Sigma-Aldrich) and then stained with a 0.5% (w/v) crystal violet (Sigma-Aldrich) solution in 2% ethanol for 10 min. The plates were then rinsed three times with water and allowed to dry. After this, the dye was solubilized in 2% SDS (w/v) (Merck Millipore) for 30 min at RT. The optical density at 590 nm was recorded on a Varioskan Flash microplate reader (Thermo Fisher Scientific). Viable cell numbers were calculated against a standard curve of known cell numbers.

- **Apoptosis**

THP1 MΦ (10^5 cells/well) were infected at MOI: 0.1 or 1 in 24-well plates as described above. At indicated time points they were then removed from plates with accutase (PAA Laboratories), washed twice in ice-cold PBS and resuspended in 100 μ L of binding buffer, cells were then incubated with 2.5 μ L of Phycoerythrin (PE) conjugated Annexin V in conjunction with 2.5 μ L of a vital dye 7-Amino-Actinomycin (7-AAD) (BD Biosciences) for 15 min in the dark. With the aim of killing the bacilli to ensure our own safety in further analysis, cells were then incubated in PBS containing 5% paraformaldehyde (Panreac, Castellar del Vallès, Catalonia, Spain) for 20 min and then analyzed with a FACSCantoll instrument and FACSDiva software (BD Biosciences). Apoptosis was expressed as the percentage of Annexin V-positive 7-AAD-negative cells.

12.2.3. Quantification of mycobacterial growth

THP1 MΦ (10^6 cells/well) were infected at MOI: 0.1 or 1 in 6-well plates as described above. At 4, 24 and 72 h infected cells were washed three times with 1 mL RPMI by centrifugation 300 xg 5 min to remove the unbound bacteria, then for collect intracellular bacteria cells were lysed by pipetting up and down repeatedly with 1 mL sterile water, this step was repeated 3 times. To pellet the bacteria, cell lysates were centrifugated at 2000 xg 20 min and pellets were resuspended vigorously in 1 mL sterile water (Dilution 0). 10-fold serial dilutions (-1, -2, -3) were prepared in sterile conical tubes vortexing thoroughly for 1 min between dilutions. The amount of intracellular bacilli was measured by plating 0.1 mL of serial dilutions on Middlebrook 7H11 agar plates (BD Biosciences) and counting bacterial

colony formation (200 colonies/plate maximum) after 21 days of incubation at 37°C.

12.2.4. Foam cell quantification

10^5 THP1 cells/well were plated in 24-well plates, PMA-differentiated and infected as described above at MOI 0.1 for 24h in RPMI 1% FBS, and subsequently stained with Nile Red as follows. Cells were fixed in PBS containing 5% PFA (Panreac) for 20 min, incubated with a 1mM Nile Red solution (Molecular Probes) in DMSO and extensively washed with cold PBS. Nile Red incorporation was analyzed using inverted microscopy (Microscopy Unit, IGTP, Badalona) and quantified by flow cytometry on a FACScalibur instrument and CellQuest software (BD Biosciences; Cytometry Unit, IGTP, Badalona) with 5,000 events acquired for each sample.

12.2.5. IL-8 measurements

M Φ (5×10^4) were infected as described above at the indicated MOIs, and culture supernatants were collected 24 h postinfection. IL-8 production was measured with the IL-8 OptEIA ELISA kit (BD Biosciences).

12.2.6. Measurements of macrophage mycobactericidal mechanisms

- **NO and ROS production**

THP1 M Φ (5×10^4 cells/well) were infected at MOI: 0.1 or 1 in 96-well plates as described above during different length of times (4 - 96h). Production of nitric oxide by THP-1 Mtb infected cells was

determined by measurement of nitrite in the culture supernatant by the Griess assay. Supernatants (100 μ L) from THP1 cultures were added in triplicate to an equal volume of Griess reagent [1% sulfanilamide, 2.5% phosphoric acid, and 0.1% *N*-(1-naphthyl) ethylenediamine dihydrochloride (Sigma-Aldrich)] and incubated at room temperature for 10 min. For measurement of ROS production, cells were loaded with 10 μ M dichloro-dihydroxy fluorescein diacetate (H₂-DCF-DA; Sigma-Aldrich) in PBS for 30 min at 37°C in the dark. Then the cells were washed twice and resuspended in 100 μ l of PBS. Absorbance at 540 nm and 485 nm for NO and ROS production, respectively, were measured using a Varioskan Flash microplate reader (Thermo Fisher Scientific). The supernatant nitrite concentrations were calculated against a standard curve of known NaNO₂ concentrations. Intracellular ROS levels were calculated as a percentage of the uninfected control (THP1-Vector cells), indicated as 100%.

- **Expression of antimicrobial peptides**

THP1 M Φ (10⁶ cells/well) were infected at MOI: 0.1 in 6-well plates as described above. At 0, 4 and 72 h post-infection mRNA expression of antimicrobial peptides Cathelididin (LL-37) and Defensin- β -4 (DEFB4) were determined by RT-PCR as previously described with specific primers listed in **Table 1**. Gene expression values were normalized to the expression levels of human acidic ribosomal protein (HuPo). Fold induction was calculated using the levels of expression of each gene at time 0 (uninfected) in THP1-Vector cells as a reference. When indicated, cells were pre-incubated with 10 ng/mL of Interferon- γ (R&D Systems) 24 h before infection.

- **Autophagy**

First, positive autophagy markers Beclin-1 and LC3 were analyzed in THP1 Mtb-infected cells. THP1 MΦ (10⁶ cells/well) were infected at MOI: 0.1 in 6-well plates and at different time points mRNA levels of Beclin 1 (mammalian Atg6), involved in the initial formation of autophagosomes, were determined by qRT-PCT as previously described with specific primers listed in **Table 1**. LC3 I-II conversion was analyzed by western blot as described above. Microscopy studies of THP1 Mtb-FITC infected cells were performed for determine the effect of hAIM in autophagy induction (LC-3 puncta per cell), formation of mycobacterial containing autophagosomes (Mtb-LC3 colocalization) and acidification of mycobacterial phagosomes (Mtb-LC3-LysoTracker colocalization) as follows. THP1 MΦ (5*10⁴ cells/well) were infected with Mtb-FITC at MOI: 5 in Millicell EZ slides (Merck Millipore) as described above. When indicated, cells were pre-incubated with the autophagy inhibitor 3-MA (Sigma-Aldrich) 45 min before infection. At 24 and 72 h post-infection, cell were washed with PBS, and medium was replaced with prewarmed RPMI containing 100 nM LysoTracker Red (Molecular Probes) and then stained with LC3 specific antibody as previously described. Slides were examined using a confocal microscope (Vall d'Hebron Research Institute Microscopy Platform, Barcelona). Mtb-LC3 and Mtb-LC3-LysoTracker colocalization were calculated by counting the overlapping of fluorescence in random fields, LC3 puncta per cell was determined using the Image J software and puncta analyzer plug-in (NIH), in thresholded images with size from 3 to 30 pixel² and puncta circularity 0.8-1.

12.2.7. Analysis of hAIM expression

THP1 MΦ (10⁶ cells/well) were infected at MOI: 0.1 in 6-well plates as described above. hAIM mRNA expression was quantified by qRT-PCR with the specific primers listed in **Table 1**. hAIM protein expression in total cell lysates was determined by SDS-PAGE and western blot, immunodetection was performed with biotinylated anti-hAIM poAb (0.2 µg/mL, R&D Systems) as previously described. Fold induction was calculated using the levels of expression of hAIM at time 0 (uninfected) in THP1-Vector cells as a reference.

12.3. Determination of hAIM in serum of *M. tuberculosis* infected mice

12.3.1. Mice infection and chemotherapy

An animal experiment was performed to evaluate the evolution of AIM presence and expression during Mtb infection *in vivo*. All the procedures were performed and approved by the Animal Experimentation Ethics Committee of the Hospital Universitari Germans Trias i Pujol (registered as B9900005) and also approved by the Dept. d'Agricultura, Ramaderia, Pesca, Alimentació i Medi Natural of the Catalan Government, in accordance with current national and European Union legislation regarding the protection of experimental animals (Law 1997 of the Catalan Government; Spanish *Real Decreto* 1201/2005; and the European 86/609/CEE; 91/628/CEE; 92/65/CEE and 90/425/CEE). 6-8-week-old specific-pathogen-free (spf) C57BL/6

female mice (Harlan Laboratories, Sant Feliu de Codines, Spain) were kept under controlled conditions in a P3 facility with access to sterile food and water *ad libitum*. Mice (n=3 to n=5 per time point) were infected with Mtb through aerosol inoculation as described (Cardona, Gordillo et al. 2003). The animals were euthanized at weeks 3, 6, 16, 19 and 21 by isoflurane (inhalation excess), following a strict protocol to prevent unnecessary suffering. Lung and spleen samples were used to evaluate tissue bacillary load, by plating serial dilutions on Middlebrook 7H11 agar plates (BD Diagnostics, Spark, USA). The number of CFUs was counted after incubation for 21 days at 37°C, and the results are expressed as CFUs/mL. Mice were orally treated with Isoniazid (INH) plus rifampicin (RIF) (25 and 10 mg/kg, respectively) once a week from weeks 6 to 14 postinfection, as previously described (Cardona, Amat et al. 2005).

12.3.1. mAIM detection in serum samples

To optimize mAIM detection in whole mouse serum by western blot, different amounts of C57BL/6 mouse control serum were analyzed under non-reducing (NR) and reducing (R, containing 25mM dithiothreitol) conditions, using the recombinant form of the protein (rmAIM) as a reference control. Samples were loaded into 8% SDS gels and immunodetection was performed with anti-mouse AIM biotinylated poAb (0.1 µg/mL, R&D Systems). As observed in **Figure 8**, western blot analysis of mouse serum showed that rmAIM used as positive control was detected at a molecular weight (MW) of 50 kDa under R conditions. A similar reactivity at 50 kDa was detected in mouse serum, suggesting that the antibody was specifically recognizing mAIM. Moreover, little

cross-reactivity was observed around this MW. However, the mAIM band was too close to that of the immunoglobulin heavy chains as well as albumin, which did not facilitate quantification under these settings. The mAIM protein was best detected under NR conditions, in which both recombinant and serum forms presented a MW of 37 kDa. The differences in MW between R and NR conditions can be explained by the elevated number of cysteine residues of the SRCR domains of mAIM (Sarrias, Gronlund et al. 2004). In these experiments, we also confirmed that the signal was dose-response dependent, given that loading different amounts of serum yielded increasing signal responses.

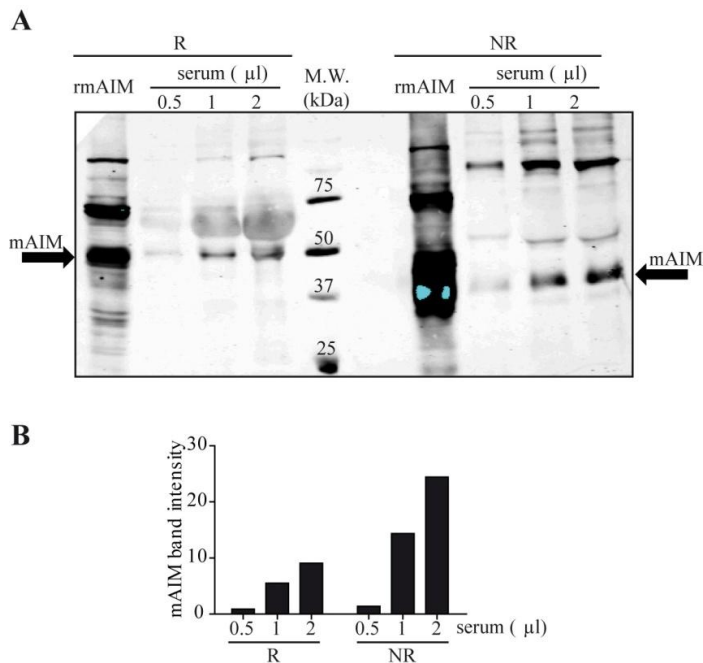


Figure 8. Optimization of mAIM detection in serum by western blot analysis. (A) Representative image of mAIM detection analyzed by Western blot of serum samples. Either rmAIM or the indicated amounts of serum were resolved in 8% SDS polyacrylamide gels under R or NR conditions and the presence of mAIM was detected with a specific antibody. (B) Graph depicting the results of the densitometric analysis performed using the Odyssey V.3 software (LI-COR).

Blood samples obtained from the euthanized *Mtb* infected animals were kept at 4°C for 8 h, and serum was obtained by centrifugation at 2500 xg, aliquoted, and kept at -20°C until required. Mouse serum (1 µL) was resolved in 8% SDS-polyacrylamide gels under non-reducing conditions as previously indicated. A pool of uninfected mice sera were used to determine basal levels of mouse AIM (mAIM) and fold increase in mAIM concentration was determined using mAIM basal levels, set as 1, as a reference.

13. Statistical analysis

Results are expressed as the mean \pm standard error means (SEM) unless otherwise stated. To minimize the effect of inter-individual variability the results are expressed in some experiments as relative values to the control situation. Comparison among two conditions was conducted using the t test for paired or unpaired observations, comparison among more than two conditions were conducted using two or one way anova. Analysis was performed using the GraphPad Prism v4.00 software (GraphPad Software, Inc., La Jolla, CA, USA). A value of $p < 0.05$ was considered significant.

RESULTS & DISCUSSION

WORK I

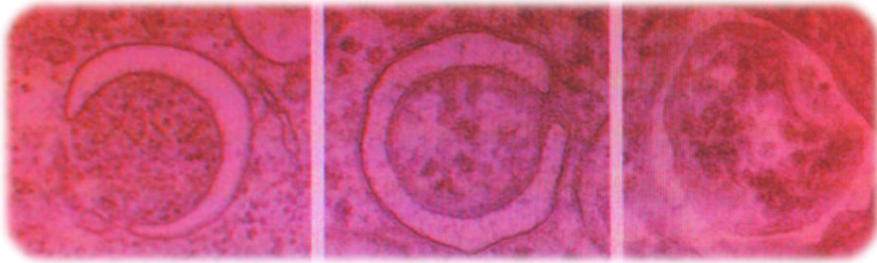
The hAIM-CD36 axis is a novel mechanism of autophagy induction in monocytes

WORK II

Human AIM enhances macrophage intracellular killing of *Escherichia coli*

WORK III

The scavenger protein AIM potentiates the antimicrobial response against *Mycobacterium tuberculosis* by enhancing autophagy



ARTophagy by Altamira Arcos.

WORK I: The hAIM-CD36 axis is a novel mechanism of autophagy induction in monocytes

Lucía Sanjurjo, Núria Amézaga, Gemma Aran, Mar Naranjo-Gómez, Lilibeth Arias, Francesc E. Borràs, Maria-Rosa Sarrias.

SUMMARY

Human Apoptosis Inhibitor of Macrophages (hAIM) is a secreted glycoprotein that participates in host response to bacterial infection. AIM influences the monocyte inflammatory response to the bacterial surface molecules lipopolysaccharide (LPS) and lipoteichoic acid (LTA) by inhibiting TNF- α secretion. Here we studied the intracellular events that lead to macrophage TNF- α inhibition by hAIM. To accomplish this goal, we performed functional analyses with human monocytic THP1 macrophages, as well as with peripheral blood monocytes. Inhibition of PI3K reversed the inhibitory effect of hAIM on TNF- α secretion. Among the various PI3K isoforms, our results indicated that hAIM activates Vps34, a PI3K involved in autophagy. Further analysis revealed a concomitant enhancement of autophagy markers such as cellular LC3-II content, increased LC3 puncta, as well as LC3-LysoTracker Red co-localization. Moreover, electron microscopy showed an increased presence of cytoplasmic autophagosomes in THP1 macrophages overexpressing hAIM. Besides preventing TNF- α secretion, hAIM also inhibited IL-1 β and enhanced IL-10 secretion. This macrophage anti-inflammatory pattern of hAIM was reverted upon silencing of autophagy protein ATG7 by siRNA transfection. Additional siRNA experiments in THP1 macrophages indicated that the induction of autophagy mechanisms by hAIM was achieved through cell surface scavenger receptor CD36, a multi-ligand receptor expressed in a wide variety of cell types. Our data represent the first evidence that CD36 is involved in autophagy and point to a significant contribution of the hAIM-CD36 axis to the induction of macrophage autophagy.

This work will be published in *Autophagy Journal*. The human AIM-CD36 axis: a novel autophagy inducer in macrophages that modulates inflammatory responses. Article in press.

RESULTS I

hAIM inhibits TLR -induced M Φ TNF- α mRNA synthesis and secretion as well as NF- κ B nuclear translocation.

To study hAIM function, we used two cellular M Φ models, namely the THP1 cell line, frequently used as a model for monocytes, and peripheral blood monocytes (PB monocytes) obtained from healthy donors. As mouse AIM expression disappears in cultured cells (Miyazaki, Hirokami et al. 1999; Joseph, Bradley et al. 2004) and neither THP1 M Φ nor PB monocytes express detectable levels of hAIM protein (Amezaga, Sanjurjo et al. 2013), we generated a M Φ cell line that stably expresses hAIM (THP1-hAIM) (Amezaga, Sanjurjo et al. 2013) and produced a new recombinant form of this protein (rhAIM) with improved yield to supplement PB monocyte cultures. We then analyzed whether THP1-hAIM M Φ transfectants and the new rhAIM produced and purified in our laboratory retained the potential to inhibit the TNF- α response to TLR stimuli in PB monocytes. Since TLR2 heterodimerizes distinctly in response to different ligands, we tested two of its agonists, Pam3CSK4 (TLR2/1 agonist) and Pam2CGDPKHPKSF [FSL1 (TLR2/6 agonist)], as well as LPS as a TLR4 agonist. THP1-hAIM M Φ secreted lower levels of TNF- α than control THP1-Vector M Φ in response to TLR2 and TLR4 agonists (**Figure 1A, left**). Similar results were obtained upon addition of rhAIM to PB monocytes prior to TLR stimulation (**Figure 1A, right**). Quantitative PCR analysis suggested that inhibition of TNF- α responses occurred at the transcriptional level, because lower levels of TNF- α mRNA were observed in LPS or Pam3CSK4-stimulated M Φ when hAIM was present (**Figure 1B**). Given that

TNF- α transcription is primarily controlled by the transcription factor NF- κ B, we next assessed nuclear translocation of NF- κ B p65 subunit as a measure of activation. A series of immunofluorescence analyses showed that hAIM reduced NF- κ B nuclear: cytoplasmic ratio, suggesting lower activation of this transcription factor (**Figure 1C**).

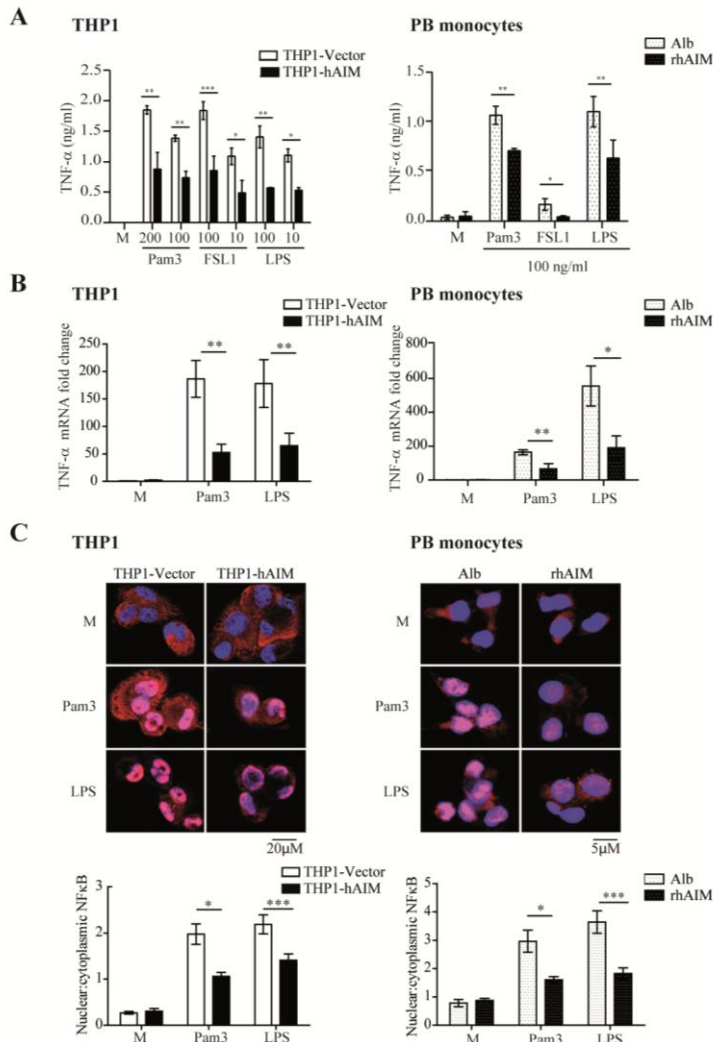


Figure 1. hAIM inhibition of TLR-induced TNF α secretion is concomitant with a decrease of mRNA transcription and lowered NF- κ B nuclear translocation. (Left) PMA-differentiated THP1-Vector (white boxes) and THP1-hAIM (black boxes) M Φ and (Right) PB monocytes incubated for 24 h with 1 μ g/ml albumin (Alb) as control protein (white-dotted boxes) or 1 μ g/ml rhAIM (black-dotted boxes) were (A) stimulated for 4 h with the indicated doses of TLR agonists Pam3CSK4 (Pam3), synthetic diacylated lipoprotein (FSL1), or Lipopolysaccharide (LPS). Culture supernatants were collected, and the amount of TNF- α was measured by ELISA. * $p \leq 0.05$; ** $p \leq 0.01$; *** $p \leq 0.001$ Two-way ANOVA. (B) Incubated with 100 ng/ml LPS or Pam3CSK4 (Pam3) for 1h, and the amount of mRNA encoding TNF- α was measured by qPCR (data show mean fold change relative to untreated THP1-Vector \pm SEM from three independent experiments). (C) Stimulated with 1 μ g/ml LPS or Pam3CSK4 (Pam3) for 1 h. Cells were fixed and NF- κ B was stained with a specific antibody (red) and nuclei with Hoechst stain (blue). Upper panel: representative confocal microscopy images. Lower panel: mean NF- κ B nuclear vs cytoplasmic fluorescence intensity ratio values \pm SEM in more than 200 cells scored in random fields. * $p \leq 0.05$; *** $p \leq 0.001$, one-way ANOVA. Data show the mean values \pm SEM from four independent experiments (for THP1 M Φ) or three blood donors (for PB monocytes). M are untreated cells (left in culture medium).

hAIM has no effect in macrophage TLR2 and TLR4 surface expression and ligand dependent internalization.

We next questioned whether hAIM-induced differences in the response to TLR ligands could be due to modulation of cell surface expression levels of TLR2 or TLR4 and/or its endocytosis rate upon activation. TLR2 and TLR4 endows internalization upon ligand binding (Husebye, Halaas et al. 2006; Triantafilou, Gamper et al. 2006), which results in a transient decrease of surface expression. Accordingly, time-course Pam3CSK4 or LPS stimulation analyzing TLR2 or TLR4 cell surface expression by flow cytometry showed a decrease on TLR2 and TLR4 levels in THP1 control cells, whit maximum rates of internalization 2 h after TLR stimulation (**Figure 2A**). Flow cytometric analysis indicated that the expression of hAIM in THP1 MΦ or its addition to PB monocyte cultures did not modify TLR2 or TLR4 surface expression levels (**Figure2B**). We also observed a decrease in surface expression of receptors 2 h after Pam3CSK4 or LPS addition, both in THP1-Vector MΦ (70.5% ± 10.4 and 13.6% ± 3.3 reduction for TLR2 and TLR4, respectively) and PB monocytes (11.4% ± 2.1 and 8.9% ± 3.6 reduction for TLR2 and TLR4, respectively). This decrease was not altered by hAIM. Overall, these data suggest that the inhibition of TNF-α secretion by hAIM is not caused by a change on TLR2 and TLR4 surface expression or ligand-dependent internalization.

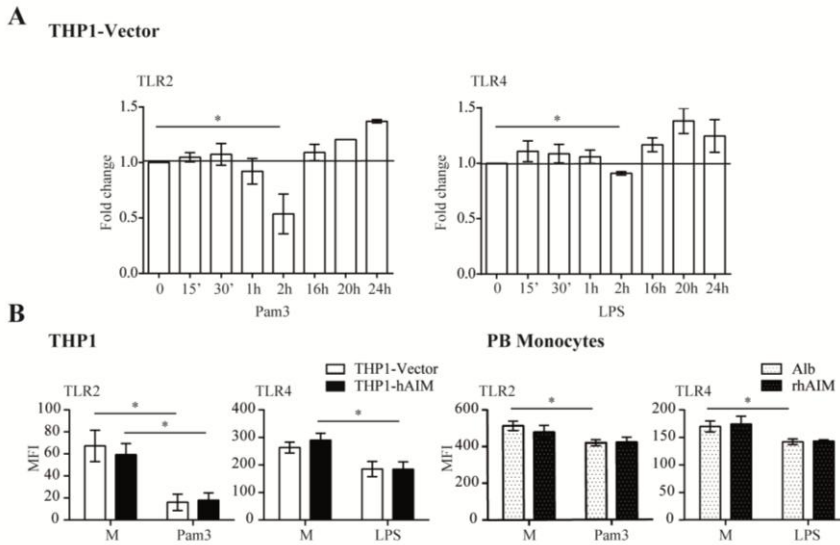


Figure 2. AIM has no effect in TLR2 or TLR4 ligand-dependent internalization and cell surface expression. TLR2 and TLR4 cell surface expression was analyzed by flow cytometry in (A) THP1-Vector cells stimulated with 1µg/ml of Pam3CSK4 or LPS during the times indicated. (B) THP1 MΦ (left) or PB monocytes preincubated during 24h with 1µg/ml rhAIM or albumin (right), untreated or stimulated with 1µg/ml of Pam3CSK4 or LPS during two hours. Results are expressed as Median Fluorescence Intensity (MFI), and show the mean ± SEM from more than three independent experiments (for THP1 cells) or more than three different blood donors (for PB Monocytes). *p≤0.05 t-test.

hAIM induced lower levels of TNF-α secretion is not due to MAPK activation.

We next examined the intracellular signaling mechanisms involved in TLR regulation by hAIM. As an initial approach, we analyzed the mitogen-activated protein kinase (MAPK) signaling cascade, because it plays a key role in regulating TLR activation. (Brown, Wang et al. 2010). As an initial approach, we tested the ability of MAPK pharmacological inhibitors to modify the AIM-dependent inhibition of TNF-α. In accordance with previous results

(Bennett, Sasaki et al. 2001; Rutault, Hazzalin et al. 2001) blockade of p38, JNK1/2 or MEK kinase reduced TNF- α levels in PB monocytes upon TLR stimulation, whereas in THP1 M Φ inhibition of p38 was no effect in TNF- α secretion in these settings. Overall, to relevance for our studies addition of pharmacological MAPK blockers did not alter the inhibitory effect of hAIM on TNF- α secretion (**Figure 3A**). Moreover, time-course determination of MAPK phosphorylation by western blot assays on total Pam3CSK4- or LPS-stimulated THP1 M Φ lysates confirmed these data. The activation of Pam3CSK4- and LPS-induced p38, JNK and ERK1/2 in hAIM-expressing cells was similar to that in control cells (**Figure 3B**).

RESULTS & DISCUSSION

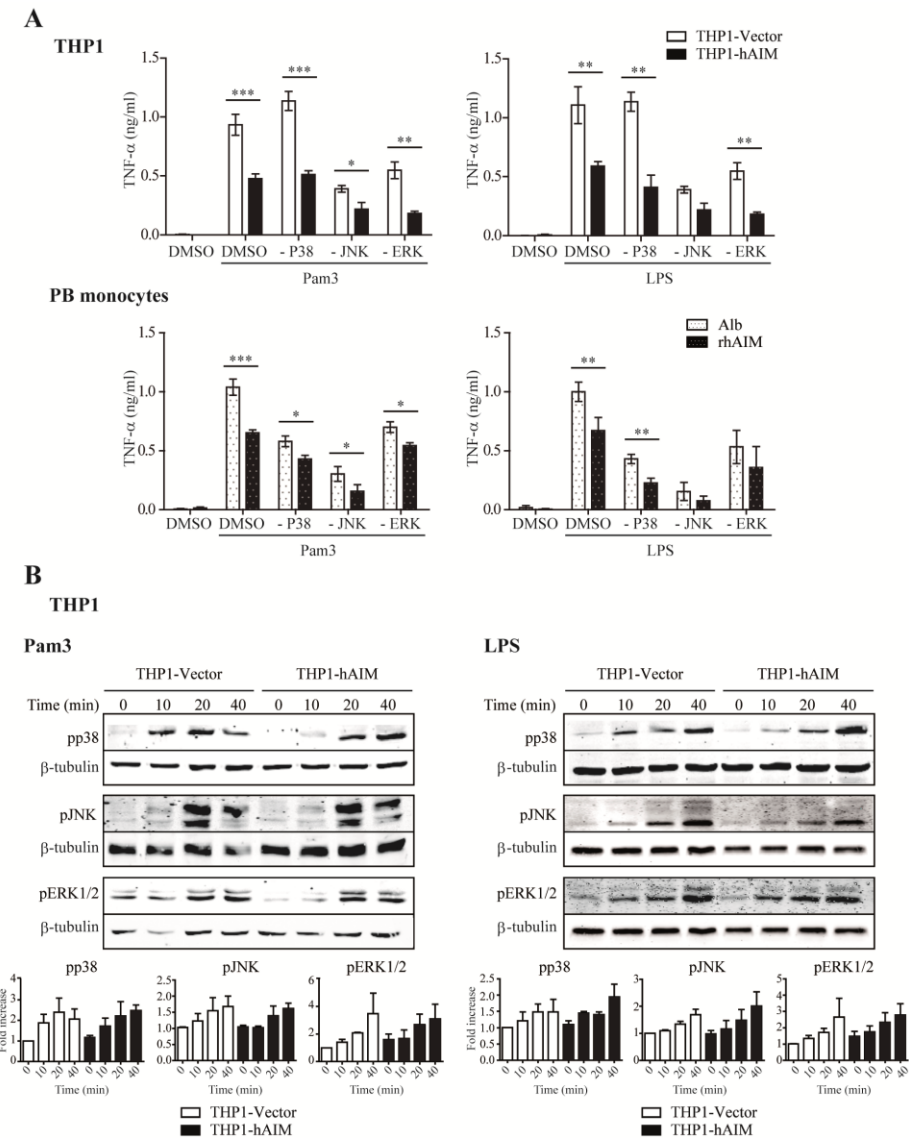


Figure 3. hAIM does not influence TLR-induced MAPK signaling. (A) THP1 M Φ (*up*) or PB monocytes preincubated with 1 μ g/ml rhAIM or albumin for 24 h (*down*) were treated for 45 min with specific MAPK inhibitors at the following concentrations: 20 μ M SB203580 (- p38, p38 inhibitor), 50 μ M SP600125 (- JNK, JNK1/2 inhibitor), 100 μ M PD98059 (- MEK, MEK inhibitor), or DMSO as a control. Then, cells were stimulated with 100 ng/ml Pam3CSK4 (*left*) or LPS (*right*) for 4h. Culture supernatants were collected and the amount of TNF- α was measured by ELISA. mean \pm SEM from more than three independent experiments (for THP1 cells) or more than three different blood donors (for PB Monocytes) performed in triplicate are shown. * $p \leq 0.05$; ** $p \leq 0.01$; *** $p \leq 0.001$ t-test. (B) THP1 M Φ were stimulated for the indicated times with 0.5 μ g/ml of Pam3CSK4 (*left*) or LPS (*right*), lysed and probed in western blotting with antibodies specific against phosphorylated MAPKs and β -tubulin. Upper panel: western blot images of a single experiment. Lower panel: mean of protein signal intensities \pm SEM of 3 independent experiments. Fold increase is relative to THP1-Vector cells at time 0 after normalization to the control protein β -tubulin.

Inhibition of TNF- α secretion by hAIM occurs via the PI3K isoform Vps34.

We then tested whether hAIM modulates the activation of PI3K-pathway, because this pathway is important in regulating the inflammatory response of M Φ (Brown, Wang et al. 2010). The PI3K superfamily comprises a large family of structurally related heterodimeric enzymes. These molecules are formed by a catalytic subunit and a regulatory or accessory subunit (Vanhaesebroeck, Leever et al. 1997), with differing phosphatidylinositol (PI) substrate requirements and modes of regulation (Foster, Traer et al. 2003), Class I and Class III being the best known PI3K isoforms involved in the control of inflammation (Ghigo, Damilano et al. 2010). To determine which of these PI3K isoforms is preferentially activated by hAIM, we stimulated THP1 M Φ with Pam3CSK4 or LPS for 4 h in the presence of the following inhibitors: Pi-104 (targeting Class I PI3K p110 α , β , δ , γ), IC87114 (targeting Class IA PI3K p110 δ), 3-methyladenine (3-MA) (targeting Class III vacuolar protein sorting, Vps34), and the pan-PI3K inhibitors wortmannin or LY294002. Subsequently, we analyzed TNF- α production by ELISA. Interestingly, when pan-PI3K was inhibited, similar concentrations of TNF- α were detected in TLR-stimulated THP1-hAIM M Φ as in control cells (**Figure 4A, Upper graphs**). These data indicate that PI3K repression reverted the inhibitory effect of hAIM over TNF- α secretion. Of note, of the two classes of PI3K molecules assayed, only by blocking the Class III PI3K Vps34 was TNF- α inhibition by hAIM abolished. Similar results were obtained in Pam3CSK4- and LPS-stimulated PB monocytes (**Figure 4A, Lower graphs**).

Vps34 phosphorylates phosphatidylinositol to generate phosphatidylinositol 3-phosphate (PI3P), a key phospholipid for membrane trafficking (Vanhaesebroeck, Leever et al. 2001). Using fluorescent microscopy and a PI3P-specific antibody, we found that the cellular content of PI3P increased slightly in THP1-Vector M Φ after Pam3CSK4 stimulation (**Figure 4B, left**). Interestingly, already without TLR stimulation, THP1-hAIM-expressing M Φ triplicated their PI3P levels as compared to control cells. Likewise, rhAIM enhanced PI3P levels in PB monocytes as compared to control Alb without the need for LPS or Pam3CSK4 addition (**Figure 4B, right**). The addition of Class III PI3K inhibitor 3-MA largely abolished PI3P staining in both cell types, suggesting a contribution of Vps34 to hAIM-enhanced PI3P levels.

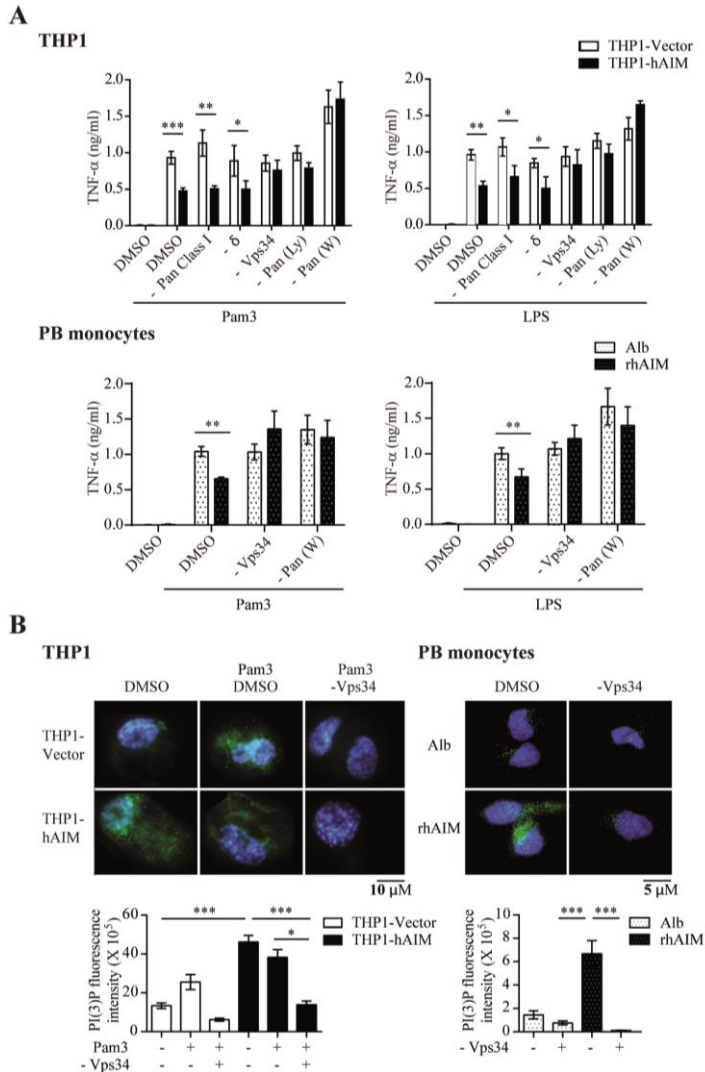


Figure 4. hAIM increases PI3K Class III activity. (A) THP1 MΦ (*top*) and PB monocytes (*bottom*) pre-incubated with 1 μg/ml rhAIM or Alb for 24 h were treated for 45 min with PI3K inhibitors at the following concentrations: 1 μM Pi-103 (-pan Class I, PI3K α, β, γ, δ inhibitor), 1 μM IC87114 (-δ, PI3Kδ inhibitor), 0.1 mM 3-MA (-Vps34, Vps34 inhibitor), 200 μM LY294002 (Ly, pan-PI3K inhibitor), 10 μM Wortmannin (W, pan-PI3K inhibitor), or with DMSO as control. Cells were then incubated for 4 h with 100 ng/ml Pam3CSK4 or 100 ng/ml LPS, and culture supernatants were collected and assayed for TNFα production by ELISA. Mean values ± SEM from four independent experiments (for THP1 MΦ) or three blood donors (for PB monocytes) performed in triplicate are shown. *p≤0.05; **p≤0.01; ***p≤0.001 t-test. (B) To assay PI3P cellular content, THP1 MΦ (*left*) and PB monocytes (*right*) pre-incubated with 1 μg/ml rhAIM or Alb for 24 h were treated for 45 min with 0.1 mM 3-MA (-Vps34) or DMSO as control, and then incubated with 1 μg/ml Pam3CSK4 for 30 min when indicated. PI3P was stained with a specific antibody (green) and nuclei with Hoechst stain (blue). Upper panel: representative confocal microscopy images of THP1 MΦ (*left*) and PB monocytes (*right*). Lower panel: mean PI3P fluorescence intensity values ± SEM in more than 20 cells from independent experiments scored in random fields. *p≤0.05; ***p≤0.001, one-way ANOVA.

hAIM increases the levels of markers of autophagy and autophagy flux in macrophages

Class III PI3K Vps34 plays a key role in autophagy induction (Jaber, Dou et al. 2012). Here we further analyzed the effects of hAIM in the induction of M Φ autophagy by bacterial Pam3CSK4 and LPS, given that these products have been described to induce autophagy (Delgado, Elmaoued et al. 2008). THP1 M Φ and PB monocytes were examined for the microtubule-associated protein 1A/1B-light chain 3 (LC3), LC3 II /LC3 I ratio as an autophagy marker in western blot of total cell lysates. AKT (Ser 473) phosphorylation status was also examined because it increases in response to TLR activation and acts as a negative regulator of autophagy (O'Farrell, Rusten et al. 2013). Pam3CSK4 stimulation increased the LC3II /LC3 I ratio and also AKT phosphorylation (Ser 473) in THP1-Vector M Φ . Most importantly, THP1-hAIM M Φ showed an enhanced LC3II/LC3 I ratio, even under no stimulation (**Figure 5A, left**). In contrast, AKT phosphorylation was markedly lower in these cells as compared to THP1-Vector M Φ . Noteworthy, total AKT protein was similar in both cell types, suggesting no differences in AKT content. Similar results were obtained in PB monocytes incubated with rhAIM vs. control Alb (**Figure 5A, right**).

We next quantified autophagosome formation and autophagy flux by analyzing the amount of LC3 puncta per cell and the colocalization of LC3 puncta with acidic organelles, respectively (Klionsky, Abdalla et al.) (**Figure 5B**). For this purpose, cells were stained with an antibody against LC3 and also with LysoTracker, an acidotropic fluorescent dye that accumulates in acidic organelles. We found that even in the absence of

Pam3CSK4 or LPS, THP1-hAIM cells almost quadruplicated the number of LC3 puncta per cell vs. THP1-Vector M Φ (13.27 ± 1.33 vs. 3.10 ± 0.33 , $p < 0.0001$ Student t test). Furthermore, a 6-fold increase in LC3-LysoTracker double-positive puncta as compared to THP1-Vector M Φ (3.77 ± 0.55 vs. 0.61 ± 0.19 , $p < 0.0001$ Student t test) was observed (**Figure 5B left**). Accordingly, incubation of PB monocytes with rhAIM almost triplicated LC3 puncta formation (4.90 ± 0.39 vs. 1.82 ± 0.18 , $p < 0.0001$ Student t test) and quadruplicated LysoTracker colocalization (1.80 ± 0.41 vs. 0.44 ± 0.16 ; $p 0.0007$ Student t test) as compared to incubation with the control protein Alb (**Figure 5B right**). These findings suggest that hAIM promotes autophagy by increasing autophagosome formation and may render phagosomes more susceptible to acidification in M Φ . Interestingly, addition of the Vps34 inhibitor 3-MA, widely used as an autophagy blocker, inhibited all these effects. To reinforce these data, we performed experiments aimed at silencing the protein ATG7, an integral component of the cellular autophagy machinery (Geng and Klionsky 2008). SiRNA transfection targeting ATG7 lowered its expression in THP1-hAIM M Φ (**Figure 5 material and methods**), with a concomitant decrease on LC3 puncta formation and LC3-LysoTracker double-positive puncta in these cells, when compared to control, non-targeting siRNA (**Figure 5C**). Together, these data further support the notion that hAIM contributes to M Φ autophagy.

RESULTS & DISCUSSION

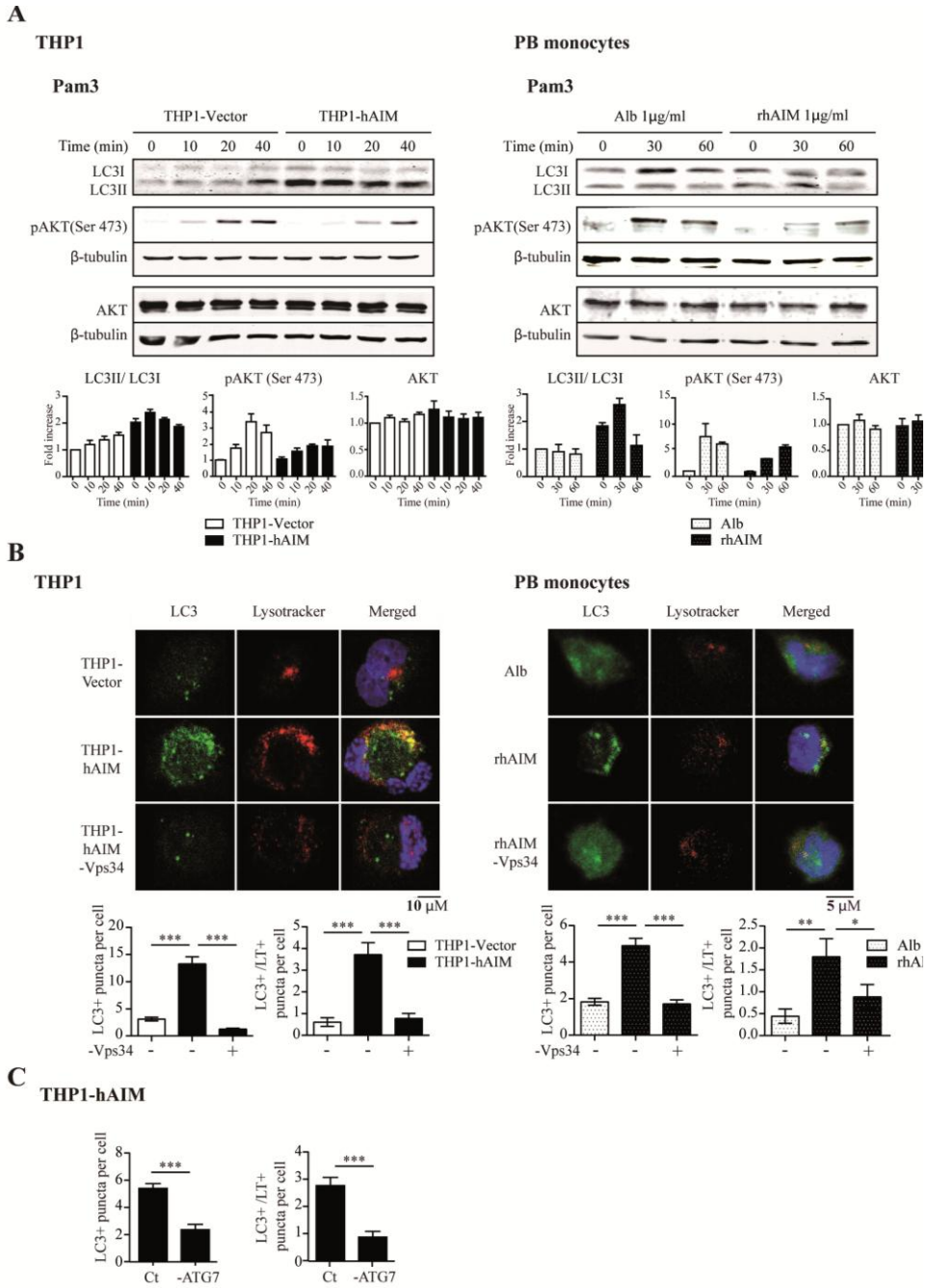


Figure 5. Please see figure legend on next page

Figure 5. hAIM promotes macrophage autophagy. (A) THP1 MΦ (*left*) and PB monocytes (*right*) pre-incubated with 1 μg/ml rhAIM or Alb for 24 h were stimulated for the indicated times with 0.5 μg/ml Pam3CSK4, lysed, and probed in western blots with specific antibodies. Upper panel: western blot images of a single experiment. Lower panel: mean of protein signal intensities ± SEM of 3 independent experiments. Fold increase is relative to untreated THP1-Vector MΦ (*left*) and untreated PB monocytes (*right*) after normalization to the control protein β-tubulin. LC3 protein signal intensities were plotted as LC3-II/LC3-I ratio. (B) To determine autophagy flux, THP1 MΦ (*left*) and PB monocytes (*right*) pre-incubated with 1 μg/ml rhAIM or Alb for 24 h were treated for 45 min with autophagy inhibitor 3-MA (- Vps34, 0.1 mM), or with DMSO used as a control. LC3 was then stained with a specific antibody (green), acidic organelles with LysoTracker (red), and nuclei with Hoechst stain (blue). Upper panel: representative confocal microscopy images showing LC3 and LysoTracker staining and colocalization (Merged). Lower Panel: mean ± SEM quantitative data showing LC3 puncta per cell (LC3+ puncta per cell) and LC3-LysoTracker colocalized puncta per cell (LC3+/LT+ puncta per cell) in three independent experiments (for THP1 MΦ) or three blood donors, including at least 50 cells scored in random fields. (C) THP1-hAIM MΦ after transfection of a siRNA targeting ATG7 (-ATG7) or a non-targeting negative control (Ct) were stained for LC3, LysoTracker and nuclear detection as in (B). Graphs depict mean ± SEM quantitative data showing LC3 puncta per cell (LC3+ puncta per cell) and LC3-LysoTracker colocalized puncta per cell (LC3+/LT+ puncta per cell) in three independent experiments, including at least 200 cells scored in random fields. *p≤0.05; **p≤0.01; ***p≤0.001, one-way ANOVA.

hAIM expression induces double-membrane vesicle formation in THP1 MΦ

To further confirm that the process detected was indeed autophagy, we studied the formation of ribosome-free, smooth double membrane vesicles in THP1 MΦ (Klionsky, Abdalla et al. 2012). The ultrastructural analysis of 25 sections/cell line using electron microscopy revealed the presence of 1 to 4 of these typical autophagosomal double-membrane vesicles in the cytoplasm of THP1-hAIM MΦ (**Figure 6**). The vesicles were absent from the control THP1-Vector MΦ.

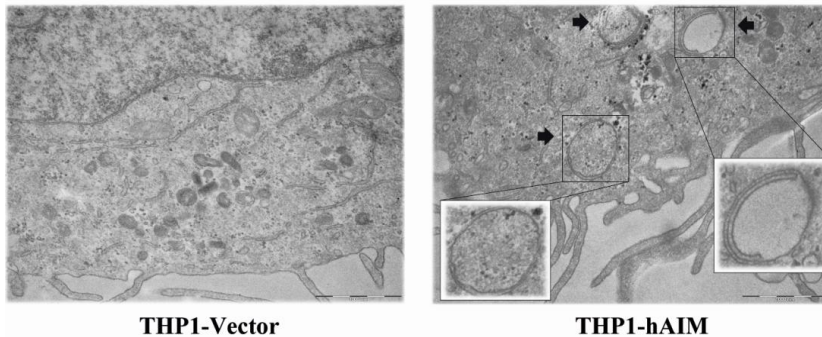


Figure 6. Assessment of autophagy induction by hAIM by ultrastructural imaging. Electron microscopy of THP1 MΦ. A representative image of 25 sections/cell line is shown (30,000 x magnification). Arrows and enlarged areas indicate autophagic organelles.

hAIM inhibits IL-1 β and enhances IL-10 secretion, but not their mRNA transcription

To obtain a wider view of the immunomodulatory capacity of hAIM, we tested whether it modulated Pam3CSK4- or LPS-induced secretion of other cytokines namely IL-1 β , IL-6 and IL-10. For this purpose, we analyzed the production of these cytokines, in supernatants of PB monocytes 24 h after TLR stimulation (**Figure 7A**). In these experiments TNF- α was also analyzed as a positive control (data not shown). The addition of rhAIM did not induce the release of any of these cytokines when compared to control protein albumin (Alb), thereby suggesting that hAIM is not involved in the secretion of these cytokines in the absence of other stimuli. Upon Pam3CSK4 or LPS stimulation, however, the presence of rhAIM lowered IL-1 β secretion and enhanced IL-10 levels, while no effect was observed on IL-6 secretion, as compared to the control Alb. Given that autophagy is known to suppress IL-1 β maturation

rather than mRNA transcription, (Shi, Shenderov et al.) we analyzed mRNA content of this cytokine in TLR- activated PB monocytes by real time PCR (**Figure 7B**). Addition of rhAIM to PB monocytes did not apparently modify mRNA levels of IL-1 β , reinforcing the notion that hAIM is modulating the secretion of this cytokine post-transcriptionally. Similarly, addition of rhAIM to PB monocytes did not affect either IL-6 or IL-10 mRNA levels in response to TLR ligands (**Figure 7B**). Similar real time PCR results were obtained when we compared mRNA levels in THP1-hAIM to those of THP1-Vector M Φ (data not shown).

To reinforce the notion of hAIM-modulated cytokine release was due to enhanced autophagy, two sets of experiments were performed. First, we observed that rhAIM-induced modulation of IL-1 β and IL-10 protein secretion in PB monocytes did not occur when PI3K phosphorylation was blocked by addition of wortmannin (data not shown). More relevantly, blockade of ATG7 expression in THP1-hAIM cells enhanced TNF- α and IL-1 β while lowering IL-10 secretion in response to TLR induction, reverting thus the modulatory effect of hAIM (**Figure 7C**). These findings suggest that hAIM downregulates Pam3CSK4 and LPS inflammatory responses and that this effect is mediated at least in part, by enhancing autophagy.

RESULTS & DISCUSSION

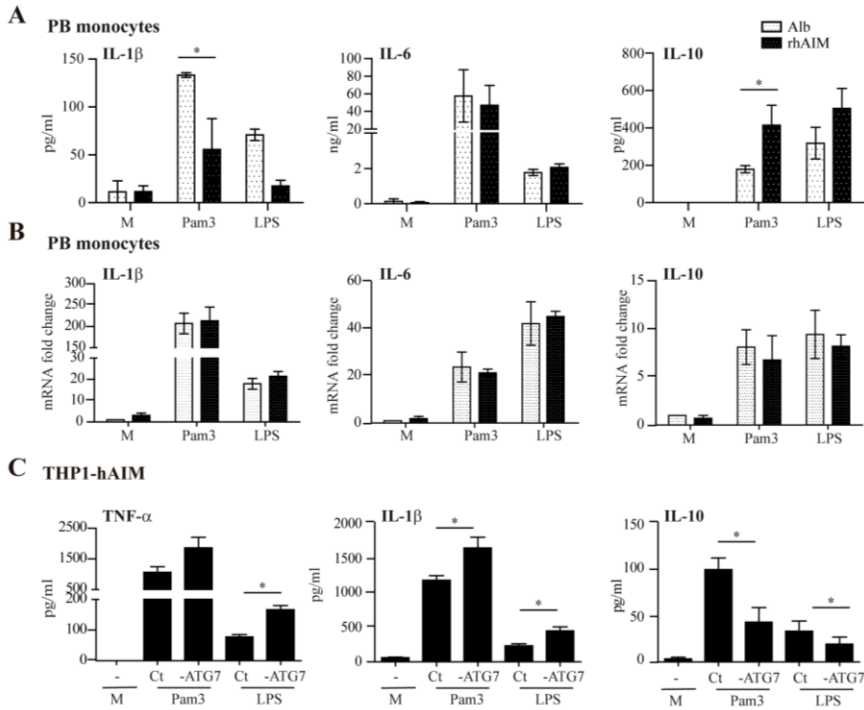


Figure 7. hAIM inhibits IL-1 β and enhances IL-10 protein secretion, which is reversed upon silencing of ATG7 expression. (A-B) PB monocytes incubated with 1 μ g/ml Alb or rhAIM for 24 h and 100 ng/ml Pam3CSK4 (Pam3) or LPS were added to the cultures. **(A)** TLR agonists were incubated for 24 h, and the amount of IL-1 β , IL-6 and IL-10 was analyzed by multiplex cytokine assay. **(B)** TLR agonists were incubated for 6h and the levels of mRNA encoding for IL-1 β , IL-6 and IL-10 were analyzed by real time RT-PCR. Mean values \pm SEM from three blood donors performed in duplicate are shown. * $p \leq 0.05$; ** $p \leq 0.01$; *** $p \leq 0.001$ t-test. **(C)** THP1-hAIM cells were transfected with siRNA targeting ATG7 (-ATG7) or a non-targeting negative control (Ct), and stimulated with TLR agonists (100 ng/ml) for 4h (for TNF- α detection) and 24 h (for IL-1 β and IL-10 detection). Cytokine production in the supernatant was quantified by ELISA. Mean values \pm SEM of four experiments performed in triplicate are shown. * $p \leq 0.05$; ** $p \leq 0.01$; *** $p \leq 0.001$ t-test.

CD36 silencing abolishes hAIM-induced autophagy and its modulation of inflammatory cytokine secretion.

AIM colocalizes with scavenger receptor CD36 on the cell surface (Kurokawa, Arai et al. 2010) and mediates M Φ uptake of oxLDL through CD36 (Amezaga, Sanjurjo et al. 2013). Consequently, we next tested whether CD36 is the receptor mediating hAIM induction of M Φ autophagy (**Figure 8**). Flow cytometry analysis of THP1 cells revealed that transfection of a pool of 4 siRNAs targeting CD36 silenced its expression in THP1 M Φ by ~60% as compared with transfection of the negative control, a pool of 4 non-targeting siRNAs (see **Figure 5B material and methods**). Noteworthy, microscopy analysis of CD36-silenced THP1-hAIM M Φ compared with THP1-hAIM ones treated with non-targeting siRNA showed a reduction in LC3 puncta per cell and LC3-LysoTracker double-positive puncta by 45% (8.95 ± 0.62 vs. 4.82 ± 0.34 $p < 0.0001$ Student t test) and 30% (3.71 ± 0.5 vs 2.49 ± 0.3 $p = 0.032$ Student t test), respectively (**Figure 8A**). We then studied whether modulation of cytokine secretion by hAIM was mediated through CD36. CD36 was silenced in THP1-hAIM M Φ prior to TLR stimulation, and the amount of TNF- α , IL-1 β and IL-10 in cell supernatants was measured by ELISA. CD36 silencing in THP1-hAIM M Φ increased TNF- α and IL-1 β release and decreased IL-10 production in response to TLR activation as compared to control siRNA-treated M Φ (**Figure 8B**). We next addressed whether CD36-dependent hAIM-triggered autophagy was induced by exogenous addition of rhAIM to THP1-Vector M Φ . With this goal, we incubated THP1-Vector M Φ with rhAIM or Alb for 24 h and determined autophagosome formation and autophagy flux in these cells

(Figure 8C). Low levels of LC3 puncta formation as well as LC3-LysoTracker colocalization were observed in Alb-incubated cells, which were not affected by silencing of CD36 expression. In contrast, rhAIM addition triplicated the number of LC3 puncta per cell (6.81 ± 0.46 rhAIM vs. 2.41 ± 0.31 Alb, $p < 0.0001$ Student t test) and that of LC3-LysoTracker double-positive puncta (2.26 ± 0.26 vs. 0.61 ± 0.19 , $p < 0.0001$ Student t test) in cells treated with non-targeting control siRNA. The effect of rhAIM was reduced upon inhibition of CD36 expression by siRNA treatment in terms of LC3 puncta formation (6.81 ± 0.46 siRNA control vs. 3.46 ± 0.30 siRNA CD36; $p < 0.0001$) as well as LC3-LysoTracker colocalization (2.26 ± 0.26 siRNA control vs. 1.4 ± 0.22 siRNA CD36, $p = 0.0164$). These results suggest that M Φ autophagy is induced by exogenous rhAIM addition to CD36-positive cells not expressing hAIM. Together, our findings indicate that CD36 is the receptor that mediates hAIM-induced autophagy and subsequent hAIM-regulated TNF- α , IL-1 β and IL-10 cytokine secretion.

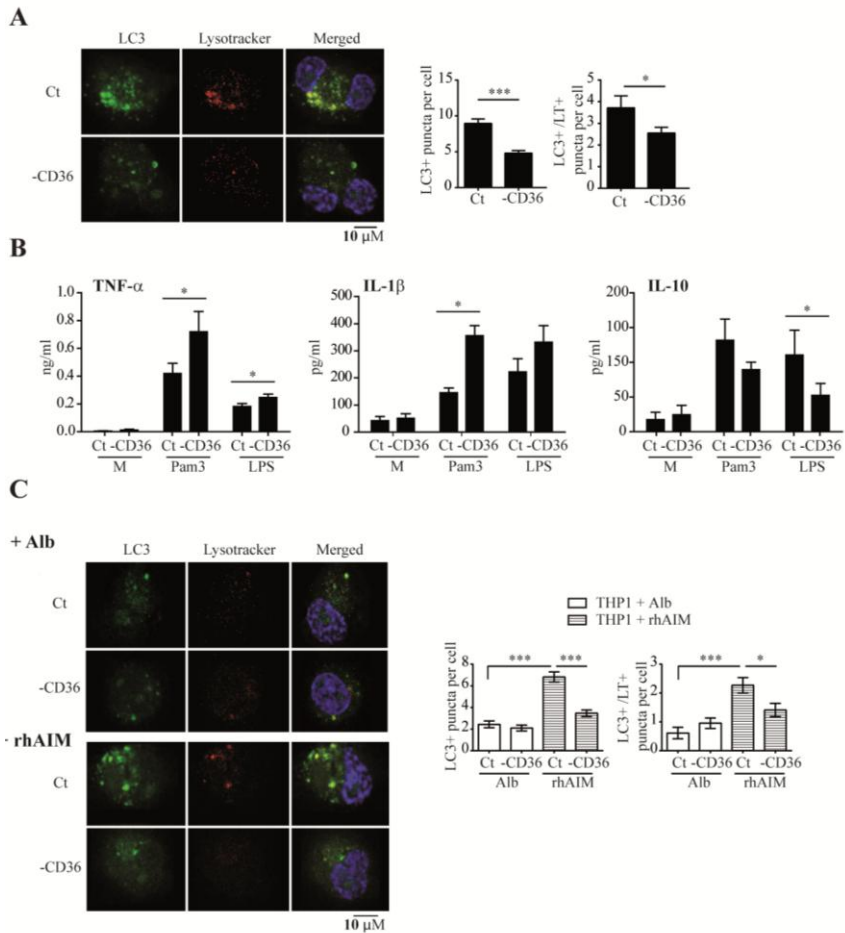


Figure 8. CD36 silencing reduces hAIM-induced autophagy and reverts hAIM-regulated cytokine secretion in THP1 MΦ. Cells were transfected with siRNA targeting CD36 (-CD36) or a non-targeting negative control (Ct). **(A)** Autophagy flux was assessed upon CD36 silencing in THP1-hAIM MΦ. Left panels: representative confocal microscopy images showing staining of LC3 with a specific antibody (green), acidic organelles with LysoTracker red (red), nuclei with Hoechst stain (blue), and colocalization (Merged). Right graphics: mean ± SEM quantitative data show LC3 puncta per cell (LC3+ puncta per cell) and LC3-LysoTracker colocalized puncta per cell (LC3+/LT+ puncta per cell) in three independent experiments including at least 50 cells scored in random fields. **(B)** SiRNA-treated THP1-hAIM MΦ were stimulated for 24 h with 100 ng/ml Pam3CSK4 or LPS, culture supernatants were collected, and the amount of TNFα, IL1-β and IL-10 was measured by ELISA. Mean values ± SEM from three independent assays performed in triplicate are shown. **(C)** Autophagy flux was assessed in CD36-silenced THP1-Vector MΦ after incubation with 1 μg/ml rhAIM or 1 μg/ml Alb for 24 h. The analysis was performed by confocal microscopy as in B). *p<0.05; **p<0.01; ***p<0.001, t-test.

DISCUSSION I

Here we report on a novel role for hAIM in the regulation of M Φ homeostasis, showing that this protein activates autophagy in this cell type through the CD36 receptor. Consequently, hAIM prevents TLR-induced TNF- α and IL-1 β secretion with a concomitant increase in IL-10 levels, thereby down-regulating the M Φ inflammatory reaction. Our findings are of relevance because inflammation can lead to excessive self-aggression and pathology when not finely regulated.

To study the regulation of M Φ TLR responses by hAIM, the amount TNF- α in the cell culture supernatant was taken as an indirect measure of hAIM activity. For that reason, a series of experiments were performed to modulate the intracellular pathways in such a way to revert the inhibitory effects of hAIM over TNF- α production. To induce M Φ TNF- α secretion, we chose the TLR agonists Pam3CSK4 and LPS as they are established TLR2/1 and TLR4 activators. In initial experiments, stable expression of hAIM in THP1 M Φ and our newly generated rhAIM inhibited TLR-induced TNF- α as we previously reported (Sarrias, Rosello et al. 2005). These results suggest that hAIM expression in the THP1 cell line and our newly generated rhAIM are adequate tools by which to study hAIM modulation of M Φ inflammatory responses.

We next sought to determine whether the lowered TNF- α response promoted by hAIM is due to modulation of TLR surface expression and/or internalization. We focused on this issue because TLRs undergo internalization upon ligand binding and this permits signaling from endosomal compartments and the

generation of distinct outcomes (Barton and Kagan 2009). In our hands, cytometry staining experiments showed that hAIM induced no change in TLR2 or 4 levels at the cell surface, thus discarding the participation of this protein in the regulation of the availability of these receptors at the cell surface.

To decipher the intracellular events modulated by hAIM, we analyzed two signaling pathways relevant for TLR signaling, namely the MAPK and PI3K pathways (Brown, Wang et al. 2010). The MAPK and PI3K signaling inhibitors were expected to revert the inhibitory effects of hAIM over TNF- α production. Data on MAPK pharmacological inhibition supported by Western blot analysis of cell lysates suggested that MAPK activity is crucial for TLR signaling (Brown, Wang et al. 2010). Of relevance for our studies, the data showed that hAIM does not modulate TLR2- or TLR4-induced MAPK activation in M Φ .

On the contrary, our results from PI3K pharmacological inhibition experiments suggested that hAIM triggers PI3K activation. This notion is supported by the observation that lower TNF- α levels induced in the presence of hAIM were restored by wortmannin and LY294002, two synthetic pan-PI3K inhibitors. Our results are in accordance with the anti-inflammatory role of PI3K (Ghigo, Damilano et al. 2010).

Analysis of the PI3K isoform that participates in the hAIM modulation of TNF- α secretion indicated that this was preferentially the Class III PI3K Vps34 pathway. These results are of relevance because Vps34 is linked to the activation of autophagy (O'Farrell, Rusten et al.) and in fact, autophagosome formation is

blocked in the absence of this PI3K isoform (Jaber, Dou et al. 2012). In support of the pharmacological inhibitor data that suggest that hAIM activates Vps34, we found that hAIM increased the cellular content of its metabolic product, PI3P, in both THP1 MΦ and PB monocytes. Interestingly, this enhancement occurred without the addition of LPS or Pam3CSK4. PI3P may also be produced via Vps34-independent mechanisms, including dephosphorylation of PI(3,4,5)P₃ by PI 5-phosphatases and 4-phosphatase (Shin, Hayashi et al. 2005) or through Class II PI3K molecules that also contribute to PI3P synthesis (Devereaux, Dall'Armi et al.). However, our data suggest that hAIM preferentially enhances PI3P levels through Vps34, since the signal was abrogated in the presence of the Vps34-specific inhibitor 3-MA.

In accordance, hAIM enhanced the LC3II/I ratio and down-modulated AKT (Ser 473) phosphorylation in both THP1 MΦ and PB monocytes. Our data support the notion that AKT is a negative regulator of autophagy (O'Farrell, Rusten et al.). Moreover, given that AKT is phosphorylated by Class I PI3K, our western blot data are consistent with the results on pharmacological inhibition of Class I PI3K, which did not affect hAIM-mediated inhibition of TNF-α.

Further examination of autophagy markers reinforced the notion that hAIM induces autophagy in MΦ. In this regard, in both THP1 MΦ and PB monocytes, hAIM increased LC3 puncta and LC3-LysoTracker-positive puncta per cell, and these effects were inhibited by the addition of 3-MA, the specific autophagy blocker. Likewise, silencing of ATG7, a key component of the autophagy

signaling network, lowered LC3 puncta and LC3-LysoTracker-positive puncta per cell in THP1-hAIM M Φ . Furthermore, the elevated number of autophagosomes observed in THP1-hAIM cells by electron microscopy reinforced the notion that hAIM is activating autophagy mechanisms in the M Φ .

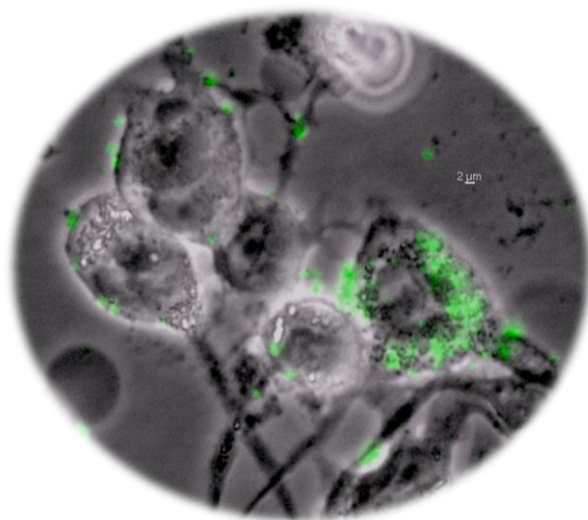
Modulation of cytokine responses by hAIM was not restricted to TNF- α . Lowered IL-1 β and enhanced IL-10 protein secretion suggest a broader anti-inflammatory role of hAIM on M Φ . However, hAIM may target a specific subset of cytokines since it did not modify IL-6 protein levels. Further research is underway to analyze modulation of M Φ chemokine/cytokine production by hAIM. Of relevance for the present study, hAIM modulation of TNF- α , IL-1 β and IL-10 were reverted by silencing of ATG7 protein. Moreover, we found that hAIM inhibited TLR-induced IL-1 β secretion but did not apparently modify mRNA synthesis, suggesting a post-translational processing of the IL-1 β protein. Because it is well known that autophagy inhibits IL-1 β protein maturation rather than mRNA synthesis (Harris, Hartman et al. 2011), these data reinforce the concept that hAIM is activating autophagy. Similarly, hAIM enhanced IL-10 protein secretion but did not alter IL-10 mRNA levels upon TLR activation, which may suggest a role of autophagy in M Φ IL-10 maturation as well.

Given that hAIM is a secreted protein, we next sought to determine the cellular receptor mediating hAIM induction of autophagy in M Φ . We analyzed the CD36 receptor because of previous evidence that links the activity of these two molecules (Kurokawa, Arai et al. 2010; Amezaga, Sanjurjo et al. 2013). Flow cytometry analysis showed that hAIM induced higher M Φ cell

surface expression of CD36, as previously observed (Amezaga, Sanjurjo et al. 2013). Interestingly, silencing of CD36 alone did not alter autophagy markers in THP1-Vector M Φ , which were almost absent, suggesting that this receptor does not modulate autophagy in basal conditions. In contrast, the reduction in CD36 cell surface receptor availability in hAIM-expressing M Φ lowered hAIM-induced LC3 puncta formation and LC3-LysoTracker colocalization. Our data from the CD36 silencing experiments further indicate that this receptor is involved in the anti-inflammatory mechanisms mediated by hAIM (i.e. enhanced TNF- α and IL-1 β and lowered IL-10 secretion). Interestingly, the addition of rhAIM to non-hAIM-expressing M Φ yielded similar results. Therefore, taken together, our data suggest that hAIM modulation of TLR activation occurs by enhancement of autophagy through CD36. The observation that a decrease in LC3 puncta/LC3-LysoTracker colocalization in THP1-Vector M Φ in which CD36 expression was silenced was not evident points towards a role for AIM in increasing PIK3C3 signaling directly, rather than indirectly by increasing CD36 levels. However, given that the levels of the autophagy markers were very low in these cells, these data are not conclusive and further experiments are needed to solve this issue.

In contrast to our results, CD36 knockout mouse macrophages have not shown an elevated reactivity to TLR ligands in previous studies (Hoebe, Georgel et al. 2005; Stewart, Stuart et al. 2009). These assays were performed under culture conditions where AIM expression has been shown to disappear (Miyazaki, Hirokami et al. 1999). The lack of AIM expression may therefore explain the observed differences on CD36 function.

In summary, our results provide a new function for the CD36 receptor as an inducer of M Φ autophagy through hAIM. Our results open a new perspective of the role of the hAIM-CD36 axis in cellular homeostasis that could be associated with the pathogenesis of those serious inflammatory conditions in which these proteins are relevant.



THP1-hAIM cells and fluorescent *E.coli* (green)

WORK II: Human AIM enhances macrophage intracellular killing of *Escherichia coli*

Lucía Sanjurjo, Núria Amézaga, Maria-Rosa Sarrias.

SUMMARY

Human and mouse AIM are secreted proteins that, as other members of the SRCR superfamily, are able to bind and aggregate microbial agents (bacteria and fungi). No data are available regarding the involvement of AIM in phagocytosis of pathogens. However, in a mice model overexpressing AIM histological studies suggested that mAIM promotes M Φ phagocytosis in response to fulminant hepatitis that may result in an efficient clearance of dead cell or toxic reagents. Supporting this finding, *in vitro* evidences showed that mAIM enhances mouse macrophage phagocytosis of latex beads. With the goal of addressing whether the prophagocytic role is conserved in the human form of the protein, the effect of hAIM in macrophage phagocytosis of latex beads, Gram-negative and Gram-positive bacteria was analyzed *in vitro* in the present work.

Not published data

RESULTS II

Human AIM does not affect macrophage phagocytosis of latex beads

Our first experiment was to assess whether hAIM retained the prophagocytic capabilities of its murine counterpart in response to latex beads. To do so, THP1-Vector and THP1-hAIM M Φ were incubated with fluorescent latex beads for 1 h and the increase in fluorescence was analyzed by flow cytometry. By incubation with different doses of beads, the percentage of fluorescein isothiocyanate (FITC)-positive cells increased in a dose-dependent way in experiment performed at 37°C but not at 4°C (**Figure 1A**), indicating that increases in fluorescence were due to uptake rather than to bead adherence to the cell surface. **Figure 1B** shows the histogram of FITC intensity in both THP1 cell lines. The histogram shows three peaks, which represent cells that had phagocytized 1 (P1), 2 (P2) or 3 or more beads (P3). In THP1-AIM cells 14.4 % of cells had phagocytized a single bead, 5.2 % phagocytized two beads, and 3.9 % phagocytized three or more beads. Overall, comparing these values with those of control (THP1-Vector) cells no significant differences in the rate of phagocytosis were observed (**Figure 1B, lower table**). These data suggested no involvement of hAIM in bead uptake. These results contrasted with the reported role of mAIM in enhancing macrophage uptake of latex beads (Haruta, Kato et al. 2001). We therefore assayed the effect of mAIM in macrophage phagocytosis in our experimental settings. Before the addition of FITC-beads, THP1-Vector M Φ and mouse bone marrow derived macrophages (BMDM) were preincubated during 1 h with 1 μ g/mL of recombinant

forms of mouse AIM (rmAIM) or human AIM (rhAIM) proteins or with human albumin (Alb) as a control protein (**Figure 1C**). Our results show that in accordance with (Haruta, Kato et al. 2001) addition of rmAIM increased by 35% the number of FITC-positive cells in both human and mouse M Φ . In contrast, no effect in bead uptake was observed by incubation with rhAIM, thus corroborating no role for this protein in latex bead uptake.

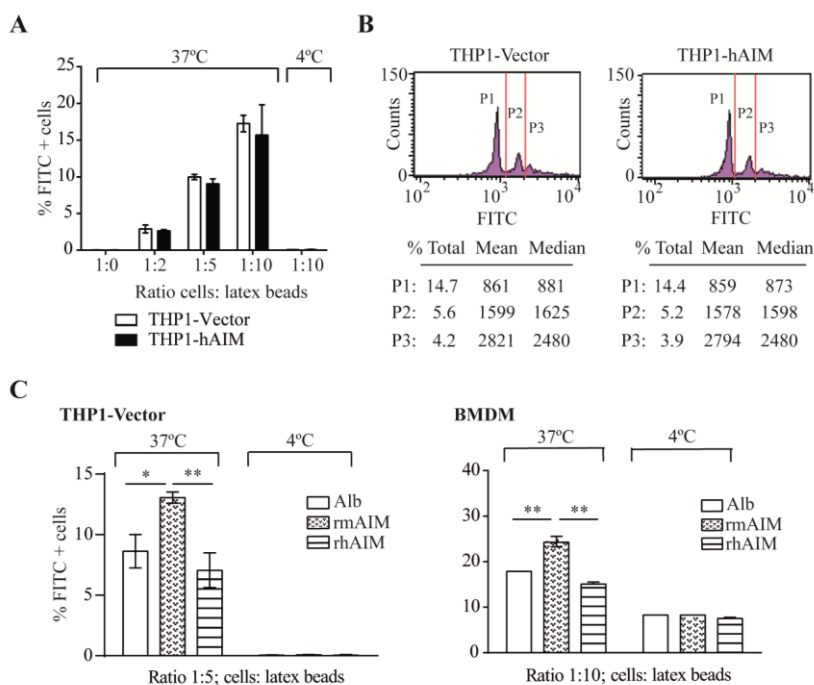


Figure 1. Role of AIM in macrophage phagocytosis of latex beads. (A-B) THP1-Vector and THP1-hAIM M Φ were incubated for 1 h with 3 μ m YG Fluoresbriht™ microspheres and their phagocytosis rate was determined by flow cytometry. **(A)** THP1 M Φ were incubated with FITC-beads at the indicated ratios and temperatures, mean \pm SEM of % FITC positive cells from three independent experiments are shown. **(B)** THP1 M Φ were incubated with latex beads at ratio 1:10 (cell:bead) at 37°C. The histograms show a representative experiment. Upper panel: FITC histograms, Lower tables: values of % FITC-positive cells, mean and median of fluorescence intensity of 3 different gates corresponding to each histogram peak. **(C)** THP1-Vector (*left*) and mouse BMDM (*right*) were preincubated for 24h with 1 μ g/ml albumin, rmAIM or rhAIM and then incubated during 1h with FITC-beads at the indicated ratios and temperature. Mean \pm SEM of % FITC-positive cells from duplicates of a single experiment are shown. Two way ANOVA * $p \leq 0.5$, ** $p \leq 0.01$.

Human AIM enhances macrophage intracellular killing of *E. coli*

Despite no effect due to hAIM was observed in macrophage phagocytosis of latex beads, phagocytosis experiments were performed using heat-killed *Escherichia coli* and *Staphylococcus aureus*. Given that microbial pathogens express multiple ligands on their cell surfaces that can be recognized by phagocytes (Ofek, Goldhar et al. 1995), and that hAIM binds to the surface of Gram-positive and Gram-negative bacteria (Sarrias, Rosello et al. 2005), we hypothesized that hAIM could act as a soluble protein influencing bacterial recognition by phagocytic receptors. To answer that question, flow cytometric analysis of THP1 M Φ incubated with fluorescent heat-killed *E. coli* or *S. aureus* were performed. **Figure 2A** shows that the percentage of FITC-positive THP1-Vector cells increased in a dose-dependent way in experiments performed at 37°C but not at 4°C in the presence of fluorescent *E. coli*. However, no significant differences in rate of *E. coli* or *S. aureus* phagocytosis were observed in hAIM expressing cells as compared with the control cell line (THP1-Vector). We next performed intracellular killing experiments, to determine the effects of hAIM in the final outcome of viable *E. coli*. With this goal, THP1 M Φ were infected with live *E. coli* for 30 or 90 min at 37 °C, then cells were extensively washed with sterile PBS and lysed. Serial dilutions of cell lysates were plated in LB-agar plates, and after 24 h of incubation, results of colony forming units (CFUs) counting (**Figure 2B**) showed that the numbers of viable *E. coli* in THP1-hAIM expressing cells were significantly lower than in THP1-Vector control cells. These results suggested that hAIM increases *E. coli* intracellular killing by M Φ .

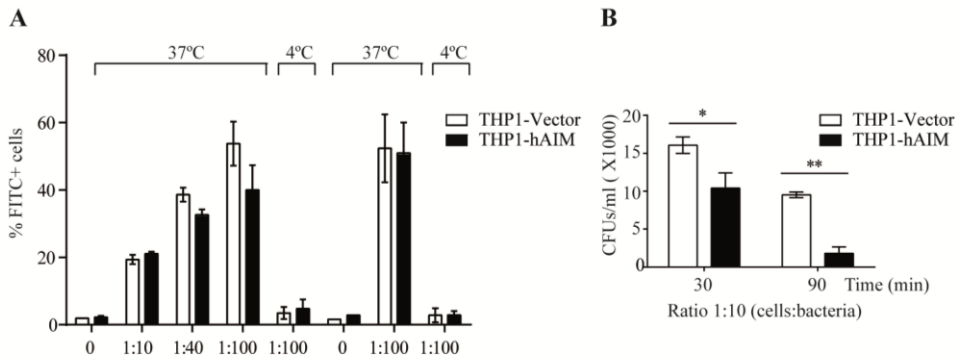


Figure 2. Effect of hAIM in phagocytosis and killing of bacteria. (A) THP1 MΦ were incubated during 1 h with fluorescent *E. coli* or *S. aureus* bioparticles at the indicated ratios (cell:bacteria) and temperatures. The graphs show the mean \pm SEM of % FITC cells from three independent experiments. (B) THP1 MΦ were infected with viable *E. Coli* at a ratio of 10 bacteria per cell during 30 or 90 min, cells were lysed and intracellular CFU numbers were determined by colony counting. The graphs show the mean \pm SEM of three different experiments. Two way ANOVA * $p \leq 0.5$, ** $p \leq 0.01$.

DISCUSSION II

Scavenger receptors (SRs) bind to a broad range of polyanionic molecules, among them PAMPs, and have been implicated in host defense against bacterial infections (Krieger 1997). Like mouse AIM (Haruta, Kato et al. 2001), it is known that other SRCR-SF members enhance the macrophage phagocytic abilities, promoting phagocytosis of pathogens, virus or apoptotic cells (Mukhopadhyay and Gordon 2004; Pluddemann, Mukhopadhyay et al. 2011). Here, we explored whether human protein AIM shares this pro-phagocytic function, essential for host defense response.

At the amino acid level, human and mouse AIM proteins are highly homologous (69% identity, 80% similarity), however, there are species-specific differences in their glycosylation patterns (Sarrias, Padilla et al. 2004) that may result in distinct activities. In this regard, a recent publication confirmed the relevance of glycosylation in mAIM function, by reporting that mutation of two N-glycosylation sites in the protein inhibited its secretion and enhanced its lipolytic function in adipocytes (Mori, Kimura et al. 2012). Therefore, it was worth analyzing whether key functions described already for mAIM were conserved in hAIM.

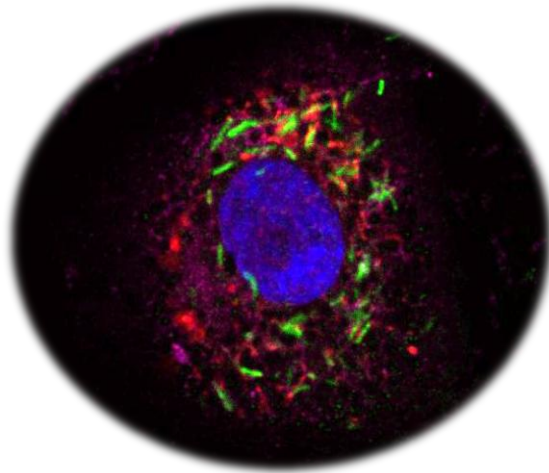
We had previously reported that the widely studied function of mAIM, its antiapoptotic role (Arai, Shelton et al. 2005; Valledor, Hsu et al. 2004; Zou, Garifulin et al. 2011; Gebe, Kiener et al. 1997; Haruta, Kato et al. 2001; Joseph, Bradley et al. 2004), is conserved in the human form of the protein (Amezaga, Sanjurjo et al. 2013). As other members of the SRCR superfamily, human and

mouse AIM also share the ability of bind and aggregate a microbial agents (bacteria and fungi), and both proteins present immunomodulatory properties in response to PAMPs in terms of reducing TNF- α secretion (Sarrias, Rosello et al. 2005; Martinez, Escoda-Ferran et al. 2014). In the other hand, distinct roles of human and mouse AIM in M Φ lipid accumulation were reported (Amezaga, Sanjurjo et al. 2013). In the context of atherosclerosis, assessment of oxLDL foam cell formation evidenced a new role for hAIM, in enhancing macrophage lipid storage through increased uptake. This enhancement is not conserved in mAIM (Arai, Shelton et al. 2005).

Here, we find another functional mismatch between both forms of the proteins. Unlike its murine counterpart our data suggest that hAIM does not induce a pro-phagocytic function in M Φ . No hAIM-dependent effects were observed in phagocytosis of latex beads, Gram-negative or Gram-positive bacteria by THP1 cells. Moreover in experiment performed with latex beads we have used mouse BMDM and the recombinant form of mAIM to corroborate our data. Haruta et al. argued that mAIM pro-phagocytic activity of latex beads may be an indirect effect, they hypothesized that mAIM may induce an unknown factor(s) that may enhance phagocytosis. Further studies of the mechanisms involved in these phenomena are needed to understand the different roles of mouse and human protein in bead uptake.

Our previous data described AIM as an autophagy inductor (Results, work I) and accumulating evidences highlight autophagy as a important process in the control of intracellular infection by

bacteria (Jo, Yuk et al. 2013). In accordance, in the present work, we observed a lower number of intracellular viable *E. coli* in MΦ after infection in the presence of hAIM. Because phagocytosis of *E. coli* was not inhibited by hAIM, we hypothesize that hAIM may enhance bactericidal mechanisms in the macrophage, possibly through autophagy induction. Our results are part of an ongoing project and further studies are needed to address the mechanism involved in AIM-dependent reduction of *E. coli* burdens. In parallel studies, involvement of hAIM in macrophage phagocytosis and bactericidal mechanisms was assayed in a *Mycobacterium tuberculosis* infection model as shown in the following work.



THP1-hAIM cell infected with Mtb-FITC (green).
Acidic structures (red), LC3 (purple), nucleus
(blue).

WORK III: The scavenger protein AIM potentiates the antimicrobial response against *Mycobacterium tuberculosis* by enhancing autophagy

Lucía Sanjurjo, Núria Amézaga, Cristina Vilaplana, Neus Cáceres, Elena Marzo, Pere-Joan Cardona, Maria-Rosa Sarrias.

SUMMARY

Apoptosis Inhibitor of Macrophages (AIM), a scavenger protein secreted by tissue macrophages, is transcriptionally regulated by the nuclear receptor Liver X Receptor (LXR) and Retinoid X Receptor (RXR) heterodimer. Given that LXR exerts a protective immune response against *M. tuberculosis*, here we analyzed whether AIM is involved in this response. In an experimental murine model of tuberculosis, AIM serum levels peaked dramatically early after infection with *M. tuberculosis*, providing an *in vivo* biological link to the disease. We therefore studied the participation of AIM in macrophage response to *M. tuberculosis in vitro*. For this purpose, we used the H37Rv strain to infect THP-1 macrophages transfected to stably express AIM, thereby increasing infected macrophage survival. Furthermore, the expression of this protein enlarged foam cell formation by enhancing intracellular lipid content. Phagocytosis assays with FITC-labeled *M. tuberculosis* bacilli indicated that this protein was not involved in bacterial uptake; however, AIM expression decreased the number of intracellular CFUs by up to 70% in bacterial killing assays, suggesting that AIM enhances macrophage mycobactericidal activity. Accordingly, *M. tuberculosis*-infected AIM-expressing cells upregulated the production of reactive oxygen species. Moreover, real-time PCR analysis showed increased mRNA levels of the antimicrobial peptides cathelicidin and defensin 4B. These increases were concomitant with greater cellular concentrations of the autophagy-related molecules Beclin 1 and LC3II, as well as enhanced acidification of mycobacterial phagosomes and LC3 co-localization. In summary, our data support the notion that AIM contributes to key macrophage responses to *M. tuberculosis*.

This work was published in PLoS ONE. The scavenger protein Apoptosis Inhibitor of Macrophages (AIM) potentiates the antimicrobial response against *Mycobacterium tuberculosis* by enhancing autophagy. PLoS ONE 8(11): e79670. doi:10.1371/journal.pone.0079670, 2013.

RESULTS III

hAIM expression increases the survival of *M. tuberculosis*-infected THP1 MΦ

Our first goal was to assess whether the anti-apoptotic role of AIM (Arai, Shelton et al. 2005; Valledor, Hsu et al. 2004; Zou, Garifulin et al. 2011; Gebe, Kiener et al. 1997; Haruta, Kato et al. 2001; Joseph, Bradley et al. 2004) is conserved in *Mtb* infection, stable THP1 cell transfectants were infected at three MOIs, and cell viability was assessed by crystal violet staining. *Mtb* infection affected MΦ viability in a MOI- and time-dependent manner (**Figure 1A**). The data further show that the numbers of uninfected THP1-hAIM cells were similar to those of THP1-Vector cells over time. Interestingly, infection at low MOI (0.1) did not significantly change THP1 cell survival when compared to that of uninfected cells. However, increasing the MOI to 1 resulted in higher THP1-Vector cell death, which was significantly greater than that observed in THP1-hAIM cells: at day 3 postinfection, the number of viable THP1-hAIM cells was double than that of THP1-Vector cells (7×10^4 vs. 3×10^4). Longer infection times (5 days) or increasing the MOI to 10 almost totally compromised cell viability. The dynamics of such infection time involve continuous uptake, killing of some bacteria, and too many organisms being internalized by MΦ, and therefore most of the subsequent experiments were performed in shorter lengths of time. The data suggest that expression of hAIM contributes to the survival of *Mtb*-infected MΦ. In accordance, hAIM conferred MΦ resistance to *Mtb*-induced apoptosis, as measured by Annexin V and 7AAD staining. In these assays, no

apoptosis was detected at MOI 0.1, while the percentage of apoptotic cells (Annexin V+, 7AAD- cells) was significantly lower in THP1-hAIM cells at MOI 1 (Figure 1B). These data strengthen the notion that hAIM supports MΦ survival in the setting of Mtb infection.

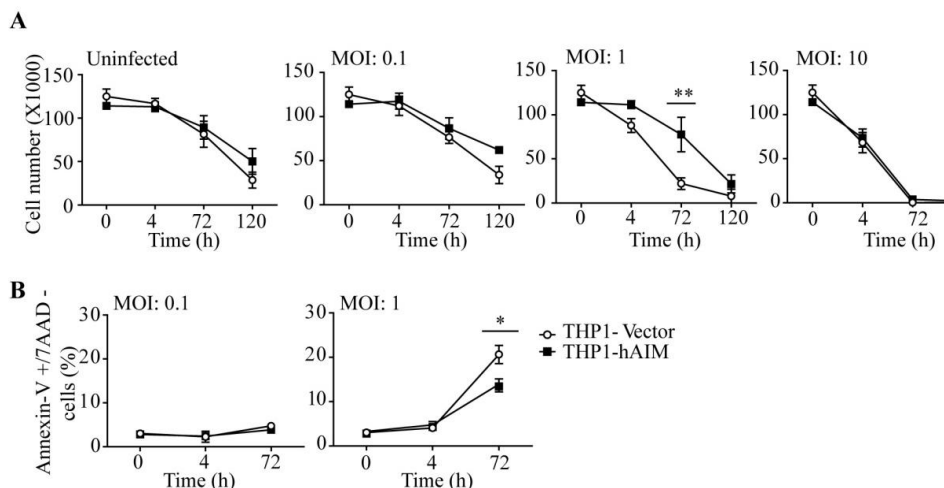


Figure 1. Expression of hAIM infection increases the survival of Mtb-infected MΦ. Stably transfected THP1-Vector (control) and THP1-hAIM MΦ were infected with Mtb at the indicated MOIs, and cell viability was analyzed at the indicated time points. **(A)** The number of viable cells was determined by crystal violet staining and quantified using a standard curve of known input cell numbers. **(B)** Apoptosis was assessed using Annexin V-7AAD staining and analyzed by flow cytometry. Results are expressed as percentage of Annexin V-positive, 7AAD-negative cells. All graphs are from three independent experiments performed in triplicate. * $p \leq 0.05$; ** $p \leq 0.01$: two-way ANOVA.

hAIM enhances MΦ foam cell formation and IL-8 secretion

MΦ foam cell formation caused by intracellular lipid accumulation is a hallmark of Mtb infection (Caceres, Tapia et al. 2009; Russell, Cardona et al. 2009). We have recently observed that in atherosclerosis hAIM increases foam cell formation induced

by modified lipoproteins (namely oxLDL) (Amezaga, Sanjurjo et al. 2013). We therefore tested whether hAIM modifies Mtb-induced MΦ lipid accumulation. For this purpose, we stained infected MΦ with the lipid specific dye Nile Red. Mtb infection increased foam cell formation in THP1-Vector cells, and this formation was enhanced in hAIM-transfected cells (upper panel), as shown by the fluorescence microscopy analysis in **Figure 2A**. Quantification by flow cytometry analysis (lower graphic) indicated that the lipid content of THP1-hAIM cells reached ~ 4-fold that of control THP1-Vector cells. Infected LXR-deficient mice show decreased pulmonary neutrophilia (Korf, Vander Beken et al. 2009). We analyzed whether AIM contributes to Mtb-infected MΦ secretion of the chemokine IL-8, a highly attractant molecule for neutrophils (Kobayashi 2008). Indeed, we found that the expression of hAIM increased MΦ IL-8 production by ~3-fold (**Figure 2B**). All together, these data indicate that hAIM contributes to infected MΦ foam cell formation as well as to IL-8 secretion.

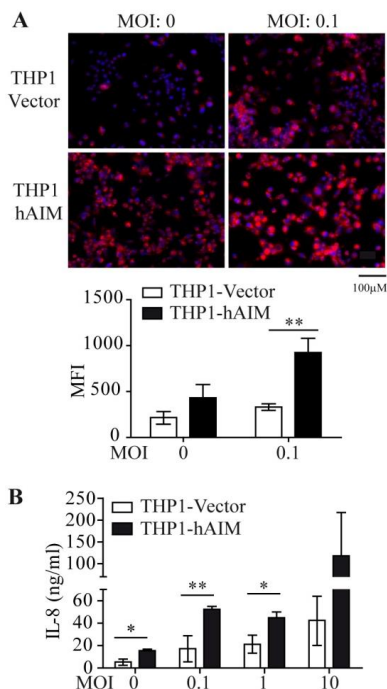


Figure 2. Human AIM enhances foam cell formation and IL-8 secretion. (A) THP1 MΦ were infected with Mtb at MOI 0.1 for 24 h in RPMI 1% FBS medium, fixed, stained with Nile Red and observed by fluorescent microscopy (*upper panel*), or quantified by flow cytometry (*lower graphic*). MFI: Median Fluorescence Intensity. **(B)** The amount of IL-8 in culture supernatants from *M. tuberculosis*-infected THP1 MΦ at the indicated MOIs during 24 h was determined by ELISA. Mean ± SEM from three independent experiments performed in triplicate are shown. *p≤0.05; **p≤0.01; two-way ANOVA.

Expression of hAIM reduces M Φ mycobacterial load

Using a colony forming unit (CFU) assay, we tested whether hAIM participates in M Φ mycobactericidal activity. Expression of hAIM significantly reduced the number of viable bacilli per cell, with ~70% of the bacteria being killed at day 5 post-infection at MOI 0.1, and ~50% at day 3 post-infection at MOI 1 (**Figure 3A**). Given that infection rate and time affected cell viability (**Figure 1**), CFUs per cell were calculated by dividing CFUs by number of viable cells, as determined by staining with the vital dye crystal violet. To discard the possibility that reduced bacterial load in hAIM-expressing cells was due to decreased initial phagocytosis, bacilli were fluorescently labeled with FITC, and THP1 M Φ bacterial uptake was analyzed by flow cytometry (**Figure 3B**) in these assays, the percentage of FITC-positive cells increased over time when the experiments were performed at 37°C, but not at 4°C. These observations thus indicate that increases in fluorescence were due to uptake rather than to bacterial adherence to the cell surface. Nevertheless, no differences were detected between THP1-Vector and THP1-hAIM cells, thereby suggesting no participation of hAIM in bacterial uptake. In summary, our data indicate that hAIM plays a crucial role in enhancing mycobactericidal responses in M Φ .

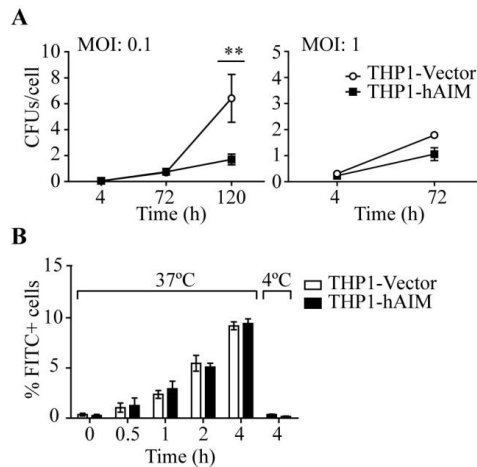


Figure 3. hAIM increases the intracellular killing of *Mtb* without modifying the phagocytic capacity of $M\Phi$. (A) Stably transfected THP1 $M\Phi$ were infected with *Mtb* at MOI 0.1 and 1. 4, 72 and 120 h later, cells were lysed and intracellular CFU numbers were determined by serial dilutions on 7h9 agar plates. CFUs per cell were calculated by dividing CFUs by number of viable cells determined by crystal violet staining at each time point. Mean \pm SEM from three independent experiments performed in duplicate. * $p \leq 0.05$; ** $p \leq 0.01$; two-way ANOVA. (B) THP1 $M\Phi$ were incubated with FITC-labelled bacilli at MOI 40 and the percentage of FITC-positive cells at the indicated time points and temperature was determined by flow cytometry. Results are expressed as the % of FITC-positive cells at each time point and show the mean \pm SEM from three independent experiments.

hAIM modulates the $M\Phi$ production of radical oxygen species

Our next set of experiments analyzed whether the hAIM-mediated mycobactericidal effect was due to increased $M\Phi$ production of NO or reactive oxygen species (ROS). NO levels in the supernatants as well as intracellular ROS in infected $M\Phi$ were analyzed by the Griess method and by H2-DCF-DA-induced fluorescence (Figure 4A and B, respectively). Although *Mtb* infection induced NO secretion in both cell lines in a time- and MOI-dependent manner, NO

production was very low (0-2 μ M) and did not differ between THP1-Vector and THP1-hAIM cells (**Figure 4A**). In fact, it is well known that NO production by human M Φ is not as high as that of murine M Φ (Weinberg, Misukonis et al. 1995) and that the involvement of this process as a mycobactericidal mechanism in humans is controversial (Yang, Yuk et al. 2009). Conversely, upon infection, a time- and dose-dependent significant rise in ROS production was observed in both cell lines. This increase was further intensified by the expression of hAIM (**Figure 4B**). Therefore our data indicate that hAIM induces increased ROS production in infected M Φ .

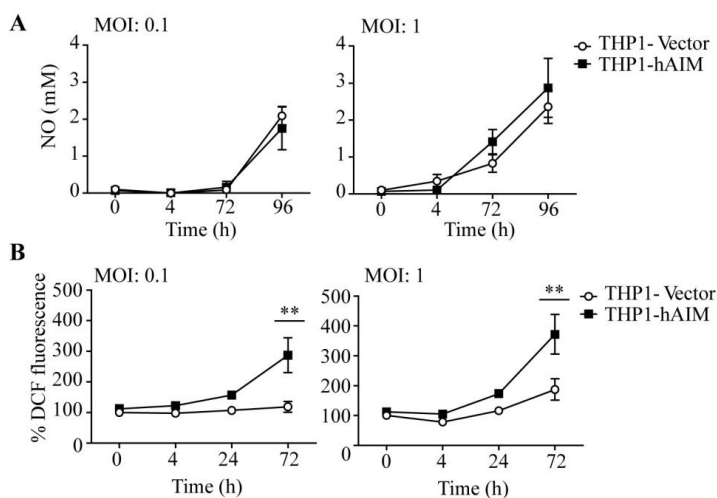


Figure 4. Effects of hAIM on NO and ROS production. THP1 M Φ were infected with Mtb at MOI 0.1 and 1 during the times indicated, and the production of NO and ROS was determined as follows. **(A)** Nitrite levels were measured in the supernatants using the Griess reagent, and values were calculated against a standard curve of known NaNO₂ concentrations. **(B)** Intracellular ROS release was quantified via the changes of DCF fluorescence. ROS levels were calculated as a percentage of the uninfected control (THP1-Vector cells), indicated as 100%. Mean \pm SEM from three independent experiments, performed in triplicate are shown. * $p \leq 0.05$; ** $p \leq 0.01$; two-way ANOVA.

hAIM upregulated the expression of the antimicrobial peptides Defensin 4B (DEF4B) and cathelicidin.

We next studied whether expression of hAIM modulates the induction of DEF4B and cathelicidin (LL-37) –two antimicrobial peptides of the vitamin D-dependent antimicrobial pathway– in infected MΦ. Interestingly, Mtb infection induced MΦ synthesis of DEF4B and cathelicidin mRNA at 72 h postinfection, and this was enhanced ~2- fold in hAIM-expressing cells (**Figure 5A**). We next tested whether hAIM was able to modulate IFN-γ-induced antimicrobial responses. In this regard, the expression of hAIM synergized with IFN-γ in further increasing the gene expression of DEF4B ~2-fold, but not that of cathelicidin (**Figure 5B**).

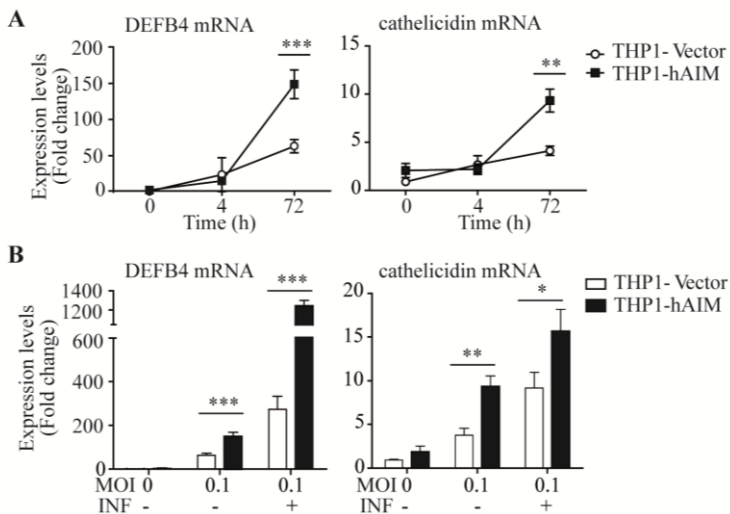


Figure 5. hAIM increases the expression of the antimicrobial peptides DEF4B and cathelicidin. (A) Stably transfected THP1 MΦ were infected with Mtb at MOI 0.1, and mRNA levels of DEF4B and cathelicidin were determined by RT-qPCR. (B) The same experiment was performed but cells were incubated with rIFN γ (10 ng/ml) 24 h prior to infection. mRNA mean fold change values is relative to uninfected THP1-Vector \pm SEM, set as 1, from three independent experiments. * $p \leq 0.05$; ** $p \leq 0.01$; *** $p \leq 0.001$ two-way ANOVA.

hAIM expression activates autophagy-dependent microbicidal mechanisms

The vitamin D-antimicrobial pathway controls autophagy and phagosome maturation (Yuk, Shin et al. 2009). We therefore analyzed whether hAIM affects this pathway by modulating the expression of the autophagosome protein Beclin 1. In this regard, the mRNA of this gene increased in THP1-Vector cells at 72 h postinfection, and the expression of hAIM further increased Beclin 1 mRNA levels 1.5-fold (**Figure 6A**). Moreover, to study autophagosome formation, we used Western blots to quantify the content of LC3-II and LC3-I (Kabeya, Mizushima et al. 2000) in cellular lysates. Mtb infection slightly increased the LC3II/ LC3 I ratio in THP1-Vector M Φ (**Figure 6B**). Interestingly, hAIM expression enhanced this ratio 5-fold, thereby suggesting increased autophagosome formation. We next tested whether hAIM enhances the acidification of mycobacterial phagosomes and whether this was due to autophagy-dependent mechanisms by analyzing the colocalization of LC3, as well as the number of LC3 puncta per cell. THP1 M Φ were infected with FITC-labeled bacilli for 24 (data not shown) and 72 h and stained with LysoTracker, an acidotropic fluorescent dye that accumulates in acidic organelles, as well as an antibody against LC3. No differences between the two cell lines were observed at 24 h postinfection regarding phagosomal acidification (data not shown). However, hAIM-expressing cells showed 43.2 % \pm 16.4 FITC-bacteria colocalization with LysoTracker vs 19.6 \pm 12.5 in THP1-Vector cells (p 0.0029 Student t test) at 72 h postinfection (**Figure 6C**). These findings show that hAIM expression in M Φ renders mycobacterial phagosomes more

susceptible to acidification. Furthermore, this was coincident with an increase of LC3 colocalization with the bacterial-containing phagosomes in hAIM-expressing cells (32.7% \pm 22) versus THP1-Vector cells (10.7% \pm 10) (p :0.0004 Student t test). We further analyzed the amount of LC3 puncta in infected cells at this time point as a measure of autophagosome formation, and found that hAIM-expressing cells almost triplicated the LC3 puncta per cell as compared to THP1-Vector cells (29.3 \pm 20 vs 11.2 \pm 11, p <0.0001 Student t test). Interestingly, addition of the autophagy inhibitor 3-MA reverted these effects, further suggesting a contribution of hAIM to autophagy. All together, our results support the notion that hAIM contributes to increasing M Φ autophagosome formation during Mtb infection.

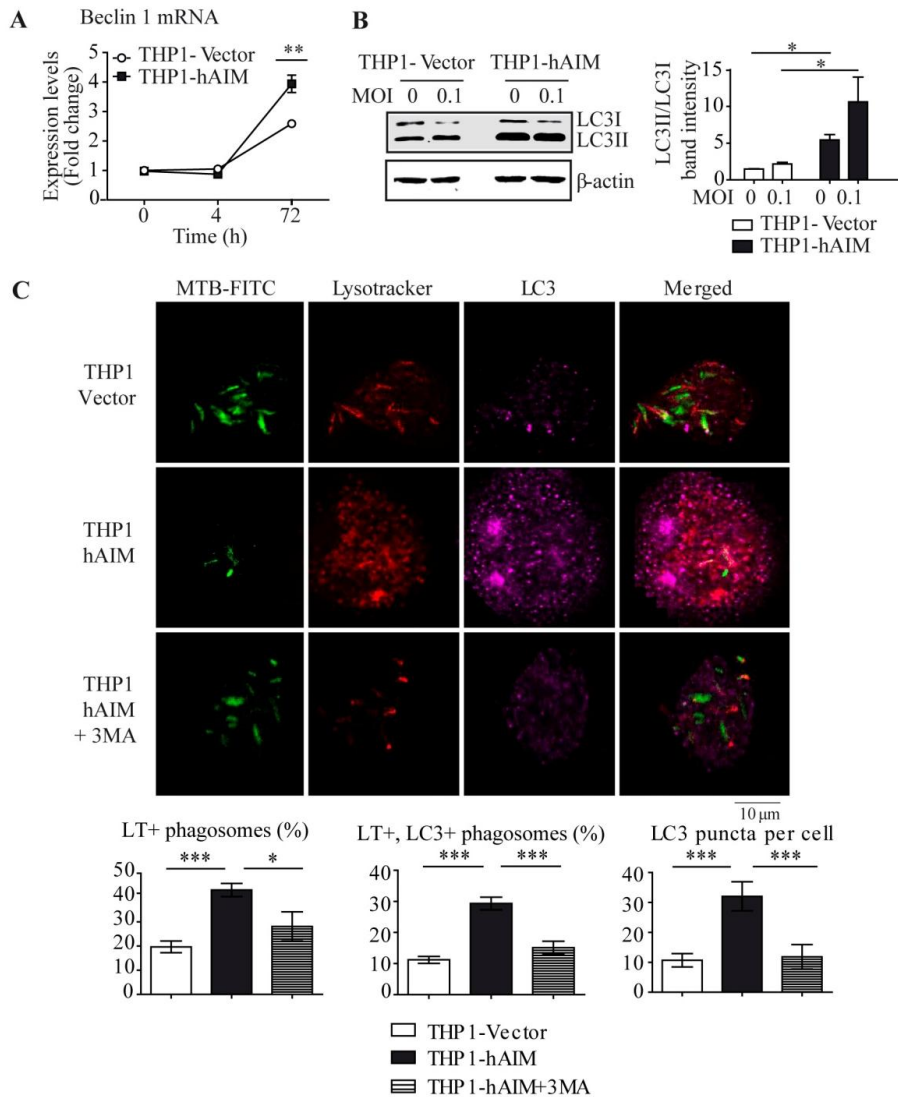


Figure 6. hAIM promotes autophagy and endosome-lysosome fusion in Mtb-infected THP1 cells. Stably transfected THP1 MΦ were infected with Mtb at MOI 0.1, and autophagy was analyzed as follows. **(A)** mRNA levels of autophagy related protein Beclin-1 were determined by RT-qPCR at the indicated times. mRNA mean fold change values are relative to uninfected THP1-Vector \pm SEM, set as 1, from three independent experiments. * $p \leq 0.05$; ** $p \leq 0.01$; *** $p \leq 0.001$ two-way ANOVA. **(B)** LC3 expression was analyzed by western blot in cell lysates of uninfected and Mtb-infected THP MΦ for 24 h. Left: representative western blot image. Right: protein signal intensities were quantified and plotted as LC3-II/LC3-I ratio after normalization to the control protein actin. Mean \pm SEM of three independent experiments. * $p \leq 0.05$; ** $p \leq 0.01$; *** $p \leq 0.001$, one-way ANOVA. **(C)** Mtb-lysosome co-localization analysis. Upper panel: representative confocal microscopy images showing co-localization of FITC-labeled Mtb bacilli (green), cellular lysosomes (red) and LC3 (purple) 72 h post-infection, in the presence or absence of the autophagy inhibitor 3-MA. Lysosomes were stained with LysoTracker Red, and LC3 with a specific antibody. Lower panel: mean \pm SEM quantitative data show Mtb-lysosome, Mtb-lysosome-LC3 co-localization and LC3 puncta per cell in three independent experiments, with each experiment including at least 200 internalized bacilli or 100 cells scored in random fields. * $p \leq 0.05$; ** $p \leq 0.01$; *** $p \leq 0.001$, one-way ANOVA.

AIM levels increases *in vitro* and *in vivo* after *M. tuberculosis* infection

Both human (hAIM) and mAIM have been detected circulating in serum (Gebe, Llewellyn et al.; Sarrias, Padilla et al. 2004). An important goal was to analyze whether, like several LXR and RXR target genes, AIM expression in MΦ is induced in response to *Mtb* infection (Korf, Vander Beken et al. 2009). First we analyzed whether AIM mRNA and protein expression is induced in the THP1 cell line *in vitro* in response to *Mtb* infection. *Mtb* infection at MOI 0.1 induced hAIM mRNA synthesis in THP1-Vector (control) and THP1-hAIM cell lines, although the increase was significant 120 h post-infection (Figure 7A). At this time point, hAIM protein was also induced in both cell lines, albeit the levels were higher in THP1-hAIM cells (Figure 7B).

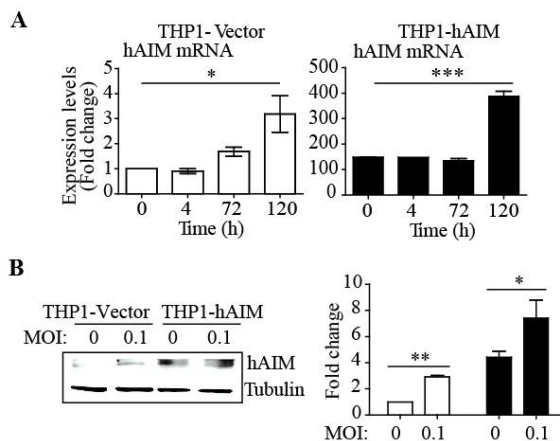


Figure 7. *Mtb* increases hAIM mRNA and protein levels in a THP1 *in vitro* infection model. Stably transfected THP1-Vector (control) and THP1-hAIM MΦ were infected with *Mtb* MOI 0.1, and hAIM expression was analyzed at the indicated time points, (A) mean ± SEM of hAIM mRNA levels were determined by RT-qPCR. hAIM mRNA values are represented as fold change vs. uninfected THP1-Vector cells, set as 1. * $p \leq 0.05$; *** $p \leq 0.001$; one-way ANOVA. (B) Western blot analysis of hAIM protein levels in cell lysates at 120 h postinfection. Equal loading was determined by probing against tubulin. Left panel, western blot; right panel, fold induction levels, which were calculated by setting the background signal of uninfected THP1-Vector cells to 1 as a reference. * $p \leq 0.05$; ** $p \leq 0.01$, one-way ANOVA.

We next examined the concentrations of serum mAIM in an experimental model of Mtb infection in order to determine an *in vivo* biological link between this protein and the disease. Mice were infected with Mtb by aerosol inoculation, and lung and spleen bacterial load, as well as serum mAIM were analyzed at several times post-infection (material and methods, Figure 9). mAIM serum detection was optimized as shown in Figure 9, material and methods. **Figure 8A** shows a representative Western blot analysis of serum mAIM levels. The graph depicting results from 3 to 5 mice per time point in **Figure 8B** shows that mAIM levels increased 5-fold immediately after infection and remained constant for 2 weeks. A second peak of this protein was detected at week 3 post-infection, reaching maximum levels (10-fold those of uninfected mice). This peak coincided with maximum CFU counts in lung and spleen. Concentrations of mAIM dropped to basal levels thereafter and during antibiotic treatment. Reactivation of the infection by antibiotic withdrawal did not affect serum mAIM levels, which remained constant for the rest of the experiment.

RESULTS & DISCUSSION

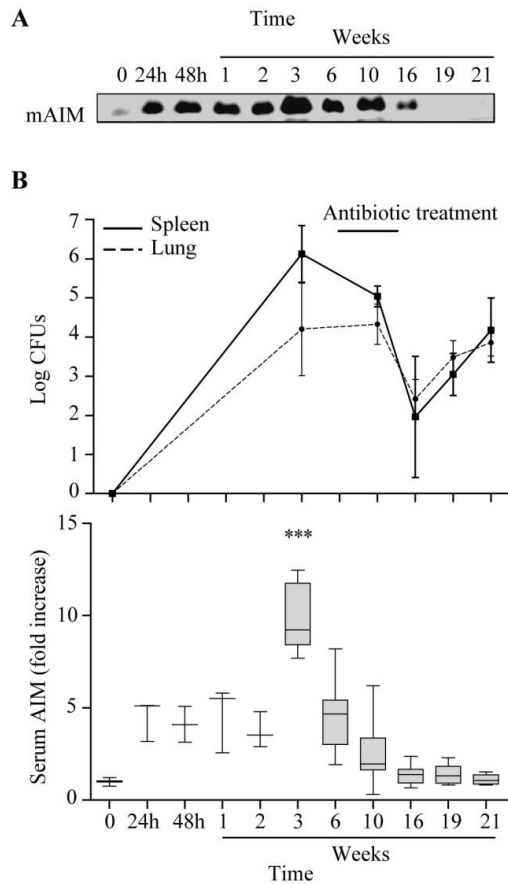


Figure 8. Mtb increases mAIM serum levels in an *in vivo* infection model. C57BL/6 mice were infected with *M. tuberculosis* H37Rv through aerosol inoculation. Mice were treated with INH/RIF for 8 weeks (w6 to w14) at which point antibiotic was withdrawn, and infection was allowed to reactivate. mAIM serum levels and bacillary load in the lung and spleen were measured at several time points post-infection (24 h - 21 weeks). **(A)** Representative image of mAIM levels analyzed by western blot of serum samples. **(B)** Graphs showing spleen and lung bacterial loads at the indicated times (upper graph) and mAIM protein intensity (lower graph) data. Box plots show median values and 5-95 percentile values, from 1 μ l serum (n=3 to n=5). Fold induction levels were calculated using as reference the serum mAIM from a pool of 5 C57BL/6 uninfected healthy animals, set as 1. *** $p \leq 0.001$ two-way ANOVA.

DISCUSSION III

Here we demonstrate that hAIM participates in several key aspects of M Φ response to Mtb. This finding is of relevance because in previous studies we showed that hAIM is involved in pattern recognition of bacteria and in the modulation of monocyte inflammatory responses (Sarrias, Rosello et al. 2005). The present study now reveals that the participation of hAIM in innate immunity goes beyond these activities. Our data support the notion that hAIM makes a relevant contribution to the M Φ autophagy mechanisms that lead to intracellular mycobacterial killing.

In our effort to decipher the functional involvement of hAIM in Mtb infection of M Φ , we performed a range of *in vitro* experiments. We used the THP1 cell line because THP1-PMA differentiated M Φ have been demonstrated to be a suitable cellular model for Mtb infection (Karim, Chandra et al. 2011; Theus, Cave et al. 2004), including the study of the vitamin D antimicrobial pathway (Liu, Stenger et al. 2007). Using this cell line, we assessed whether the anti-apoptotic activity of AIM is conserved in response to Mtb infection. Indeed, THP1-hAIM cells were more resistant to infection-induced cell death and apoptosis, thereby confirming a pro-survival role for this protein in these settings. These results also served to determine that, under our experimental conditions, Mtb did not affect THP1 cell survival when infected at MOI 0.1. Therefore, our studies at MOI 0.1 helped to decipher the contribution of hAIM to M Φ responses, independent of its anti-apoptotic effects.

We also observed that hAIM expression enhanced foam cell formation both in uninfected and infected cells, thus conferring a role for the human form of this protein in M Φ lipid accumulation. This finding contrasts with previous results, in which Mtb-infected LXR-deficient mice showed enhanced foam cell formation (Korf, Vander Beken et al. 2009). This apparent contradiction is consistent with our own observations, which point to a distinct role of human and mouse AIM in M Φ lipid accumulation (Amezaga, Sanjurjo et al. 2013). In the context of atherosclerosis, assessment of oxLDL foam cell formation evidenced a new role for hAIM, which enhances macrophage lipid storage through increased uptake (Amezaga, Sanjurjo et al. 2013). This enhancement is not conserved in mAIM (Arai, Shelton et al.). Foamy M Φ are key participants in both sustaining persistent bacteria and contributing to the tissue pathology which might lead to cavitation and the release of infectious bacilli (Caceres, Tapia et al. 2009; Russell, Cardona et al. 2009). The lipid may serve as a source of nutrients for the pathogen, enabling its survival within the cell. On the other hand, lipids play multiple roles as determinants of phagosomal formation and fate and as coordinators of the recruitment and retention of key phagocytic proteins (Steinberg and Grinstein 2008; Melo and Dvorak 2012). The participation of hAIM in Mtb-induced foam cell formation and its specific consequences deserves further study.

Given that LXR-deficient mice fail to mount an effective early neutrophilic airway response to infection (Korf, Vander Beken et al. 2009) and that THP1-hAIM-expressing cells showed increased secretion of IL-8, a highly chemoattractant chemokine for neutrophils, we hypothesize that AIM contributes to neutrophil

attraction. Furthermore, our studies provide strong evidence that this protein participates in the intracellular mycobactericidal activity of M Φ . Functional studies suggest that this activity is mediated through enhanced ROS secretion and autophagy mechanisms in M Φ . The expression of hAIM induced an increase in the transcription of the antimicrobial peptides DEF4B and cathelicidin in Mtb-infected M Φ .

Given that hAIM expression synergized with IFN- γ in further increasing DEF4B mRNA levels ~2 fold, but not those of cathelicidin, our results suggest that, in addition to the vitamin D pathway, hAIM also activates the IL-1 β pathway of DEF4B production (Liu, Schenk et al. 2009). hAIM-enhanced cathelicidin and DEF4B production was concomitant with increased transcription of the autophagy-related gene Beclin-1. Consequently, we observed enhanced flux of bacteria through phagosomes to phagolysosomes as evidenced by the significantly higher number of bacilli localized in the phagolysosomal compartments. Several additional evidences point to a role for hAIM in enhancing autophagy mechanisms. Its expression induced increased cleavage of the autophagosome marker LC3 protein as well as enhanced colocalization of this protein with the bacterial-containing phagolysosomes. The elevated LC3 puncta in hAIM-expressing cells further suggest a contribution of hAIM to autophagy. Moreover, the autophagy inhibitor 3-MA (Klionsky, Abdalla et al. 2012) reverted these effects. Overall, our data indicate that hAIM protein boosts ROS production and antimicrobial peptide synthesis, concomitant with an increase in autophagy mechanisms, which could explain enhanced mycobactericidal capacity of hAIM-expressing M Φ .

Our studies confirmed that, like other LXR target genes such as ApoE and ABCA1 (Korf, Vander Beken et al. 2009), AIM MΦ mRNA expression was induced in response to infection. This finding is relevant because MΦ expression of AIM is tightly regulated. In this regard, low levels of hAIM mRNA and null protein expression were detected by real-time PCR and Western blot, respectively, in differentiated THP1 cells (Amezaga, Sanjurjo et al. 2013). In our study, due to stable transfection of the cDNA encoding hAIM in these cells, the levels of hAIM mRNA were higher in THP1-hAIM cells over time. The data indicate that the upregulation of hAIM expression in THP1-Vector cells occurred later than the observed increase in anti-mycobacterial activity in THP1-hAIM cells.

The involvement of AIM in the initial innate immune response to Mtb infection is illustrated by the observation that 24 h after infection its serum levels increased 5-fold and peaked at 10-fold at 3 weeks, during the exponential growth of the bacilli (Torrado, Robinson et al.). At this point, when bacterial growth control by the adaptive immune response takes place, AIM serum levels dropped to almost basal levels. Antibiotic treatment or reactivation by antibiotic removal did not result in a second peak of serum AIM, thus reinforcing the notion that hAIM is involved in the initial inflammatory burst of the host response to infection. It also suggests that a high threshold of bacterial load and subsequent inflammation are needed for hAIM to increase its plasma levels. Our results are of relevance because the protein AIM is composed exclusively of Scavenger Receptor Cysteine-Rich (SRCR) domains (Sarrias, Gronlund et al. 2004). The SRCR domain is present in proteins that contribute to the immune defense against Mtb infection, such as macrophage SR-AI (Sever-Chroneos,

Tvinnereim et al. 2011) and Macrophage Receptor with Collagenous Structure (MARCO) (Bowdish, Sakamoto et al. 2009). Moreover, genetic variations of MARCO have been associated with susceptibility to pulmonary tuberculosis in a Gambian population (Bowdish, Sakamoto et al. 2013). It is interesting that the ectodomain of CD163 (sCD163), another member of the SRCR protein family expressed by M Φ , has been found to be elevated in serum of TB patients (Knudsen, Gustafson et al. 2005). In that study increased pre-treatment serum levels of sCD163 appeared to be an independent predictor of mortality during treatment, as well as of long-term mortality in verified cases of TB from Guinea-Bissau (Knudsen, Gustafson et al. 2005). These observations open up the possibility that related SRCR proteins are predictors of TB disease in humans.

Here we studied whether the LXR-target gene AIM further contributes to host innate immunity by modulating key M Φ responses to Mtb. Our results indicate that AIM expression peaks in the early phase of infection, thereby inducing the synthesis of vitamin D-dependent antimicrobial peptides and subsequent autophagy mechanisms that lead to mycobacterial killing. All together, our data support the notion that AIM enhances the mycobactericidal activity of M Φ , thus actively participating in the innate response against Mtb. In summary, our *in vivo* observations and *in vitro* results indicate that hAIM is a key orchestrator of M Φ bactericidal responses to Mtb.

GENERAL DISCUSSION

In recent years, the understanding of the role/s of the protein AIM has greatly expanded. Besides its initially described anti-apoptotic role (Gebe, Kiener et al. 1997; Miyazaki, Hirokami et al. 1999; Haruta, Kato et al. 2001; Joseph, Bradley et al. 2004; Valledor, Hsu et al. 2004; Arai, Shelton et al. 2005; Zou, Garifulin et al. 2011), other highly relevant functional features have been reported in several pathological scenarios related to lipid metabolism, namely atherosclerosis, obesity, and metabolic disorders subsequent to obesity. (Arai, Shelton et al. 2005; Kurokawa, Arai et al. 2010; Kurokawa, Nagano et al. 2011; Miyazaki, Kurokawa et al. 2011; Amezaga, Sanjurjo et al. 2013; Arai, Maehara et al. 2013; Arai and Miyazaki 2014).

In the context of bacterial infection, AIM influences the monocyte inflammatory response to PAMPs by reducing TNF- α secretion (Sarrias, Rosello et al. 2005; Martinez, Escoda-Ferran et al. 2014). However, no AIM-dependent regulation of other inflammatory mediators nor the mechanisms involved in its anti-inflammatory function had been described at the beginning of our work. Furthermore, AIM belongs to the SRCR superfamily of proteins, whose high degree of structural and phylogenetic conservation has helped elucidate several common functions. Among these, their bacterial-binding capacity (Dunne, Resnick et al. 1994; Brannstrom, Sankala et al. 2002; Bikker, Ligtenberg et al. 2004; Sarrias, Farnos et al. 2007; Fabriek, van Bruggen et al. 2009; Loimaranta, Hytonen et al. 2009; Vera, Fenutria et al. 2009; Miro-

Julia, Rosello et al. 2011). In this regard, like other SRCR members, AIM binds to and aggregates pathogens (Sarrias, Rosello et al. 2005; Martinez, Escoda-Ferran et al. 2014). But to our knowledge, reports studying its role in macrophage uptake of bacteria (i.e. phagocytosis) did not exist before the beginning of our work.

Considering all this information, the first objective of the present work was to deepen the analysis of AIM possible anti-inflammatory properties in the context of macrophage responses to PAMPs. Our goal was to try to decipher the macrophage signalling pathways that could be affected by AIM resulting in its inhibition of TNF- α . These findings are of relevance because although inflammation is a physiological response mechanism that protects organisms from damage, it can also lead to excessive self-aggression and pathology when not finely regulated (Kundu and Surh 2008; Mantovani, Allavena et al. 2008). Therefore, the ability to impair PAMP-induced pro-inflammatory cytokine production could be useful in protecting tissues from local damage by inflammation, and from more generalized effects such as sepsis. In fact, other members of the SRCR family such as CD5 and CD6 have been shown to inhibit septic shock in a mouse model (Sarrias, Farnos et al. 2007; Vera, Fenutria et al. 2009).

We thus aimed at elucidating the intracellular events that lead to inflammatory modulation by hAIM. Our results show that hAIM is able to activate basal autophagy flux. To our knowledge, AIM is the first protein belonging to the SRCR family to be proven to induce autophagy. Therefore, our findings open up the possibility that other SRCR-containing proteins may act in a

similar way. Our data suggest that AIM-induced autophagy can regulate TLR-induced cytokine production, and thus reinforce the novel role of autophagy as an anti-inflammatory mechanism (Levine, Mizushima et al. 2011; Deretic, Saitoh et al. 2013). However, hAIM may target a specific subset of cytokines since it modulated TNF- α , IL-1 β and IL-10 but it did not affect IL-6 protein levels in response to TLR activation. Further research is needed to analyze modulation and of M Φ chemokine/cytokine production by hAIM and their relation to autophagy.

siRNA experiments in THP1 macrophages indicated that the induction of autophagy mechanisms by hAIM was achieved through cell surface scavenger receptor CD36. Our data provide a new scenario where the AIM-CD36 axis could act to promote autophagy and the subsequent anti-inflammatory profile in macrophages. Moreover, given that AIM is a soluble protein that circulates in blood and that CD36 is a multi-ligand receptor expressed in a wide variety of cell types, our results raise the possibility that AIM could act as autophagy inducer in other CD36⁺ cell types, such as dendritic cells, microglia, or adipocytes, among others.

In this regard, although adipocytes do not express AIM, AIM is internalized in these cells through CD36-mediated endocytosis. Once in the cytoplasm, AIM is able to inhibit FASN activity (Kurokawa, Arai et al. 2010). It is possible that in our work, rhAIM endeavors the same process. It would therefore be interesting to assess whether hAIM inhibits FASN in the M Φ , and whether this in turn is linked to its induction of autophagy. It is also possible that the intracellular targets of AIM could vary in different cell types. The mediators for AIM internalization might also vary, given that

thymocytes and NK-T cells, in which AIM is also effective (Miyazaki, Hirokami et al. 1999; Kuwata, Watanabe et al. 2003), do not express CD36. This may explain the multiple AIM functions observed in different cell types.

Further studies are needed to assess the ability of AIM to modulate inflammation mediated by other PAMPs or even DAMPs through enhanced autophagy. In this regard, it would be interesting to propose AIM as a candidate to be considered in the context of inflammatory or autoimmune pathologies that have been associated to autophagy dysfunction such as type II diabetes, liver and heart diseases or neuronal disorders (Jiang and Mizushima 2013).

Phagocytosis, like autophagy, is an ancient and highly conserved cellular function. However, the nature of the interactions between these two critical processes remains unclear. The second goal of the present work was to analyze hAIM role in macrophage phagocytosis. In order to achieve this goal, a set of *in vitro* experiments were performed comparing the phagocytic abilities of murine and human AIM proteins. Our data suggested that hAIM does not share the pro-phagocytic function of its murine homolog (Haruta, Kato et al. 2001).

AIM mRNA is synthesized in the same human and mouse tissues (spleen, lymph node, thymus, bone marrow, liver and fetal liver). However, three AIM mRNA transcripts expressed by human lymphoid tissues contrast with the single mRNA transcript found in the mouse, probably reflecting differences in mRNA regulation in these two species (Gebe, Kiener et al. 1997; Gebe, Llewellyn et al.

2000). At the amino acid level they are highly homologous (69% identity, 80% similarity), and their predicted molecular weight is 37 kDa; however, there are species-specific differences in their glycosylation patterns which may result in distinct activities (Sarrias, Gronlund et al. 2004). In this regard, a recent publication confirmed the relevance of glycosylation in mAIM function, by reporting that mutation of two N-glycosylation sites in the protein inhibited its secretion and enhanced its lipolytic function in adipocytes (Mori, Kimura et al. 2012). Our results regarding their distinct ability to regulate phagocytosis reinforce the notion that important functional differences may exist between human and mouse AIM.

The control of infectious diseases relies on the integration of a multitude of host cellular signaling pathways. The biological consequences of altered apoptosis, phagocytosis or autophagy should vary depending on the type of pathogen and the integrity of other host defense machinery (Bonilla, Bhattacharya et al. 2013). Previous studies in two different AIM KO models suggested contradictory contributions of AIM regarding its antibacterial function against *Listeria monocytogenes* infection (Joseph, Bradley et al. 2004; Zou, Garifulin et al. 2011). The authors hypothesized that these differences could be explained by different dynamics of AIM antiapoptotic effects between the two experimental models. However, a lack in direct evidences of the role of AIM in macrophage bactericidal mechanisms brought us to our third objective: to analyze the involvement of AIM in the response of macrophages to infection by bacteria. Our preliminary experiments performed with *E. coli*, showed lower bacterial burdens

concomitant with no effect in M Φ phagocytosis in the presence of hAIM. These data suggest that hAIM may enhance bactericidal mechanisms in the M Φ . The study of AIM involvement in M Φ bactericidal mechanisms was extended to an Mtb infection model. Three main reasons led us to choose Mtb for our model. First, because our research could contribute to increase the knowledge and help solve its burden in worldwide health in the long term. Second, because AIM is direct target of regulation of LXR/RXR receptors, and it was known that LXR protects against Mtb infection in mice (Korf, Vander Beken et al. 2009). Third, the availability of bacteria, facilities and know-how thanks to a collaboration established with the Unitat de Tuberculosi Experimental, UTE, IGTP, Badalona.

An *in vitro* model of Mtb infection of differentiated THP1-M Φ was established in the laboratory. This helped us to corroborate first that hAIM preserves its anti-apoptotic function in the settings of Mtb infection and, more interestingly, that AIM potentiates the antimicrobial response against Mtb by enhancing autophagy, suggesting that the previous described AIM-dependent autophagy induction in M Φ could be effective in the settings of an Mtb challenge.

We also observed that hAIM expression enhanced foam cell formation in uninfected and infected cells, thus conferring a role for the human form of this protein in macrophage lipid accumulation. Foamy M Φ are key participants in sustaining persistent bacteria and contributing to the tissue pathology that leads to cavitation and release of infectious bacilli (Caceres, Tapia et al. 2009; Russell, Cardona et al. 2009). Moreover, in the

presence of hAIM we detected increased IL-8 secretion, a highly chemoattractant chemokine for neutrophils. This finding contrasted with our previous results on AIM-dependent inhibition of NF- κ B activity in response to PAMPs. Interestingly, IL-8 production is induced in the presence of AIM also in basal (uninfected) conditions. The mechanisms of AIM-dependent IL-8 induction are under study. In response to PAMPs AIM-induced autophagy can regulate TLR-induced cytokine production, promoting an anti-inflammatory profile. It is possible that in the context of Mtb infection rhAIM endeavors the same process. It was recently suggested that inflammation plays a very important role in the outcome of tuberculosis lesions. Ibuprofen (a nonsteroidal anti-inflammatory drug) reduced the percentage of affected lung area, reduced the bacillary load, and increased survival in a mouse model mimicking active tuberculosis in humans (Vilaplana, Marzo et al. 2013). In brief, our findings regarding AIM-dependent foam cell formation, IL-8 induction and promotion of anti-inflammatory profile could be relevant in the progression of TB granuloma and its consequences in the final outcome of the disease deserves further study.

The observation that 24 h after infection mAIM serum levels increased 5-fold and peaked at 10-fold at 3 weeks, during the exponential growth of the bacilli suggests that AIM is involved in the initial innate immune response to Mtb infection. Accordingly, in a proteomic study, hAIM was identified as potential biomarker for early diagnosis of TB infection, because its serum levels were found significantly higher in patients with pulmonary TB (n:76) as compared with healthy controls (n:56) (Xu, Deng et al. 2013). In

this regard, several plasma proteomic studies have proposed AIM as biomarker of different pathologies, liver cirrhosis, (Gangadharan, Antrobus et al. 2007; Gray, Chattopadhyay et al. 2009; Sarvari, Mojtahedi et al. 2013) and allergic asthma, (Wu, Kobayashi et al. 2005) among others. However, because both in mouse models and in humans elevated AIM plasma levels occur in conditions with inflammatory components, we believe that AIM would have to be included in a panel along with other plasma biomarkers for the proposed diseases.

AIM circulates in blood associated to IgM (Tissot, Sanchez et al. 2002; Sarrias, Padilla et al. 2004). Whereas free AIM is excreted in the urine, its association with IgM stabilizes AIM in blood (Arai, Maehara et al. 2013). Recently, a novel strategy based in a synthetic fragment crystallizable (Fc) portion of IgM heavy chain was developed to safely control AIM blood levels (Kai, Yamazaki et al. 2014). The authors proposed that this could be applied in obese patients to promote lipolysis, and at the same time avoiding inflammation. Based on the increasingly understanding of AIM function this strategy or others based in anti/pro-AIM compounds could form the basis for developing novel therapies in different pathological settings.

In summary, our results provide new findings on hAIM that are highly relevant for our knowledge of M Φ in homeostasis as well as in response to inflammation and infection. They further provide a new function for the CD36 receptor as an inducer of M Φ autophagy through hAIM, and therefore they open a new perspective of the role of the hAIM-CD36 axis participating in the cross-talk between

the immune (pathogen-sensing) and metabolic systems that is emerging as a crucial homeostatic mechanism (Hotamisligil 2006).

CONCLUSIONS

- 1. hAIM displays an anti-inflammatory role in macrophages.** Both in THP1 cells and PB monocytes hAIM inhibited TLR induced p65 NF- κ B nuclear translocation with a concomitant decrease in TNF- α and IL-1 β as well as enhancement of IL-10 secretion.
- 2. hAIM induces macrophage autophagy.** Analysis of autophagy-related proteins (LC3, AKT, PI3P), autophagy flux and ultrastructural analysis by electron microscopy suggested that hAIM induces autophagy in macrophages. Abolition of hAIM autophagy induction by 3-MA treatment and ATG7 silencing further corroborated this data.
- 3. hAIM may act as an autophagy inductor that helps regulating TLR2 and TLR4-induced inflammatory responses.** ATG7 silencing reverted hAIM effects over TNF- α , IL-1 β and IL-10 secretion by M Φ in response to TLR2 and TLR4 ligands.
- 4. hAIM induces autophagy through CD36.** CD36 silencing abolished hAIM-induced autophagy and its modulation of inflammatory cytokine secretion.
- 5. hAIM has no effect on macrophage phagocytosis** of latex beads, *Escherichia coli* and *Staphylococcus aureus*.

- 6. hAIM enhances macrophage intracellular killing of *Escherichia coli*.** Lower intracellular bacterial burdens concomitant with no effect in phagocytosis in the presence of hAIM suggested a bactericidal function of the protein.

- 7. hAIM potentiates the antimicrobial response against *Mycobacterium tuberculosis*.** The boosting of ROS production and antimicrobial peptide synthesis and increase in autophagy mechanisms, could explain the enhanced mycobacterial capacity of hAIM-expressing cells.

- 8. AIM levels increases *in vitro* and *in vivo* after *Mycobacterium tuberculosis* infection.** *M. tuberculosis* increased hAIM mRNA and protein levels in a THP1 *in vitro* infection model and we observed increased mAIM serum levels in an *in vivo* infection model.

REFERENCES

REFERENCES

- Abe, T., M. Shimamura, et al. (2010) "Key role of CD36 in Toll-like receptor 2 signaling in cerebral ischemia." *Stroke* 41(5): 898-904.
- Akira, S. and K. Takeda (2004). "Toll-like receptor signalling." *Nat Rev Immunol* 4(7): 499-511.
- Akira, S., S. Uematsu, et al. (2006). "Pathogen recognition and innate immunity." *Cell* 124(4): 783-801.
- Aksoy, E., S. Taboubi, et al. (2012). "The p110delta isoform of the kinase PI(3)K controls the subcellular compartmentalization of TLR4 signaling and protects from endotoxic shock." *Nat Immunol* 13(11): 1045-54.
- Alers, S., A. S. Loffler, et al. (2011). "Role of AMPK-mTOR-Ulk1/2 in the regulation of autophagy: cross talk, shortcuts, and feedbacks." *Mol Cell Biol* 32(1): 2-11.
- Amezaga, N. (2013). Paper de la proteïna scavenger AIM en l'activació de macròfags i desenvolupament de cèl·lules escumoses. Barcelona, University of Barcelona. PhD Thesis in Biomedicine
- Amezaga, N., L. Sanjurjo, et al. (2013). "Human scavenger protein AIM increases foam cell formation and CD36-mediated oxLDL uptake." *J Leukoc Biol*.
- Amiel, E., A. Alonso, et al. (2009). "Pivotal Advance: Toll-like receptor regulation of scavenger receptor-A-mediated phagocytosis." *J Leukoc Biol* 85(4): 595-605.
- Arai, S., N. Maehara, et al. (2013). "Obesity-associated autoantibody production requires AIM to retain the immunoglobulin M immune complex on follicular dendritic cells." *Cell Rep* 3(4): 1187-98.
- Arai, S. and T. Miyazaki (2014). "Impacts of the apoptosis inhibitor of macrophage (AIM) on obesity-associated inflammatory diseases." *Semin Immunopathol* 36(1): 3-12.
- Arai, S., J. M. Shelton, et al. (2005). "A role for the apoptosis inhibitory factor AIM/Spalpha/Ap16 in atherosclerosis development." *Cell Metab Mar*;1(3):201-13.
- Arbibe, L., J. P. Mira, et al. (2000). "Toll-like receptor 2-mediated NF-kappa B activation requires a Rac1-dependent pathway." *Nat Immunol* 1(6): 533-40.
- Armengol, C., R. Bartoli, et al. (2013). "Role of scavenger receptors in the pathophysiology of chronic liver diseases." *Crit Rev Immunol* 33(1): 57-96.
- Armstrong, J. A. and P. D. Hart (1975). "Phagosome-lysosome interactions in cultured macrophages infected with virulent tubercle bacilli. Reversal of the usual nonfusion pattern and observations on bacterial survival." *J Exp Med* 142(1): 1-16.
- Asch, A. S., J. Barnwell, et al. (1987). "Isolation of the thrombospondin membrane receptor." *J Clin Invest* 79(4): 1054-61.

REFERENCES

- Backer, J. M. (2008). "The regulation and function of Class III PI3Ks: novel roles for Vps34." *Biochem J* 410(1): 1-17.
- Balakrishnan, L., M. Bhattacharjee, et al. (2014). "Differential proteomic analysis of synovial fluid from rheumatoid arthritis and osteoarthritis patients." *Clin Proteomics* 11(1): 1.
- Balfoussia, E., K. Skenderi, et al. (2013). "A proteomic study of plasma protein changes under extreme physical stress." *J Proteomics* 98: 1-14.
- Barbe, F., T. Douglas, et al. (2014). "Advances in Nod-like receptors (NLR) biology." *Cytokine Growth Factor Rev.*
- Barnwell, J. W., A. S. Asch, et al. (1989). "A human 88-kD membrane glycoprotein (CD36) functions in vitro as a receptor for a cytoadherence ligand on *Plasmodium falciparum*-infected erythrocytes." *J Clin Invest* 84(3): 765-72.
- Barton, G. M. (2008). "A calculated response: control of inflammation by the innate immune system." *J Clin Invest* 118(2): 413-20.
- Barton, G. M. and J. C. Kagan (2009). "A cell biological view of Toll-like receptor function: regulation through compartmentalization." *Nat Rev Immunol* 9(8): 535-42.
- Bell, J. K., I. Botos, et al. (2006). "The molecular structure of the TLR3 extracellular domain." *J Endotoxin Res* 12(6): 375-8.
- Bennett, B. L., D. T. Sasaki, et al. (2001). "SP600125, an anthranyrazolone inhibitor of Jun N-terminal kinase." *Proc Natl Acad Sci U S A* 98(24): 13681-6.
- Bikker, F. J., A. J. Ligtenberg, et al. (2004). "Bacteria binding by DMBT1/SAG/gp-340 is confined to the VEVLXXXXW motif in its scavenger receptor cysteine-rich domains." *J Biol Chem* 279(46): 47699-703.
- Biswas, S. K. and E. Lopez-Collazo (2009). "Endotoxin tolerance: new mechanisms, molecules and clinical significance." *Trends Immunol* 30(10): 475-87.
- Blasius, A. L. and B. Beutler (2010). "Intracellular toll-like receptors." *Immunity* 32(3): 305-15.
- Bonilla, D. L., A. Bhattacharya, et al. (2013). "Autophagy regulates phagocytosis by modulating the expression of scavenger receptors." *Immunity* 39(3): 537-47.
- Bowdish, D. M., K. Sakamoto, et al. (2009). "MARCO, TLR2, and CD14 are required for macrophage cytokine responses to mycobacterial trehalose dimycolate and *Mycobacterium tuberculosis*." *PLoS Pathog* 5(6): e1000474.
- Bowdish, D. M., K. Sakamoto, et al. (2013). "Genetic variants of MARCO are associated with susceptibility to pulmonary tuberculosis in a Gambian population." *BMC Med Genet* 14(1): 47.
- Brandt, K. J., C. Fickentscher, et al. (2013). "TLR2 Ligands Induce NF-kappaB Activation from Endosomal Compartments of Human Monocytes." *PLoS One* 8(12): e80743.
- Brannstrom, A., M. Sankala, et al. (2002). "Arginine residues in domain V have a central role for bacteria-binding activity of macrophage

- scavenger receptor MARCO." *Biochem Biophys Res Commun* 290(5): 1462-9.
- Brown, J., H. Wang, et al. (2010). "TLR-signaling networks: an integration of adaptor molecules, kinases, and cross-talk." *J Dent Res* 90(4): 417-27.
- Brown, J., H. Wang, et al. (2011). "Mammalian target of rapamycin complex 2 (mTORC2) negatively regulates Toll-like receptor 4-mediated inflammatory response via FoxO1." *J Biol Chem* 286(52): 44295-305.
- Brown, M. S. and J. L. Goldstein (1979). "Receptor-mediated endocytosis: insights from the lipoprotein receptor system." *Proc Natl Acad Sci U S A* 76(7): 3330-7.
- Broz, P. and D. M. Monack (2013). "Noncanonical inflammasomes: caspase-11 activation and effector mechanisms." *PLoS Pathog* 9(2): e1003144.
- Bull, H. A., P. M. Brickell, et al. (1994). "Src-related protein tyrosine kinases are physically associated with the surface antigen CD36 in human dermal microvascular endothelial cells." *FEBS Lett* 351(1): 41-4.
- Caceres, N., G. Tapia, et al. (2009). "Evolution of foamy macrophages in the pulmonary granulomas of experimental tuberculosis models." *Tuberculosis (Edinb)* 89(2): 175-82.
- Campbell, G. R. and S. A. Spector (2012). "Vitamin D inhibits human immunodeficiency virus type 1 and *Mycobacterium tuberculosis* infection in macrophages through the induction of autophagy." *PLoS Pathog* 8(5): e1002689.
- Cannizzo, E. S., C. C. Clement, et al. (2012). "Age-related oxidative stress compromises endosomal proteostasis." *Cell Rep* 2(1): 136-49.
- Canton, J., D. Neculai, et al. (2013). "Scavenger receptors in homeostasis and immunity." *Nat Rev Immunol* 13(9): 621-34.
- Cardona, P. J., I. Amat, et al. (2005). "Immunotherapy with fragmented *Mycobacterium tuberculosis* cells increases the effectiveness of chemotherapy against a chronic infection in a murine model of tuberculosis." *Vaccine* 23(11): 1393-8.
- Cardona, P. J., S. Gordillo, et al. (2003). "Widespread bronchogenic dissemination makes DBA/2 mice more susceptible than C57BL/6 mice to experimental aerosol infection with *Mycobacterium tuberculosis*." *Infect Immun* 71(10): 5845-54.
- Castillo, E. F., A. Dekonenko, et al. (2012). "Autophagy protects against active tuberculosis by suppressing bacterial burden and inflammation." *Proc Natl Acad Sci U S A* 109(46): E3168-76.
- Celada, A., P. W. Gray, et al. (1984). "Evidence for a gamma-interferon receptor that regulates macrophage tumoricidal activity." *J Exp Med* 160(1): 55-74.
- Cemma, M. and J. H. Brumell (2012). "Interactions of pathogenic bacteria with autophagy systems." *Curr Biol* 22(13): R540-5.
- Circu, M. L. and T. Y. Aw (2010). "Reactive oxygen species, cellular redox systems, and apoptosis." *Free Radic Biol Med* 48(6): 749-62.

REFERENCES

- Coburn, C. T., T. Hajri, et al. (2001). "Role of CD36 in membrane transport and utilization of long-chain fatty acids by different tissues." *J Mol Neurosci* 16(2-3): 117-21; discussion 151-7.
- Court, N., V. Vasseur, et al. (2010). "Partial redundancy of the pattern recognition receptors, scavenger receptors, and C-type lectins for the long-term control of *Mycobacterium tuberculosis* infection." *J Immunol* 184(12): 7057-70.
- Chan, E. D., J. Chan, et al. (2001). "What is the role of nitric oxide in murine and human host defense against tuberculosis? Current knowledge." *Am J Respir Cell Mol Biol* 25(5): 606-12.
- Chang, C. P., Y. C. Su, et al. (2012). "TLR2-dependent selective autophagy regulates NF-kappaB lysosomal degradation in hepatoma-derived M2 macrophage differentiation." *Cell Death Differ* 20(3): 515-23.
- Chang, C. P., Y. C. Su, et al. (2013). "Targeting NFKB by autophagy to polarize hepatoma-associated macrophage differentiation." *Autophagy* 9(4): 619-21.
- Cherra, S. J., 3rd, S. M. Kulich, et al. (2010). "Regulation of the autophagy protein LC3 by phosphorylation." *J Cell Biol* 190(4): 533-9.
- Dall'Armi, C., K. A. Devereaux, et al. (2013). "The role of lipids in the control of autophagy." *Curr Biol* 23(1): R33-45.
- Davis, B. K., H. Wen, et al. (2011). "The inflammasome NLRs in immunity, inflammation, and associated diseases." *Annu Rev Immunol* 29: 707-35.
- Deffert, C., J. Cachat, et al. (2014). "Phagocyte NADPH oxidase, chronic granulomatous disease and mycobacterial infections." *Cell Microbiol*.
- Delgado, M. A., R. A. Elmaoued, et al. (2008). "Toll-like receptors control autophagy." *EMBO J* 27(7): 1110-21.
- Deretic, V. (2008). "Autophagy, an immunologic magic bullet: *Mycobacterium tuberculosis* phagosome maturation block and how to bypass it." *Future Microbiol* 3(5): 517-24.
- Deretic, V. and B. Levine (2009). "Autophagy, immunity, and microbial adaptations." *Cell Host Microbe* 5(6): 527-49.
- Deretic, V., T. Saitoh, et al. (2013). "Autophagy in infection, inflammation and immunity." *Nat Rev Immunol* 13(10): 722-37.
- Devereaux, K., C. Dall'Armi, et al. (2013). "Regulation of mammalian autophagy by class II and III PI 3-kinases through PI3P synthesis." *PLoS One* 8(10): e76405.
- Dheda, K., J. F. Huggett, et al. (2004). "Validation of housekeeping genes for normalizing RNA expression in real-time PCR." *Biotechniques* 37(1): 112-4, 116, 118-9.
- Dunne, D. W., D. Resnick, et al. (1994). "The type I macrophage scavenger receptor binds to gram-positive bacteria and recognizes lipoteichoic acid." *Proc Natl Acad Sci U S A* 91(5): 1863-7.

- Elmore, S. (2007). "Apoptosis: a review of programmed cell death." *Toxicol Pathol* 35(4): 495-516.
- Endemann, G., L. W. Stanton, et al. (1993). "CD36 is a receptor for oxidized low density lipoprotein." *J Biol Chem* 268(16): 11811-6.
- Engelman, J. A., J. Luo, et al. (2006). "The evolution of phosphatidylinositol 3-kinases as regulators of growth and metabolism." *Nat Rev Genet* 7(8): 606-19.
- Fabri, M., S. Stenger, et al. (2012). "Vitamin D is required for IFN-gamma-mediated antimicrobial activity of human macrophages." *Sci Transl Med* 3(104): 104ra102.
- Fabrick, B. O., R. van Bruggen, et al. (2009). "The macrophage scavenger receptor CD163 functions as an innate immune sensor for bacteria." *Blood* 113(4): 887-92.
- Falasca, M. and T. Maffucci (2012). "Regulation and cellular functions of class II phosphoinositide 3-kinases." *Biochem J* 443(3): 587-601.
- Feng, Y., D. He, et al. (2013). "The machinery of macroautophagy." *Cell Res* 24(1): 24-41.
- Fimia, G. M., G. Kroemer, et al. (2012). "Molecular mechanisms of selective autophagy." *Cell Death Differ* 20(1): 1-2.
- Flannagan, R. S., G. Cosio, et al. (2009). "Antimicrobial mechanisms of phagocytes and bacterial evasion strategies." *Nat Rev Microbiol* 7(5): 355-66.
- Florey, O., S. E. Kim, et al. (2011). "Autophagy machinery mediates macroendocytic processing and entotic cell death by targeting single membranes." *Nat Cell Biol* 13(11): 1335-43.
- Flynn, J. L. and J. Chan (2003). "Immune evasion by *Mycobacterium tuberculosis*: living with the enemy." *Curr Opin Immunol* 15(4): 450-5.
- Foster, F. M., C. J. Traer, et al. (2003). "The phosphoinositide (PI) 3-kinase family." *J Cell Sci* 116(Pt 15): 3037-40.
- Foukas, L. C. and D. J. Withers (2010). "Phosphoinositide signalling pathways in metabolic regulation." *Curr Top Microbiol Immunol* 346: 115-41.
- Franco, I., F. Gulluni, et al. (2014). "PI3K class II alpha controls spatially restricted endosomal PtdIns3P and Rab11 activation to promote primary cilium function." *Dev Cell* 28(6): 647-58.
- Franchi, L., N. Warner, et al. (2009). "Function of Nod-like receptors in microbial recognition and host defense." *Immunol Rev* 227(1): 106-28.
- Fremont, C. M., V. Yermeev, et al. (2004). "Fatal *Mycobacterium tuberculosis* infection despite adaptive immune response in the absence of MyD88." *J Clin Invest* 114(12): 1790-9.
- Fukao, T. and S. Koyasu (2003). "PI3K and negative regulation of TLR signaling." *Trends Immunol* 24(7): 358-63.
- Fukao, T., M. Tanabe, et al. (2002). "PI3K-mediated negative feedback regulation of IL-12 production in DCs." *Nat Immunol* 3(9): 875-81.

REFERENCES

- Fukao, T., T. Yamada, et al. (2002). "Selective loss of gastrointestinal mast cells and impaired immunity in PI3K-deficient mice." *Nat Immunol* 3(3): 295-304.
- Gangadharan, B., R. Antrobus, et al. (2007). "Novel serum biomarker candidates for liver fibrosis in hepatitis C patients." *Clin Chem* 53(10): 1792-9.
- Gebe, J. A., P. A. Kiener, et al. (1997). "Molecular cloning, mapping to human chromosome 1 q21-q23, and cell binding characteristics of Spalpha, a new member of the scavenger receptor cysteine-rich (SRCR) family of proteins." *J Biol Chem* 272(10): 6151-8.
- Gebe, J. A., M. Llewellyn, et al. (2000). "Molecular cloning, genomic organization and cell-binding characteristics of mouse Spalpha." *Immunology* 99(1): 78-86.
- Geng, J. and D. J. Klionsky (2008). "The Atg8 and Atg12 ubiquitin-like conjugation systems in macroautophagy. 'Protein modifications: beyond the usual suspects' review series." *EMBO Rep* 9(9): 859-64.
- Ghigo, A., F. Damilano, et al. (2010). "PI3K inhibition in inflammation: Toward tailored therapies for specific diseases." *Bioessays* 32(3): 185-96.
- Gibson, S. B. (2013). "Investigating the role of reactive oxygen species in regulating autophagy." *Methods Enzymol* 528: 217-35.
- Girardin, S. E., R. Tournebize, et al. (2001). "CARD4/Nod1 mediates NF-kappaB and JNK activation by invasive *Shigella flexneri*." *EMBO Rep* 2(8): 736-42.
- Gong, L., R. J. Devenish, et al. (2012). "Autophagy as a macrophage response to bacterial infection." *IUBMB Life* 64(9): 740-7.
- Gray, J., D. Chattopadhyay, et al. (2009). "A proteomic strategy to identify novel serum biomarkers for liver cirrhosis and hepatocellular cancer in individuals with fatty liver disease." *BMC Cancer* 9: 271.
- Greaves, D. R. and S. Gordon (2009). "The macrophage scavenger receptor at 30 years of age: current knowledge and future challenges." *J Lipid Res* 50 Suppl: S282-6.
- Guha, M. and N. Mackman (2002). "The phosphatidylinositol 3-kinase-Akt pathway limits lipopolysaccharide activation of signaling pathways and expression of inflammatory mediators in human monocytic cells." *J Biol Chem* 277(35): 32124-32.
- Guo, J. and S. L. Friedman (2010). "Toll-like receptor 4 signaling in liver injury and hepatic fibrogenesis." *Fibrogenesis Tissue Repair* 3: 21.
- Gutierrez, M. G., S. S. Master, et al. (2004). "Autophagy is a defense mechanism inhibiting BCG and *Mycobacterium tuberculosis* survival in infected macrophages." *Cell* 119(6): 753-66.
- Gwinn, D. M., D. B. Shackelford, et al. (2008). "AMPK phosphorylation of raptor mediates a metabolic checkpoint." *Mol Cell* 30(2): 214-26.
- Hagar, J. A., D. A. Powell, et al. (2013). "Cytoplasmic LPS activates caspase-11: implications in TLR4-independent endotoxic shock." *Science* 341(6151): 1250-3.

- Hamada, M., M. Nakamura, et al. (2014). "MafB promotes atherosclerosis by inhibiting foam-cell apoptosis." *Nat Commun* 5: 3147.
- Harris, J., M. Hartman, et al. (2011). "Autophagy controls IL-1beta secretion by targeting pro-IL-1beta for degradation." *J Biol Chem* 286(11): 9587-97.
- Hart, P. D. and J. A. Armstrong (1974). "Strain virulence and the lysosomal response in macrophages infected with *Mycobacterium tuberculosis*." *Infect Immun* 10(4): 742-6.
- Haruta, I., Y. Kato, et al. (2001). "Association of AIM, a novel apoptosis inhibitory factor, with hepatitis via supporting macrophage survival and enhancing phagocytotic function of macrophages." *J Biol Chem* 276(25): 22910-4.
- He, J., J. H. Lee, et al. (2011). "The emerging roles of fatty acid translocase/CD36 and the aryl hydrocarbon receptor in fatty liver disease." *Exp Biol Med (Maywood)* 236(10): 1116-21.
- Heit, B., H. Kim, et al. (2013). "Multimolecular signaling complexes enable Syk-mediated signaling of CD36 internalization." *Dev Cell* 24(4): 372-83.
- Hoebe, K., P. Georgel, et al. (2005). "CD36 is a sensor of diacylglycerides." *Nature* 433(7025): 523-7.
- Hossain, M. M. and M. N. Norazmi (2013). "Pattern recognition receptors and cytokines in *Mycobacterium tuberculosis* infection--the double-edged sword?" *Biomed Res Int* 2013: 179174.
- Hotamisligil, G. S. (2006). "Inflammation and metabolic disorders." *Nature* 444(7121): 860-7.
- Huang, M. M., J. B. Bolen, et al. (1991). "Membrane glycoprotein IV (CD36) is physically associated with the Fyn, Lyn, and Yes protein-tyrosine kinases in human platelets." *Proc Natl Acad Sci U S A* 88(17): 7844-8.
- Hume, D. A. (2008). "Macrophages as APC and the dendritic cell myth." *J Immunol* 181(9): 5829-35.
- Hung, P. H., Y. W. Chen, et al. (2011). "Plasma proteomic analysis of the critical limb ischemia markers in diabetic patients with hemodialysis." *Mol Biosyst* 7(6): 1990-8.
- Husebye, H., O. Halaas, et al. (2006). "Endocytic pathways regulate Toll-like receptor 4 signaling and link innate and adaptive immunity." *EMBO J* 25(4): 683-92.
- Ibrahimi, A. and N. A. Abumrad (2002). "Role of CD36 in membrane transport of long-chain fatty acids." *Curr Opin Clin Nutr Metab Care* 5(2): 139-45.
- Im, S. S. and T. F. Osborne (2012). "Protection from bacterial-toxin-induced apoptosis in macrophages requires the lipogenic transcription factor sterol regulatory element binding protein 1a." *Mol Cell Biol* 32(12): 2196-202.
- Iwamura, Y., M. Mori, et al. (2012). "Apoptosis inhibitor of macrophage (AIM) diminishes lipid droplet-coating proteins leading to lipolysis in adipocytes." *Biochem Biophys Res Commun* 422(3): 476-81.

REFERENCES

- Jaber, N., Z. Dou, et al. (2012). "Class III PI3K Vps34 plays an essential role in autophagy and in heart and liver function." *Proc Natl Acad Sci U S A* 109(6): 2003-8.
- Janeway, C. A., Jr. (1989). "Approaching the asymptote? Evolution and revolution in immunology." *Cold Spring Harb Symp Quant Biol* 54 Pt 1: 1-13.
- Janeway, C. A., Jr. and R. Medzhitov (2002). "Innate immune recognition." *Annu Rev Immunol* 20: 197-216.
- Jiang, P. and N. Mizushima (2013). "Autophagy and human diseases." *Cell Res* 24(1): 69-79.
- Jimenez-Dalmaroni, M. J., N. Xiao, et al. (2009). "Soluble CD36 ectodomain binds negatively charged diacylglycerol ligands and acts as a co-receptor for TLR2." *PLoS One* 4(10): e7411.
- Jin, M. S. and J. O. Lee (2008). "Structures of the toll-like receptor family and its ligand complexes." *Immunity* 29(2): 182-91.
- Jo, E. K., J. M. Yuk, et al. (2013). "Roles of autophagy in elimination of intracellular bacterial pathogens." *Front Immunol* 4: 97.
- Joseph, S. B., M. N. Bradley, et al. (2004). "LXR-dependent gene expression is important for macrophage survival and the innate immune response." *Cell* 119(2): 299-309.
- Jung, C. H., S. H. Ro, et al. (2010). "mTOR regulation of autophagy." *FEBS Lett* 584(7): 1287-95.
- Kabeya, Y., N. Mizushima, et al. (2000). "LC3, a mammalian homologue of yeast Apg8p, is localized in autophagosome membranes after processing." *EMBO J* 19(21): 5720-8.
- Kagan, J. C., T. Su, et al. (2008). "TRAM couples endocytosis of Toll-like receptor 4 to the induction of interferon-beta." *Nat Immunol* 9(4): 361-8.
- Kai, T., T. Yamazaki, et al. (2014). "Stabilization and augmentation of circulating AIM in mice by synthesized IgM-Fc." *PLoS One* 9(5): e97037.
- Kang, R., H. J. Zeh, et al. (2011). "The Beclin 1 network regulates autophagy and apoptosis." *Cell Death Differ* 18(4): 571-80.
- Karim, A. F., P. Chandra, et al. (2011). "Express path analysis identifies a tyrosine kinase Src-centric network regulating divergent host responses to Mycobacterium tuberculosis infection." *J Biol Chem*. 2011 Nov 18;286(46):40307-19. doi: 10.1074/jbc.M111.266239.
- Kaufmann, S. H. (2001). "How can immunology contribute to the control of tuberculosis?" *Nat Rev Immunol* 1(1): 20-30.
- Kawai, T. and S. Akira (2007). "TLR signaling." *Semin Immunol* 19(1): 24-32.
- Kawai, T. and S. Akira (2010). "The role of pattern-recognition receptors in innate immunity: update on Toll-like receptors." *Nat Immunol* 11(5): 373-84.
- Kayagaki, N., S. Warming, et al. (2011). "Non-canonical inflammasome activation targets caspase-11." *Nature* 479(7371): 117-21.

- Kennedy, D. J. and S. R. Kashyap (2011). "Pathogenic role of scavenger receptor CD36 in the metabolic syndrome and diabetes." *Metab Syndr Relat Disord* 9(4): 239-45.
- Kihara, A., T. Noda, et al. (2001). "Two distinct Vps34 phosphatidylinositol 3-kinase complexes function in autophagy and carboxypeptidase Y sorting in *Saccharomyces cerevisiae*." *J Cell Biol* 152(3): 519-30.
- Kim, J., Y. C. Kim, et al. (2013). "Differential regulation of distinct Vps34 complexes by AMPK in nutrient stress and autophagy." *Cell* 152(1-2): 290-303.
- Kim, S., H. Takahashi, et al. (2009). "Carcinoma-produced factors activate myeloid cells through TLR2 to stimulate metastasis." *Nature* 457(7225): 102-6.
- Kim, W. K., H. R. Hwang, et al. (2008). "Glycoproteomic analysis of plasma from patients with atopic dermatitis: CD5L and ApoE as potential biomarkers." *Exp Mol Med* 40(6): 677-85.
- Kiss, M., Z. Czimmerer, et al. (2013). "The role of lipid-activated nuclear receptors in shaping macrophage and dendritic cell function: From physiology to pathology." *J Allergy Clin Immunol* 132(2): 264-86.
- Kleinnijenhuis, J., M. Oosting, et al. (2011). "Innate immune recognition of *Mycobacterium tuberculosis*." *Clin Dev Immunol* 2011: 405310.
- Klionsky, D. J., F. C. Abdalla, et al. (2012). "Guidelines for the use and interpretation of assays for monitoring autophagy." *Autophagy* 8(4): 445-544.
- Klug-Micu, G. M., S. Stenger, et al. (2013). "CD40L and IFN-gamma induce an antimicrobial response against *M. tuberculosis* in human monocytes." *Immunology*.
- Knudsen, T. B., P. Gustafson, et al. (2005). "Predictive value of soluble haemoglobin scavenger receptor CD163 serum levels for survival in verified tuberculosis patients." *Clin Microbiol Infect* 11(9): 730-5.
- Kobayashi, Y. (2008). "The role of chemokines in neutrophil biology." *Front Biosci*. 2008 Jan 1;13:2400-7.
- Kok, K., B. Geering, et al. (2009). "Regulation of phosphoinositide 3-kinase expression in health and disease." *Trends Biochem Sci* 34(3): 115-27.
- Kolialexi, A., A. K. Anagnostopoulos, et al. (2010). "Potential biomarkers for Turner in maternal plasma: possibility for noninvasive prenatal diagnosis." *J Proteome Res* 9(10): 5164-70.
- Kondo, T., T. Kawai, et al. (2012). "Dissecting negative regulation of Toll-like receptor signaling." *Trends Immunol* 33(9): 449-58.
- Korf, H., S. Vander Beken, et al. (2009). "Liver X receptors contribute to the protective immune response against *Mycobacterium tuberculosis* in mice." *J Clin Invest* 119(6): 1626-37.
- Koyasu, S. (2003). "The role of PI3K in immune cells." *Nat Immunol* 4(4): 313-9.

REFERENCES

- Krieger, M. (1997). "The other side of scavenger receptors: pattern recognition for host defense." *Curr Opin Lipidol* 8(5): 275-80.
- Krutzik, S. R., M. Hewison, et al. (2008). "IL-15 links TLR2/1-induced macrophage differentiation to the vitamin D-dependent antimicrobial pathway." *J Immunol* 181(10): 7115-20.
- Kumar, D., L. Nath, et al. (2010). "Genome-wide analysis of the host intracellular network that regulates survival of *Mycobacterium tuberculosis*." *Cell* 140(5): 731-43.
- Kumar, H., T. Kawai, et al. (2009). "Pathogen recognition in the innate immune response." *Biochem J* 420(1): 1-16.
- Kundu, J. K. and Y. J. Surh (2008). "Inflammation: gearing the journey to cancer." *Mutat Res* 659(1-2): 15-30.
- Kurokawa, J., S. Arai, et al. (2010). "Macrophage-derived AIM is endocytosed into adipocytes and decreases lipid droplets via inhibition of fatty acid synthase activity." *Cell Metab* 11(6): 479-92.
- Kurokawa, J., H. Nagano, et al. (2011). "Apoptosis inhibitor of macrophage (AIM) is required for obesity-associated recruitment of inflammatory macrophages into adipose tissue." *Proc Natl Acad Sci U S A* 108(29): 12072-7.
- Kuwata, K., H. Watanabe, et al. (2003). "AIM inhibits apoptosis of T cells and NKT cells in *Corynebacterium*-induced granuloma formation in mice." *Am J Pathol* 162(3): 837-47.
- Laird, M. H., S. H. Rhee, et al. (2009). "TLR4/MyD88/PI3K interactions regulate TLR4 signaling." *J Leukoc Biol* 85(6): 966-77.
- Lau, Y. L., G. C. Chan, et al. (1998). "The role of phagocytic respiratory burst in host defense against *Mycobacterium tuberculosis*." *Clin Infect Dis* 26(1): 226-7.
- Lee, H. K., J. M. Lund, et al. (2007). "Autophagy-dependent viral recognition by plasmacytoid dendritic cells." *Science* 315(5817): 1398-401.
- Lee, S. M., K. H. Kok, et al. (2014). "Toll-like receptor 10 is involved in induction of innate immune responses to influenza virus infection." *Proc Natl Acad Sci U S A* 111(10): 3793-8.
- Levine, B. and G. Kroemer (2008). "Autophagy in the pathogenesis of disease." *Cell* 132(1): 27-42.
- Levine, B., N. Mizushima, et al. (2011). "Autophagy in immunity and inflammation." *Nature* 469(7330): 323-35.
- Li, Y., P. Qu, et al. (2011). "Api6/AIM/Spalpha/CD5L overexpression in alveolar type II epithelial cells induces spontaneous lung adenocarcinoma." *Cancer Res* 71(16): 5488-99.
- Libby, P. (2002). "Inflammation in atherosclerosis." *Nature* 420(6917): 868-74.
- Liu, P. T., M. Schenk, et al. (2009). "Convergence of IL-1beta and VDR activation pathways in human TLR2/1-induced antimicrobial responses." *PLoS One* 4(6): e5810.
- Liu, P. T., S. Stenger, et al. (2007). "Cutting edge: vitamin D-mediated human antimicrobial activity against *Mycobacterium tuberculosis*

- is dependent on the induction of cathelicidin." *J Immunol* 179(4): 2060-3.
- Loimaranta, V., J. Hytonen, et al. (2009). "Leucine-rich repeats of bacterial surface proteins serve as common pattern recognition motifs of human scavenger receptor gp340." *J Biol Chem* 284(28): 18614-23.
- Long, R., B. Light, et al. (1999). "Mycobacteriocidal action of exogenous nitric oxide." *Antimicrob Agents Chemother* 43(2): 403-5.
- Luyendyk, J. P., G. A. Schabbauer, et al. (2008). "Genetic analysis of the role of the PI3K-Akt pathway in lipopolysaccharide-induced cytokine and tissue factor gene expression in monocytes/macrophages." *J Immunol* 180(6): 4218-26.
- MacMicking, J. D., R. J. North, et al. (1997). "Identification of nitric oxide synthase as a protective locus against tuberculosis." *Proc Natl Acad Sci U S A* 94(10): 5243-8.
- Mantovani, A., P. Allavena, et al. (2008). "Cancer-related inflammation." *Nature* 454(7203): 436-44.
- Mari, M., S. A. Tooze, et al. (2011). "The puzzling origin of the autophagosomal membrane." *F1000 Biol Rep* 3: 25.
- Martineau, A. R. (2011). "Old wine in new bottles: vitamin D in the treatment and prevention of tuberculosis." *Proc Nutr Soc* 71(1): 84-9.
- Martinez, J., J. Almendinger, et al. (2011). "Microtubule-associated protein 1 light chain 3 alpha (LC3)-associated phagocytosis is required for the efficient clearance of dead cells." *Proc Natl Acad Sci U S A* 108(42): 17396-401.
- Martinez, V. G., C. Escoda-Ferran, et al. (2014). "The macrophage soluble receptor AIM/Ap16/CD5L displays a broad pathogen recognition spectrum and is involved in early response to microbial aggression." *Cell Mol Immunol*.
- Martinon, F., K. Burns, et al. (2002). "The inflammasome: a molecular platform triggering activation of inflammatory caspases and processing of proIL-beta." *Mol Cell* 10(2): 417-26.
- Martinon, F., A. Mayor, et al. (2009). "The inflammasomes: guardians of the body." *Annu Rev Immunol* 27: 229-65.
- Massey, A., R. Kiffin, et al. (2004). "Pathophysiology of chaperone-mediated autophagy." *Int J Biochem Cell Biol* 36(12): 2420-34.
- Matzinger, P. (2002). "The danger model: a renewed sense of self." *Science* 296(5566): 301-5.
- Means, T. K., E. Mylonakis, et al. (2009). "Evolutionarily conserved recognition and innate immunity to fungal pathogens by the scavenger receptors SCARF1 and CD36." *J Exp Med* 206(3): 637-53.
- Medzhitov, R. and C. A. Janeway, Jr. (1997). "Innate immunity: impact on the adaptive immune response." *Curr Opin Immunol* 9(1): 4-9.
- Medzhitov, R. and C. A. Janeway, Jr. (2002). "Decoding the patterns of self and nonself by the innate immune system." *Science* 296(5566): 298-300.

REFERENCES

- Medzhitov, R., P. Preston-Hurlburt, et al. (1997). "A human homologue of the *Drosophila* Toll protein signals activation of adaptive immunity." *Nature* 388(6640): 394-7.
- Medzhitov, R., P. Preston-Hurlburt, et al. (1998). "MyD88 is an adaptor protein in the hToll/IL-1 receptor family signaling pathways." *Mol Cell* 2(2): 253-8.
- Melo, R. C. and A. M. Dvorak (2012). "Lipid body-phagosome interaction in macrophages during infectious diseases: host defense or pathogen survival strategy?" *PLoS Pathog* 8(7): e1002729.
- Mera, K., H. Uto, et al. (2014). "Serum levels of apoptosis inhibitor of macrophage are associated with hepatic fibrosis in patients with chronic hepatitis C." *BMC Gastroenterol* 14: 27.
- Mijaljica, D., M. Prescott, et al. (2011). "Microautophagy in mammalian cells: revisiting a 40-year-old conundrum." *Autophagy* 7(7): 673-82.
- Mikolajczyk, T. P., J. E. Skrzeczynska-Moncznik, et al. (2009). "Interaction of human peripheral blood monocytes with apoptotic polymorphonuclear cells." *Immunology* 128(1): 103-13.
- Miller, J. L., K. Velmurugan, et al. (2010). "The type I NADH dehydrogenase of *Mycobacterium tuberculosis* counters phagosomal NOX2 activity to inhibit TNF-alpha-mediated host cell apoptosis." *PLoS Pathog* 6(4): e1000864.
- Miro-Julia, C., S. Rosello, et al. (2011). "Molecular and functional characterization of mouse S5D-SRCRB: a new group B member of the scavenger receptor cysteine-rich superfamily." *J Immunol* 186(4): 2344-54.
- Mishra, B. B., V. A. Rathinam, et al. (2012). "Nitric oxide controls the immunopathology of tuberculosis by inhibiting NLRP3 inflammasome-dependent processing of IL-1beta." *Nat Immunol* 14(1): 52-60.
- Miyazaki, T., Y. Hirokami, et al. (1999). "Increased susceptibility of thymocytes to apoptosis in mice lacking AIM, a novel murine macrophage-derived soluble factor belonging to the scavenger receptor cysteine-rich domain superfamily." *J Exp Med* 189(2): 413-22.
- Miyazaki, T., J. Kurokawa, et al. (2011). "AIMing at metabolic syndrome. - Towards the development of novel therapies for metabolic diseases via apoptosis inhibitor of macrophage (AIM)." *Circ J* 75(11): 2522-31.
- Mori, M., H. Kimura, et al. (2012). "Modification of N-glycosylation modulates the secretion and lipolytic function of apoptosis inhibitor of macrophage (AIM)." *FEBS Lett* 586(20): 3569-74.
- Mosser, D. M. and J. P. Edwards (2008). "Exploring the full spectrum of macrophage activation." *Nat Rev Immunol* 8(12): 958-69.
- Mukhopadhyay, S. and S. Gordon (2004). "The role of scavenger receptors in pathogen recognition and innate immunity." *Immunobiology* 209(1-2): 39-49.

- Nagelkerke, A., J. Bussink, et al. (2014). "Therapeutic targeting of autophagy in cancer. Part II: Pharmacological modulation of treatment-induced autophagy." *Semin Cancer Biol.*
- Nakagawa, I., A. Amano, et al. (2004). "Autophagy defends cells against invading group A *Streptococcus*." *Science* 306(5698): 1037-40.
- Naranjo-Gomez, M., M. A. Fernandez, et al. (2005). "Primary alloproliferative TH1 response induced by immature plasmacytoid dendritic cells in collaboration with myeloid DCs." *Am J Transplant* 5(12): 2838-48.
- Nathan, C. and M. U. Shiloh (2000). "Reactive oxygen and nitrogen intermediates in the relationship between mammalian hosts and microbial pathogens." *Proc Natl Acad Sci U S A* 97(16): 8841-8.
- Nixon, R. A. (2013). "The role of autophagy in neurodegenerative disease." *Nat Med* 19(8): 983-97.
- Noursadeghi, M., J. Tsang, et al. (2008). "Quantitative imaging assay for NF-kappaB nuclear translocation in primary human macrophages." *J Immunol Methods* 329(1-2): 194-200.
- O'Farrell, F., T. E. Rusten, et al. (2013). "Phosphoinositide 3-kinases as accelerators and brakes of autophagy." *FEBS J* 280(24): 6322-37.
- O'Neill, L. A., D. Golenbock, et al. (2013). "The history of Toll-like receptors - redefining innate immunity." *Nat Rev Immunol* 13(6): 453-60.
- Obara, K., T. Sekito, et al. (2006). "Assortment of phosphatidylinositol 3-kinase complexes--Atg14p directs association of complex I to the pre-autophagosomal structure in *Saccharomyces cerevisiae*." *Mol Biol Cell* 17(4): 1527-39.
- Ockenhouse, C. F., N. N. Tandon, et al. (1989). "Identification of a platelet membrane glycoprotein as a falciparum malaria sequestration receptor." *Science* 243(4897): 1469-71.
- Ofek, I., J. Goldhar, et al. (1995). "Nonopsonic phagocytosis of microorganisms." *Annu Rev Microbiol* 49: 239-76.
- Ogawa, M., H. Mimuro, et al. (2011). "Manipulation of autophagy by bacteria for their own benefit." *Microbiol Immunol* 55(7): 459-71.
- Ohtani, M., S. Nagai, et al. (2008). "Mammalian target of rapamycin and glycogen synthase kinase 3 differentially regulate lipopolysaccharide-induced interleukin-12 production in dendritic cells." *Blood* 112(3): 635-43.
- Okkenhaug, K. (2013). "Signaling by the phosphoinositide 3-kinase family in immune cells." *Annu Rev Immunol* 31: 675-704.
- Pampliega, O., I. Orhon, et al. (2013). "Functional interaction between autophagy and ciliogenesis." *Nature* 502(7470): 194-200.
- Parzych, K. R. and D. J. Klionsky (2013). "An overview of autophagy: morphology, mechanism, and regulation." *Antioxid Redox Signal* 20(3): 460-73.
- Paul, S., A. K. Kashyap, et al. (2012). "Selective autophagy of the adaptor protein Bcl10 modulates T cell receptor activation of NF-kappaB." *Immunity* 36(6): 947-58.

REFERENCES

- Peiser, L. and S. Gordon (2001). "The function of scavenger receptors expressed by macrophages and their role in the regulation of inflammation." *Microbes Infect* 3(2): 149-59.
- Petiot, A., E. Ogier-Denis, et al. (2000). "Distinct classes of phosphatidylinositol 3'-kinases are involved in signaling pathways that control macroautophagy in HT-29 cells." *J Biol Chem* 275(2): 992-8.
- Philpott, D. J., M. T. Sorbara, et al. (2013). "NOD proteins: regulators of inflammation in health and disease." *Nat Rev Immunol* 14(1): 9-23.
- Philpott, D. J., S. Yamaoka, et al. (2000). "Invasive *Shigella flexneri* activates NF-kappa B through a lipopolysaccharide-dependent innate intracellular response and leads to IL-8 expression in epithelial cells." *J Immunol* 165(2): 903-14.
- Pieters, J. (2008). "Mycobacterium tuberculosis and the macrophage: maintaining a balance." *Cell Host Microbe* 3(6): 399-407.
- Pluddemann, A., S. Mukhopadhyay, et al. (2011). "Innate immunity to intracellular pathogens: macrophage receptors and responses to microbial entry." *Immunol Rev* 240(1): 11-24.
- Prabhudas, M., D. Bowdish, et al. (2014). "Standardizing scavenger receptor nomenclature." *J Immunol* 192(5): 1997-2006.
- Qu, P., H. Du, et al. (2009). "Myeloid-specific expression of Api6/AIM/Sp alpha induces systemic inflammation and adenocarcinoma in the lung." *J Immunol* 182(3): 1648-59.
- Raetz, M., A. Kibardin, et al. (2013). "Cooperation of TLR12 and TLR11 in the IRF8-dependent IL-12 response to *Toxoplasma gondii* profilin." *J Immunol* 191(9): 4818-27.
- Rahaman, S. O., D. J. Lennon, et al. (2006). "A CD36-dependent signaling cascade is necessary for macrophage foam cell formation." *Cell Metab* 4(3): 211-21.
- Rathinam, V. A. and K. A. Fitzgerald (2013). "Immunology: Lipopolysaccharide sensing on the inside." *Nature* 501(7466): 173-5.
- Ravikumar, B., S. Sarkar, et al. (2010). "Regulation of mammalian autophagy in physiology and pathophysiology." *Physiol Rev* 90(4): 1383-435.
- Reggiori, F. and D. J. Klionsky (2002). "Autophagy in the eukaryotic cell." *Eukaryot Cell* 1(1): 11-21.
- Reggiori, F., M. Komatsu, et al. (2012). "Autophagy: more than a nonselective pathway." *Int J Cell Biol* 2012: 219625.
- Repa, J. J., G. Liang, et al. (2000). "Regulation of mouse sterol regulatory element-binding protein-1c gene (SREBP-1c) by oxysterol receptors, LXRalpha and LXRbeta." *Genes Dev* 14(22): 2819-30.
- Resnick, D., A. Pearson, et al. (1994). "The SRCR superfamily: a family reminiscent of the Ig superfamily." *Trends Biochem Sci* 19(1): 5-8.
- Rhee, S. H., H. Kim, et al. (2006). "Role of MyD88 in phosphatidylinositol 3-kinase activation by flagellin/toll-like receptor 5 engagement in colonic epithelial cells." *J Biol Chem* 281(27): 18560-8.

- Ross, R. (1999). "Atherosclerosis is an inflammatory disease." *Am Heart J* 138(5 Pt 2): S419-20.
- Russell, D. G. (2001). "Mycobacterium tuberculosis: here today, and here tomorrow." *Nat Rev Mol Cell Biol* 2(8): 569-77.
- Russell, D. G., P. J. Cardona, et al. (2009). "Foamy macrophages and the progression of the human tuberculosis granuloma." *Nat Immunol* 10(9): 943-8.
- Rutault, K., C. A. Hazzalin, et al. (2001). "Combinations of ERK and p38 MAPK inhibitors ablate tumor necrosis factor-alpha (TNF-alpha) mRNA induction. Evidence for selective destabilization of TNF-alpha transcripts." *J Biol Chem* 276(9): 6666-74.
- Saitoh, T., N. Fujita, et al. (2008). "Loss of the autophagy protein Atg16L1 enhances endotoxin-induced IL-1beta production." *Nature* 456(7219): 264-8.
- Sanjuan, M. A., C. P. Dillon, et al. (2007). "Toll-like receptor signalling in macrophages links the autophagy pathway to phagocytosis." *Nature* 450(7173): 1253-7.
- Santos-Sierra, S., S. D. Deshmukh, et al. (2009). "Mal connects TLR2 to PI3Kinase activation and phagocyte polarization." *EMBO J* 28(14): 2018-27.
- Sarkar, S. N., K. L. Peters, et al. (2004). "Novel roles of TLR3 tyrosine phosphorylation and PI3 kinase in double-stranded RNA signaling." *Nat Struct Mol Biol* 11(11): 1060-7.
- Sarrias, M. R., M. Farnos, et al. (2007). "CD6 binds to pathogen-associated molecular patterns and protects from LPS-induced septic shock." *Proc Natl Acad Sci U S A* 104(28): 11724-9.
- Sarrias, M. R., J. Gronlund, et al. (2004). "The Scavenger Receptor Cysteine-Rich (SRCR) domain: an ancient and highly conserved protein module of the innate immune system." *Crit Rev Immunol* 24(1): 1-37.
- Sarrias, M. R., O. Padilla, et al. (2004). "Biochemical characterization of recombinant and circulating human Spalpha." *Tissue Antigens* 63(4): 335-44.
- Sarrias, M. R., S. Rosello, et al. (2005). "A role for human Sp alpha as a pattern recognition receptor." *J Biol Chem* 280(42): 35391-8.
- Sarvari, J., Z. Mojtahedi, et al. (2013). "Differentially Expressed Proteins in Chronic Active Hepatitis, Cirrhosis, and HCC Related to HCV Infection in Comparison With HBV Infection: A proteomics study." *Hepat Mon* 13(7): e8351.
- Schabbauer, G., M. Tencati, et al. (2004). "PI3K-Akt pathway suppresses coagulation and inflammation in endotoxemic mice." *Arterioscler Thromb Vasc Biol* 24(10): 1963-9.
- Schroder, K. and J. Tschopp (2010). "The inflammasomes." *Cell* 140(6): 821-32.
- Schu, P. V., K. Takegawa, et al. (1993). "Phosphatidylinositol 3-kinase encoded by yeast VPS34 gene essential for protein sorting." *Science* 260(5104): 88-91.

REFERENCES

- Segal, B. H., T. L. Leto, et al. (2000). "Genetic, biochemical, and clinical features of chronic granulomatous disease." *Medicine (Baltimore)* 79(3): 170-200.
- Seimon, T. A., M. J. Nadolski, et al. (2010). "Atherogenic lipids and lipoproteins trigger CD36-TLR2-dependent apoptosis in macrophages undergoing endoplasmic reticulum stress." *Cell Metab* 12(5): 467-82.
- Sever-Chroneos, Z., A. Tvinnereim, et al. (2011). "Prolonged survival of scavenger receptor class A-deficient mice from pulmonary Mycobacterium tuberculosis infection." *Tuberculosis (Edinb)* 91 Suppl 1: S69-74.
- Shi, C. S., K. Shenderov, et al. (2012). "Activation of autophagy by inflammatory signals limits IL-1beta production by targeting ubiquitinated inflammasomes for destruction." *Nat Immunol* 13(3): 255-63.
- Shin, H. W., M. Hayashi, et al. (2005). "An enzymatic cascade of Rab5 effectors regulates phosphoinositide turnover in the endocytic pathway." *J Cell Biol* 170(4): 607-18.
- Shoelson, S. E., J. Lee, et al. (2006). "Inflammation and insulin resistance." *J Clin Invest* 116(7): 1793-801.
- Silverstein, R. L. (2009). "Inflammation, atherosclerosis, and arterial thrombosis: role of the scavenger receptor CD36." *Cleve Clin J Med* 76 Suppl 2: S27-30.
- Silverstein, R. L. and M. Febbraio (2009). "CD36, a scavenger receptor involved in immunity, metabolism, angiogenesis, and behavior." *Sci Signal* 2(72): re3.
- Silverstein, R. L., W. Li, et al. (2010). "Mechanisms of cell signaling by the scavenger receptor CD36: implications in atherosclerosis and thrombosis." *Trans Am Clin Climatol Assoc* 121: 206-20.
- Simonsen, A., A. E. Wurmser, et al. (2001). "The role of phosphoinositides in membrane transport." *Curr Opin Cell Biol* 13(4): 485-92.
- Skeldon, A. and M. Saleh (2011). "The inflammasomes: molecular effectors of host resistance against bacterial, viral, parasitic, and fungal infections." *Front Microbiol* 2: 15.
- Sonawane, A., J. C. Santos, et al. (2011). "Cathelicidin is involved in the intracellular killing of mycobacteria in macrophages." *Cell Microbiol* 13(10): 1601-17.
- Spooner, R. and O. Yilmaz (2011). "The role of reactive-oxygen-species in microbial persistence and inflammation." *Int J Mol Sci* 12(1): 334-52.
- Sridharan, S., K. Jain, et al. (2011). "Regulation of autophagy by kinases." *Cancers (Basel)* 3(2): 2630-54.
- Steinberg, B. E. and S. Grinstein (2008). "Pathogen destruction versus intracellular survival: the role of lipids as phagosomal fate determinants." *J Clin Invest* 118(6): 2002-11.
- Stewart, C. R., L. M. Stuart, et al. (2009). "CD36 ligands promote sterile inflammation through assembly of a Toll-like receptor 4 and 6 heterodimer." *Nat Immunol* 11(2): 155-61.

- Stuart, L. M., J. Deng, et al. (2005). "Response to *Staphylococcus aureus* requires CD36-mediated phagocytosis triggered by the COOH-terminal cytoplasmic domain." *J Cell Biol* 170(3): 477-85.
- Takeshige, K., M. Baba, et al. (1992). "Autophagy in yeast demonstrated with proteinase-deficient mutants and conditions for its induction." *J Cell Biol* 119(2): 301-11.
- Takeuchi, O. and S. Akira (2010). "Pattern recognition receptors and inflammation." *Cell* 140(6): 805-20.
- Theus, S. A., M. D. Cave, et al. (2004). "Activated THP-1 cells: an attractive model for the assessment of intracellular growth rates of *Mycobacterium tuberculosis* isolates." *Infect Immun* 72(2): 1169-73.
- Thornberry, N. A., H. G. Bull, et al. (1992). "A novel heterodimeric cysteine protease is required for interleukin-1 beta processing in monocytes." *Nature* 356(6372): 768-74.
- Tissot, J. D., J. C. Sanchez, et al. (2002). "IgM are associated to Sp alpha (CD5 antigen-like)." *Electrophoresis* 23(7-8): 1203-6.
- Torrado, E., R. T. Robinson, et al. (2011). "Cellular response to mycobacteria: balancing protection and pathology." *Trends Immunol* 32(2): 66-72.
- Triantafilou, M., F. G. Gamper, et al. (2006). "Membrane sorting of toll-like receptor (TLR)-2/6 and TLR2/1 heterodimers at the cell surface determines heterotypic associations with CD36 and intracellular targeting." *J Biol Chem* 281(41): 31002-11.
- Valledor, A. F., L. C. Hsu, et al. (2004). "Activation of liver X receptors and retinoid X receptors prevents bacterial-induced macrophage apoptosis." *Proc Natl Acad Sci U S A* 101(51): 17813-8.
- van Crevel, R., T. H. Ottenhoff, et al. (2003). "Innate immunity to *Mycobacterium tuberculosis*." *Adv Exp Med Biol* 531: 241-7.
- Vanhaesebroeck, B., J. Guillermet-Guibert, et al. (2010). "The emerging mechanisms of isoform-specific PI3K signalling." *Nat Rev Mol Cell Biol* 11(5): 329-41.
- Vanhaesebroeck, B., S. J. Leever, et al. (2001). "Synthesis and function of 3-phosphorylated inositol lipids." *Annu Rev Biochem* 70: 535-602.
- Vanhaesebroeck, B., S. J. Leever, et al. (1997). "Phosphoinositide 3-kinases: a conserved family of signal transducers." *Trends Biochem Sci* 22(7): 267-72.
- Vera, J., R. Fenutria, et al. (2009). "The CD5 ectodomain interacts with conserved fungal cell wall components and protects from zymosan-induced septic shock-like syndrome." *Proc Natl Acad Sci U S A* 106(5): 1506-11.
- Vilaplana, C., E. Marzo, et al. (2013). "Ibuprofen therapy resulted in significantly decreased tissue bacillary loads and increased survival in a new murine experimental model of active tuberculosis." *J Infect Dis* 208(2): 199-202.

REFERENCES

- Vural, A. and J. H. Kehrl (2014). "Autophagy in macrophages: impacting inflammation and bacterial infection." *Scientifica (Cairo)* 2014: 825463.
- Weinberg, J. B., M. A. Misukonis, et al. (1995). "Human mononuclear phagocyte inducible nitric oxide synthase (iNOS): analysis of iNOS mRNA, iNOS protein, biopterin, and nitric oxide production by blood monocytes and peritoneal macrophages." *Blood* 86(3): 1184-95.
- Weisberg, S. P., D. McCann, et al. (2003). "Obesity is associated with macrophage accumulation in adipose tissue." *J Clin Invest* 112(12): 1796-808.
- Werts, C., S. E. Girardin, et al. (2006). "TIR, CARD and PYRIN: three domains for an antimicrobial triad." *Cell Death Differ* 13(5): 798-815.
- West, A. P., A. A. Koblansky, et al. (2006). "Recognition and signaling by toll-like receptors." *Annu Rev Cell Dev Biol* 22: 409-37.
- Winer, D. A., S. Winer, et al. (2011). "B cells promote insulin resistance through modulation of T cells and production of pathogenic IgG antibodies." *Nat Med* 17(5): 610-7.
- Wirawan, E., T. Vanden Berghe, et al. (2011). "Autophagy: for better or for worse." *Cell Res* 22(1): 43-61.
- Wong, K. K., J. A. Engelman, et al. (2009). "Targeting the PI3K signaling pathway in cancer." *Curr Opin Genet Dev* 20(1): 87-90.
- Wu, J., M. Kobayashi, et al. (2005). "Differential proteomic analysis of bronchoalveolar lavage fluid in asthmatics following segmental antigen challenge." *Mol Cell Proteomics* 4(9): 1251-64.
- Xie, Z. and D. J. Klionsky (2007). "Autophagosome formation: core machinery and adaptations." *Nat Cell Biol* 9(10): 1102-9.
- Xu, D. D., D. F. Deng, et al. (2013). "Discovery and identification of serum potential biomarkers for pulmonary tuberculosis using iTRAQ-coupled two-dimensional LC-MS/MS." *Proteomics* 14(2-3): 322-31.
- Xu, H., G. T. Barnes, et al. (2003). "Chronic inflammation in fat plays a crucial role in the development of obesity-related insulin resistance." *J Clin Invest* 112(12): 1821-30.
- Yang, C. S., J. M. Yuk, et al. (2009). "The role of nitric oxide in mycobacterial infections." *Immune Netw* 9(2): 46-52.
- Yang, Z. and D. J. Klionsky (2009). "Mammalian autophagy: core molecular machinery and signaling regulation." *Curr Opin Cell Biol* 22(2): 124-31.
- Yorimitsu, T. and D. J. Klionsky (2005). "Autophagy: molecular machinery for self-eating." *Cell Death Differ* 12 Suppl 2: 1542-52.
- Yoshimori, T. and T. Noda (2008). "Toward unraveling membrane biogenesis in mammalian autophagy." *Curr Opin Cell Biol* 20(4): 401-7.
- Yoshioka, K., K. Yoshida, et al. (2012). "Endothelial PI3K-C2alpha, a class II PI3K, has an essential role in angiogenesis and vascular barrier function." *Nat Med* 18(10): 1560-9.

- Yu, H. R., H. C. Kuo, et al. (2009). "A unique plasma proteomic profiling with imbalanced fibrinogen cascade in patients with Kawasaki disease." *Pediatr Allergy Immunol* 20(7): 699-707.
- Yuk, J. M., D. M. Shin, et al. (2009). "Vitamin D3 induces autophagy in human monocytes/macrophages via cathelicidin." *Cell Host Microbe* 6(3): 231-43.
- Yusa, S., S. Ohnishi, et al. (1999). "AIM, a murine apoptosis inhibitory factor, induces strong and sustained growth inhibition of B lymphocytes in combination with TGF-beta1." *Eur J Immunol* 29(4): 1086-93.
- Zahrt, T. C. and V. Deretic (2002). "Reactive nitrogen and oxygen intermediates and bacterial defenses: unusual adaptations in *Mycobacterium tuberculosis*." *Antioxid Redox Signal* 4(1): 141-59.
- Zhou, X., J. Takatoh, et al. (2011). "The mammalian class 3 PI3K (PIK3C3) is required for early embryogenesis and cell proliferation." *PLoS One* 6(1): e16358.
- Zou, T., O. Garifulin, et al. (2011). "Listeria monocytogenes infection induces prosurvival metabolic signaling in macrophages." *Infect Immun* 79(4): 1526-35.

ACKNOWLEDGMENTS

(agradecimientos, agraïments)

Este trabajo no hubiese sido posible sin la ayuda de un montón de personas a las cuales quiero dar las gracias.

En primer lugar, me gustaría expresar lo afortunada que me siento por haber podido realizar este trabajo bajo la dirección de la Dra. María Rosa Sarrias. Estoy muy agradecida por todo lo que he aprendido de ella durante estos años y por el enorme apoyo tanto a nivel científico como personal que he recibido desde el primer día.

Al Dr. Blázquez Caeiro y a Pilar Pérez, dos grandes personas con los que descubrí el mundo de la investigación, gracias por transmitirme su entusiasmo por la ciencia.

A todos los compañeros y ex compañeros de grupo y poyata, en especial a la Dra. Núria Amézaga y a Gemma Arán, gracias amigas por toda vuestra ayuda con los experimentos y por el día a día.

Al equipo de la UTE, Dr. Cardona, Dra. Vilaplana, Dra. Cáceres y Dra. Marzo. Por toda la ayuda y colaboración, y por dejar que me asomase a vuestro mundo.

A los buenos amigos que me llevo de mi paso por el servicio de Inmunología del Hospital Clínico.

A todos los compañeros del IGTP. Por una gran acogida, y por los buenos momentos que me habéis dado a lo largo de estos años.

A mi familia por su grandísimo apoyo. A mis amigos queridos que me han hecho sentir desde hace tiempo que mi familia se extiende a mis niñas de Ferrol, Pontedeume y a mis locos de Compostela. Llegando también hasta uBadalona, gracias por estar siempre ahí. Y en estos últimos años hasta Barcelona, mis frikis/hipsters no sé que hubiese hecho sin vosotros, sois lo más!

E por suposto, ao mellor pai do mundo ao que quero moitísimo.

